

Research on Sediment Distribution and Management in South-West Region of Bangladesh

WARPO TEAM

Md. Aminul Haque
Md. Jahid Hossain
Md. Jamal Haider
Md. Anwar Hossain
Shuvro Bhowmick
Md. Sakib Mahdi Aziz

BUET TEAM

Anisul Haque
Quamrul Ahsan
Md. Munsur Rahman
Sadmina Razzaque
Delowar Hossain
Imran Hossain Newton
Anika Tahsin
Afroza Akther

Interim Report
September 2020

Table of Contents

	Contents	Page No
	Table of Contents	1
	List of Figures	2
	List of Tables	5
	EXECUTIVE SUMMARY	6
	CHAPTER ONE	
	Introduction	
1.1	Background	14
1.2	Objectives of the Study	15
1.3	Previous Studies	15
1.4	Organization of the Report	18
	CHAPTER TWO	
	Study Area	
2.1	Introduction	19
2.2	Estuarine Systems	21
2.3	Sediment Regime	22
2.4	Existing Sediment Management Practices	26
	CHAPTER THREE	
	Methodology	
3.1	Introduction	30
3.2	Integrated Modelling Framework: The Bangladesh Delta Model (BDM)	30
3.3	Model Calibration and Validation	42
	CHAPTER FOUR	
	Results from BDM	
4.1	Introduction	52
4.2	Simulation of Tide in the Bay of Bengal	52
4.2.1	Tide propagation in the Bay of Bengal	52
4.2.2	Distribution of freshwater plume	54
4.2.3	Vertical stratification	55
4.3	Simulation of Storm Surge in the Bay of Bengal	58
4.3.1	Cyclone model	58
4.3.2	Past cyclone scenarios	59
4.3.3	Effect of cyclone wind on tidal current	72
4.4	Simulation of Land Inundation during Monsoon Flood in Bangladesh	74
4.5	Simulation of Land Inundation during Storm Surge Flood in the Coast	81
4.6	Simulation of Sedimentation	82
4.6.1	Sediment movement path along the coast	82
4.6.2	Sedimentation in the floodplains	83
	CHAPTER FIVE	
	Conclusions	92
	References	94

List of Figures

Figure No	Title	Page No.
1.1	Measurement locations by Rogers et al. (2013).	16
1.2	Land status and cross-dam location almost 16 years before the construction of the cross-dam. Cross-dam is constructed just west of red-circled zone during the year 2010.	17
1.3	Reclaimed and eroded lands as a system response almost after 8 years due to construction of cross-dam. The green, red, blue and yellow circles show reclaimed land. The white circle south of char Kukri Mukri show the lost land. The cross dam is shown by red line in between Char Islam and Char Montaz.	18
2.1	Study Area.	19
2.2	Oceanic circulation zone.	20
2.3	Protected land inside polders in the study area.	20
2.4	Estuarine systems of coastal zone.	22
2.5	Outlet of the Ganges-Brahmaputra-Meghna (GBM) delta (Source Hussain et al., 2014).	23
2.6	Yearly sedimentation during an extreme flood condition in the coastal zone for (a) with polder and (b) without polder condition (source: WARPO and BUET, 2019).	24
2.7	Model simulated oceanic circulation during the dry season.	25
2.8	Model simulated oceanic circulation during the monsoon.	25
2.9	Model simulated sedimentation and erosion in the Meghna estuary region.	26
2.10	Impact of dredging of Hari river on water-logging condition inside polders 24 and 25. In the left image (before dredging) the blue areas are the additional water-logged area due to sedimentation of the Hari river. In the right image (after dredging) the green areas are free from water-logging due to dredging of Hari river (Source WARPO and BUET 2019).	27
2.11	Concept of Tidal River Management TRM (Source: Rocky et al., 2020).	28
2.12	Proposed cross dam locations by BWDB (Source; EDP 2007).	29
3.1	Model domain and grid of Bangladesh Delta Model (BDM). The figure also shows locations of different hydrological zones and the Bay of Bengal. These zones are (1) South West (SW) (2) South Central (SC) (3) South East (SE) (4) Eastern Hills (EH) (5) North West (NW) (6) North Central (NC) (7) North East (NE) (8) Bay of Bengal (BoB).	32
3.2a	Model grid for North East (NE) region.	33
3.2b	Model grid for North Central (NC) region.	34
3.2c	Model grid for North East (NE) region.	35
3.2d	Model grid for South West (SW) region.	36
3.2e	Model grid for South Central (SC) region.	37
3.2f	Model grid for South East (SE) region.	38
3.2g	Model grid for Eastern Hill (EH) region.	39
3.2h	Model grid for Bay of Bengal (BoB) region.	40
3.3	GEBCO bathymetry of Bay of Bengal used in the model.	41
3.4	WARPO DEM for Bangladesh used as model topography.	41

3.5	Water level data at two open boundary locations Colombo of Sri Lanka and Ko Taphao Noi of Thailand. Data are shown for March to May in 2020.	42
3.6	Calibration and validation locations of BDM.	43
3.7	Wind station locations maintained by BMD. Data from these stations are used during different phases of model calibration, validation, and application. Note that all wind stations are land-based stations.	44
3.8	Results of model calibration at different water level stations. Calibration results are supplemented by wind stick diagrams at nearest wind station to show the wind effects on resultant water levels.	46
3.9	Synthesis of calibration result at Kutubdia-1 station. From top to bottom (a) comparison between model and measured water level (b) 34 HLP (c) 34 HHP and (d) wind stick diagram at Cox's Bazar station.	47
3.10	Synthesis of calibration result at Kutubdia-2 station. From top to bottom (a) comparison between model and measured water level (b) 34 HLP (c) 34 HHP and (d) wind stick diagram at Cox's Bazar station.	48
3.11	Results of validation for BDM. To show the wind effects, the results also show wind stick diagram at Khepupara wind station of BMD.	50
4.1	Simulated (a) flood and (b) ebb tides in the Bay of Bengal.	53
4.2	Location of Swatch-of-no-ground in the Bay of Bengal.	54
4.3	Distribution of freshwater plume from the Lower Meghna estuary.	55
4.4	Vertical distribution of freshwater plume (a) cross section during dry season (b) cross section during monsoon (c) longitudinal section during dry season (d) longitudinal section during monsoon.	57
4.5	Comparison of cyclone wind field generated from Delft3D Dashboard, Holland's equation and CCMP data.	58
4.6	Cyclone wind speed (top), sea surface elevation (middle) and water level variation at Kutubdia-1 station during unnamed cyclone which made landfall on December 18, 1990.	60
4.7	Cyclone wind speed (top), sea surface elevation (middle) and water level variation at Kutubdia-1 station during 1991 Chittagong cyclone which made landfall on April 29, 1991.	61
4.8	Cyclone wind speed (top), sea surface elevation (middle) and water level variation at Kutubdia-1 station during unnamed cyclone which made landfall on June 2, 1991.	62
4.9	Cyclone wind speed (top), sea surface elevation (middle) and water level variation at Kutubdia-1 station during cyclone SIDR which made landfall on November 15, 2007.	63
4.10	Cyclone wind speed (top), sea surface elevation (middle) and water level variation at Kutubdia-1 station during cyclone RASHMI which made landfall on October 26, 2008.	64
4.11	Cyclone wind speed (top), sea surface elevation (middle) and water level variation at Kutubdia-1 station during cyclone BIJLI which made landfall on April 17, 2009.	65
4.12	Cyclone wind speed (top), sea surface elevation (middle) and water level variation at Kutubdia-1 station during cyclone AILA which made landfall on May 25, 2009.	66

4.13	Cyclone wind speed (top), sea surface elevation (middle) and water level variation at Kutubdia-1 station during cyclone MOHASEN which made landfall on May 16, 2013.	67
4.14	Cyclone wind speed (top), sea surface elevation (middle) and water level variation at Kutubdia-1 station during cyclone KOMEN which made landfall on July 30, 2015.	68
4.15	Cyclone wind speed (top), sea surface elevation (middle) and water level variation at Kutubdia-1 station during cyclone ROANU which made landfall on May 21, 2016.	69
4.16	Cyclone wind speed (top), sea surface elevation (middle) and water level variation at Kutubdia-1 station during cyclone MORA which made landfall on May 30, 2017.	70
4.17	Cyclone wind speed (top), sea surface elevation (middle) and water level variation at Kutubdia-1 station during cyclone AMPHAN which made landfall on May 20, 2020.	71
4.18	Cyclone effect on water velocity in the Bay of Bengal. The example shown here is for cyclone SIDR. The left figure shows the case without cyclone and the right figure shows the case with cyclone. The right figure is supplemented by a wind stick diagram at Khepupara wind station of BMD.	72
4.19	Flux along selected sections along the coast for three different hydrodynamic forcing: wind and tide, tide only and cyclone.	73
4.20	Variation of bed shear stress along the ocean and estuarine mouths during three different hydrodynamic forcing: tide, tide & wind, and cyclone.	73
4.21	Comparison of 1998 flood extent between model simulation (left) and satellite (right).	74
4.22	Flood depth maps for the (a) entire country (b) north-west region (c) north-central region (d) north-east region (e) south-west region (f) south-central region (g) south-east region and (h) eastern-hill region.	81
4.23	Inundation in the coast simulated from BDM (left image) and extracted from satellite image (right image).	82
4.24	Sediment movement path along the coast. The red color shows high sediment concentration, green and blue colors show relatively low sediment concentration.	83
4.25	Yearly erosion-sedimentation maps for the (a) entire country (b) north-west region (c) north-central region (d) north-east region (e) south-west region (f) Sundarban region (g) south-central region (h) south-east region (i) eastern-hill region and (j) Meghna estuary region.	91

List of Tables

Table No.	Title	Page No.
1.1	Incoming sediment load in the region.	15
1.2	Measured sedimentation by Rogers et al. (2013).	16
3.1	BDM integrated modeling framework.	30
3.2	Statistical indicators along with performance evaluation criteria that determines the model calibration and validation performance.	51

EXECUTIVE SUMMARY

The sedimentation in the coast is part of an integrated processes of flow and sediment transport from the inland river systems, erosion-deposition in the inland rivers and floodplain, transport of these sediments in the estuaries and coastal floodplains, discharge of sediments to the ocean, deposition of sediment in marine environment, transport of sediment with the oceanic processes and re-entry of part of these sediments into the estuarine systems. Any sediment management practice implemented in this system becomes an integral part of this complex system. So, to study effectiveness and impacts of any specific sediment management practice or combination of different practices – the entire system need be considered in an integrated way. The only way to make this integrated system is to construct a seamless model setup that will combine the entire system in a single modelling framework. Application of this integrated modelling framework is a research gap in this region. By considering these research gaps, the specific objectives of this research are set as:

1. To quantify the sediment loads that comes from upstream and its dispersion process in the south-west region.
2. To identify and analyze the present sediment management practices in the region.
3. To generate scenarios of sediment management strategy for uniform distribution of sediment which will divert sediments from sediment-excess region to sediment-starve region.
4. To prepare a sediment management manual that will highlight solution of water-logging problem in the region.

The entire coastal zone comprising the south-west region including part of the Bay of Bengal within the oceanic circulation zone is considered as the study area. It is seen that most of the lands in the study area lie within 5m contour line. The clockwise oceanic circulation driven by Coriolis force drives the sediments from Lower Meghna estuary towards the western estuarine systems. A total of 139 coastal polders in the region largely determine the pattern of coastal floodplain sedimentation. The lands inside these polders are considered as ‘protected’ and do not allow any sediments to be deposited on the floodplain.

[Rahman et al. \(2018\)](#) made an extensive study to determine total amount of sediment load coming into the region. The study compiled sediment load estimation from secondary literature and calculated the same data from 48 years (1960-2008) of measured sediment concentration by BWDB. Comparison of incoming sediment load in the region from three major rivers are shown in [Table 1](#). These ranges will be used during generation of scenarios of sediment management practices.

Table 1: Incoming sediment load in the region

River	Sediment load from secondary literature	Sediment load calculated by Rahman et al. (2018)
	Million Ton / year	Million Ton / year
Ganges	260 - 680	150 - 590
Brahmaputra	390 - 1160	135 - 615
Upper Meghna	6 - 12	N/A
Total	1000 - 2400	Average 500

The known sediment management practices in the region are (1) Dredging (2) Tidal River Management TRM (3) Cross dam

Dredging

Dredging is the most common sediment management practice in the south-west region. The impact of dredging of Hari river is studied by [WARPO and BUET \(2019\)](#) and the result show that sedimentation in the main river indeed increases the water-logging. Dredging in the main river improves the water-logging condition in the area which are within the drainage zone of the river. Outside the drainage zone, dredging impact is not visible. Except being unusually expensive, sustainability of dredging is questionable when long-term morphological time scale is considered.

TRM

To solve the long-standing problems of water-logging in the region, the Khulna-Jessore drainage rehabilitation project known as KJDRP was implemented during 1994-2002. Later, a popular concept based on generations of indigenous water management practices, formally known as Tidal River Management (TRM), was adopted. TRM allows natural movement of sediment with tidal water into a beel which is called tidal basin and allows deposition of sediment in the beel. The benefits of TRM concept was assessed by [Al Masud et. al. \(2018\)](#) by satellite data analysis and noticed that the TRM concept have reduced water-logging up to 4243 ha of land on August, 2011 compared to 2006 in Hari-Teka and Bhadra basins. Hence, the total agricultural land was increased by 3005 ha of land in 2011 (during TRM operation) as compared to 2006. The vegetation was also improved by 2851 ha of land in the floodplain.

Although TRM is a process-based sediment management practice but its impact is dominantly local. Moreover, the implementation process of TRM creates social conflict as during TRM a certain part of the area (including the beel area) become water-logged for a long time. [Amir et al. \(2013\)](#) suggested an ‘embankment option’ coupled with TRM which will allow construction of embankment along both banks of the main channel and then cutting the embankment sequentially from upstream to downstream to ensure gradual sedimentation of beels. A geo-spatial analysis by [Hussain et al. \(2018\)](#) denoted that during TRM implementation in Pakhimara Beel at Tala upazila

of Satkhira district, about 5090 acres of agricultural land and about 729 acres of homestead land was water-logged.

Cross-dam is another well-known sediment management practice which is used for land reclamation in off-shore region (EDP, 2007). BWDB proposed 18 probable cross dam locations in the coast. Impact of these cross-dams on local or overall sedimentation in the region has not yet been studied.

This study is based on application of numerical model. The numerical model used in this study is Delft3D. Three modules of Delft3D modeling suite (Deltares, 2014) are applied in the present study. These are (a) hydrodynamic model (b) morphology model and (c) storm surge model. The Delft3D has a long track records of using in different environments, such as, oceans, coastal oceans, estuarine and river systems all over the world (Thanh et al., 2019; Sandbach et al., 2018; Hu et al., 2018; Salehi, 2018; Li et al. 2018; Bennett et al., 2018; Al Azad et al., 2018). This model has been used in many applications in Bangladesh as well (Haque, et al., 2016, for hydrodynamic model, WARPO and BUET, 2019, for morphology model, Akter et al., 2019 for salinity model and Al Azad et al., 2018 and Haque et al., 2018 for storm surge model).

Based on Delft3D, a new modelling framework named Bangladesh Delta Model (BDM) is developed in this study. BDM modeling framework integrates the entire processes of ocean, coast, Sundarban, polders, canal network, estuaries, inland rivers of different scales, embankments, wetlands, beels and haors. The model domain is extended southward to the Bay of Bengal down to Sri Lanka & Thailand coast and northward to the inflow points of all 54 transboundary rivers. To capture these complicated network and processes in different scales – we have divided BDM into three categories in terms of grid resolution. These are: low resolution (BDM-L), medium resolution (BDM-M) and high resolution (BDM-H). The main reason of these divisions is to optimize the computational resources based on the objective of model application. The three categories of BDM are briefly summarized in Table 2.

Table 2: BDM integrated modeling framework

Model Name	Resolution	Description	Application
BDM-L	Grid resolution coarse. 40-layer model.	Captures BoB, Islands & Chars, All Major, Intermediate and Minor river/estuarine systems, Polders.	Macro level study. Can be applied to resolve ocean processes, coastal and inland flooding, storm surge.
BDM-M	Grid resolution medium. 40-layer model.	Captures BoB, Islands & Chars, All Major, Intermediate and Minor river/estuarine systems, Polders, Inland	Micro level study. Application in addition to BDM-L : flooding inside polders, major river processes, river and floodplain sedimentation, salinity intrusion.

		embankments, Road networks, Few canals inside polders.	
BDM-H	Grid resolution high. 40-layer model.	Captures BoB, Islands & Chars, All Major, Intermediate and Minor river systems, Polders, Inland embankments, Road networks, Small canals inside polders, Haor and Beel systems.	Micro level study. Application in addition to BDM-M : impacts of canal and road networks inside polders, beel and haor processes.
Model output for all model resolutions are: water level, water depth, velocity, discharge, salinity concentration, temperature, cyclone wind speed, surge depth, surge velocity, sediment concentration, sedimentation & erosion thickness and sedimentation volume in river-beds & floodplains and bank erosion.			

Model Grid

Relatively coarser grids are used in the ocean (12km x 35km) compared to the coast (200m x 300m). As the tidal wave scale in the Bay of Bengal is several hundred kilometers, we do not need fine grid in the ocean part. Instead, the high-resolution model can capture a canal of width 5m or in few places, even less. The bathymetry of the Bay of Bengal is adopted from the global source of 2019 General Bathymetric Chart of the Ocean (GEBCO) data (<https://www.gebco.net/>).

Model Bathymetry and Topography

The bathymetry of the Bay of Bengal is adopted from the global source of 2019 General Bathymetric Chart of the Ocean (GEBCO) data (<https://www.gebco.net/>). For model topography, the DEM available at WARPO for the entire Bangladesh is used. For bathymetry of rivers and estuaries, measured data from various secondary sources are used.

Boundary Conditions

Two types of boundaries are used in the model. Open boundary at the southern end of the model domain where temporal variation of water level is imposed and river flow input at the northern end of the model domain. Western coast of the open boundary is Sri Lanka and eastern coast is Thailand. These southern boundary locations are selected to encompass the genesis of cyclones in the Bay of Bengal. For river boundaries, inflows of rivers from all the inlets are provided. These include discharges from all major rivers and all transboundary river flows. For Sri Lanka coast, times series of water level is provided at water level station Colombo and for Thailand coast, time

series of water level is provided at water level station Ko Taphao Noi. The time series data of these water levels are collected from global source (<https://uhslc.soest.hawaii.edu/>).

Model Calibration and Validation

Model is calibrated against measured water level data at five water level station during the period from May 19 to June 21, 2017. Sources of these data are BIWTA and Bangladesh Navy. During calibration and validation, wind fields are generated in the model domain by using measured wind data of BDM.

In general, the model simulation slightly overestimates and underestimates the measured water level based on different periods of simulation. The reason of this discrepancies can be explained with the help of 34 HLP and wind stick diagram. The 34 HLP plots represents water level variations which have a period greater than 34 hours which means there are no tides in these plots. Therefore, these plots represent residuals in the water levels where tides are filtered out. Underestimation and overestimation of water levels of the model compared to the measurements are associated with the underestimation and overestimation of residuals. Residuals in these applications are largely dominated by wind stresses exerted on the water surface. The winds in these calibration simulations are represented by the wind data at the Cox's Bazar station. All the wind station data that can be used in the model are land-based stations. The wind stress on the sea surface is due to the winds blowing over the ocean. Therefore, the discrepancies between the model water levels and measured water levels are mainly due to inappropriate representation of winds in the model. This is further stressed in the 34 HHP plots. 34 HHP plots represent water levels which have a period less than 34 hours and are mainly represented by the dominant tides in the area. The model performs far better when only tides are considered. Therefore, it is expected that the model calibration against observed water level can be significantly improved if the buoy based observed wind in the Bay of Bengal are used in the modeling framework, rather than the land based wind data. In the subsequent application of the model, wind fields will be provided by using wind data from global source, for example data from Cross-Calibrated-Multi-Platform (CCMP) <https://climatedataguide.ucar.edu/climate-data/ccmp-cross-calibrated-multi-platform-wind-vector-analysis>.

Model validation is made at two water level stations. Validation time is selected as May 5 to June 4, 2009. It is noted here that cyclone Aila made landfall in the Indian Sundarban coast on May 25, 2009. The wind stick diagram at Khepupara captured the cyclone signal correctly. But the model results show underprediction in both the stations during the cyclone landfall time. The reason of this underprediction is the absence of synoptic wind fields in the model which is explained before. Application of synoptic wind fields from CCMP data will certainly improve the model result. CCMP data also captures the cyclone signals.

Model calibration and validation performance is quantified through several statistical indicators. Statistical indicators determining the model calibration and validation performance is shown in Table 3. Evaluating different statistical indicators, overall model performance during calibration is found as ‘Very Good’. For validation, results are mixed. For Rangadia station, model evaluation is ‘Very Good’. But for Hiron Point station, model evaluation is ‘Unsatisfactory’. As mentioned before, model could not capture the impact of cyclone Aila properly due to absence of synoptic wind field in the model domain. Only cyclone wind cannot solve the problem. This will be resolved in subsequent application of the model.

Table 3: Statistical indicators along with performance evaluation criteria that determines the model calibration and validation performance.

Model Calibration							Model Validation						
Station	Statistical Indicators					Calibration Performance	Station	Statistical Indicators					Validation Performance
	RMSE	MAE	NSE	RSR	R ²			RMSE	MAE	NSE	RSR	R ²	
Kutubdia 1	0.53	0.42	0.80 (VG)	0.45(VG)	0.82 (VG)	Very Good	Rangadia	0.67	0.56	0.77 (VG)	0.49 (VG)	0.78 (G)	Very Good
Kutubdia 2	0.43	0.34	0.85 (VG)	0.38 (VG)	0.87 (VG)	Very Good							
Rangadia	0.67	0.57	0.77 (VG)	0.48 (VG)	0.79 (G)	Very Good							
Hiron Point	0.35	0.29	0.85 (VG)	0.39 (VG)	0.91 (VG)	Very Good	Hiron Point	0.71	0.55	0.35 (U)	0.81 (U)	0.66 (S)	Unsatisfactory (Poor)
Khepupara	0.59	0.51	0.60 (S)	0.63 (S)	0.63 (S)	Satisfactory (Fair)							
Qualitative Evaluation of Statistical Indicators													
Statistics	Very Good		Good		Satisfactory (Fair)		Unsatisfactory (Poor)		Reference				
R ²	0.80 < R ² ≤ 1		0.70 < R ² ≤ 0.80		0.60 < R ² ≤ 0.70		R ² ≤ 0.60		(Duda et al. 2012)				
NSE	0.75 < NSE ≤ 1.00		0.65 < NSE ≤ 0.75		0.50 < NSE ≤ 0.65		NSE ≤ 0.50		(Moriassi et al. 2007)				
RSR	0.00 ≤ RSR ≤ 0.50		0.50 < RSR ≤ 0.60		0.60 < RSR ≤ 0.70		RSR > 0.70		(Moriassi et al. 2007)				

Calibrated and validated model is applied to generate different scenarios and to understand various processes related to sediment management issues in this region. Some preliminary findings from model simulations are:

Tide propagation in the Bay of Bengal

Tides arrive almost at the same time along the coast. Flood tide slows down along the Lower Meghna estuary due to the impact of freshwater. Relatively higher velocity along the mouth of the estuaries of the western coast during the flood tide causes ocean sediments to enter inside the western estuarine systems. Sources of these ocean sediments are Lower Meghna estuary which propagates along the continental shelf during the ebb tide and later re-enter into the system during the flood tide. Just at the beginning of the ebb tide in the ocean, there is a flow disaggregation line

and a zone of stagnation occurs. This zone has significant impact on the sedimentation all along the estuary mouths. The Swatch-of-no-ground acts like a fast flowing channel and divides the entire oceanic circulation into two distinct patterns – eastern circulation and western circulation. Eastern circulation is dominated by the Lower Meghna flow and the western circulation is dominated by the western estuarine systems and flows from the West Bengal coast. Due to this fast-moving flow separation line, it appears that the sediments from the Lower Meghna system may not be able to deposit in the Swatch-of-no-ground – which is a popular hypothesis these days.

Distribution of freshwater plume

The freshwater plume is concentrated along the continental shelf. If we take freshwater plume as a proxy of sediment-laden water, the sediments from the Lower Meghna estuary is mainly distributed along the continental shelf. There is hardly any freshwater plume goes into the deep ocean. This means that sediment concentration in the deep ocean is low. This also shows that assumption of a low sediment concentration in the deep ocean is valid (WARPO and BUET, 2019). Freshwater plume from Lower Meghna propagates a long distance up to the coast of Thailand. This simulation does not consider all the freshwater sources from India, Sri Lanka, Myanmar, and Thailand.

Vertical stratification

The vertical distribution inside *swatch of no ground* shows that the entire canyon is filled with denser fluid both in dry season and in monsoon. This means there is no vertical infiltration of freshwater inside the canyon even during the monsoon. The sediments are mainly carried in suspension by freshwater from the estuarine system. This sediment laden freshwater cannot enter inside the canyon, rather it is distributed within the first 50m zone from MSL. This shows that the popular belief of “*all the sediments in the system ultimately deposits in the swatch of no ground*” is not true. If vertical profile of freshwater plume is taken as a proxy of density stratification, it is seen that stratification exists along the east coast throughout the year. Longitudinal section along the coast shows dominant influence of Meghna flow in vertical flow structure particularly during the monsoon.

Effect of cyclone wind on tidal current

Cyclonic wind suddenly increases the flood flow velocity (hydrodynamic shock). As sediment flux is related to water velocity, increased water velocity creates increased sediment flux for the same sediment concentration. So, for a similar sediment regime, cyclonic event creates increased sediment flux. This will drive increased volume of sediments to re-enter into the estuarine systems through increased flood flow velocity created by cyclone. This proves that the general belief of impact of cyclones on increased sediment flow into the system is correct.

Flooding in Bangladesh

Flooding is observed in the north-eastern haor systems in the Sylhet region and the central part of the country by Brahmaputra-Jamuna system. In the coastal region, fluvial flooding is observed in the central part of unprotected region. During cyclone (SIDR in this example), there is no land inundation inside polders. Inundation is observed only in unprotected regions.

River, estuary, and floodplain sedimentation in Bangladesh

The sediments from the Ganges-Brahmaputra-Meghna systems discharges into the Bay of Bengal through the Lower Meghna mouth, turn clockwise, part of the sediments deposit in the ocean and the rest of the sediments re-enter into the western estuarine systems. During cyclonic events, this equilibrium breaks down and bulk amount of sediments re-enters into the system through the estuary mouths. Sedimentation, as expected, is the maximum in the unprotected regions of the coast. No sedimentation is observed inside polders. Among the rivers and estuaries, maximum sedimentation is observed in the Sundarban system. In Meghna estuary region, a distinct sedimentation is observed in the region between Sandwip and Urir char which will eventually join these two land forms. Sedimentation is also observed in the Pyra port region in the mouth of Tetulia river, in the Kutubdia channel and in the Moheshkhali channel.

CHAPTER ONE

Introduction

1.1 Background

In the south-west region of Bangladesh (which is also part of the coastal zone), the main sources of sediments are mainly from Lower Meghna estuary. Due to clockwise oceanic circulation, major part of these sediments re-enter into the south-west region through the mouths of large number of estuaries (Haque et al., 2016). From a gross estimate, Goodbred and Kuehl (2000) assumed that one-third of in-coming sediments might have been deposited on the floodplain. In a later study, it was found that about 23% to 47% of in-coming sediments are deposited on the floodplain (WARPO and BUET, 2019). The same study reveals the fact that sedimentation in the coastal floodplain is spatially variable. In addition, sedimentation in this region is largely impacted by anthropogenic and climatic interventions (WARPO and BUET, 2019). Due to spatial variability of sedimentation and impacts due to intervention, sediment management in the region is particularly complicated. Most of the estuaries and rivers in the western part lost their conveyance due to sedimentation causing large scale water-logging (WARPO and BUET, 2018). On the other hand, sediment is a primary ingredient for land reclamation in the off-shore region. So, there are regions which can be termed as sediment-excess region (mainly rivers and estuaries) and there are regions which can be termed as ‘sediment-starve’ region (mainly off-shore region). One of the widely known sediment management practice in the region is Tidal River Management (TRM). TRM is a process-based sediment management practice but its impact is dominantly local. Moreover, the implementation process of TRM creates social conflict. Other known sediment management practice in the region is dredging. Except being unusually expensive, sustainability of dredging is questionable when long-term morphological time scale is considered. Cross-dam is another well-known sediment management practice which is used for land reclamation in off-shore region. But study on system impact of cross-dam is still lacking. Controlled flooding is a much-talked sediment management option which is thought to be an alternative to TRM.

The sedimentation in the coast is part of an integrated processes of flow and sediment transport from the inland river systems, erosion-deposition in the inland rivers and floodplain, transport of these sediments in the estuaries and coastal floodplains, discharge of sediments to the ocean, deposition of sediment in marine environment, transport of sediment with the oceanic processes and re-entry of part of these sediments into the estuarine systems. Any sediment management practice implemented in this system becomes an integral part of this complex system. So, to study effectiveness and impacts of any specific sediment management practice or combination of different practices – the entire system need be considered in an integrated way. The only way to make this integrated system is to construct a seamless model setup that will combine the entire system in a single modelling framework. Application of this integrated modelling framework is a research gap in this region.

1.2 Objectives of the Study

By considering the research gaps mentioned above, the specific objectives of this research are set as:

1. To quantify the sediment loads that comes from upstream and its dispersion process in the south-west region.
2. To identify and analyze the present sediment management practices in the region.
3. To generate scenarios of sediment management strategy for uniform distribution of sediment which will divert sediments from sediment-excess region to sediment-starve region.
4. To prepare a sediment management manual that will highlight solution of water-logging problem in the region.

1.3 Previous Studies

Incoming sediment load in the region

Rahman et al. (2018) made an extensive study to determine total amount of sediment load coming into the region. The study compiled sediment load estimation from secondary literature and calculated the same data from 48 years (1960-2008) of measured sediment concentration by BWDB. Comparison of incoming sediment load in the region from three major rivers are shown in Table 1.1. These ranges will be used during generation of scenarios of sediment management practices.

Table 1.1: Incoming sediment load in the region

River	Sediment load from secondary literature Million Ton / year	Sediment load calculated by Rahman et al. (2018) Million Ton / year
Ganges	260 - 680	150 - 590
Brahmaputra	390 - 1160	135 - 615
Upper Meghna	6 - 12	N/A
Total	1000 - 2400	Average 500

Sedimentation in coastal floodplain

Secondary data related to sedimentation in the coastal floodplain is limited. Rogers et al. (2013) measured sedimentation in the Sundarbans region from March 2008 to October 2008. Later they converted these 8 months data into sedimentation/year. Measurement locations of Rogers et al. (2013) is shown in Figure 1.1 and sedimentation magnitude is shown in Table 1.2.

Table 1.2: Measured sedimentation by Rogers et al. (2013)

Location	Location-1	Location-2	Location-3	Location-4
Sedimentation thickness (cm)	0.92	0.93	1.12	0.96



Figure 1.1: Measurement locations by Rogers et al. (2013).

All the measurement locations are within the Sundarban region which is part of the western system. Sedimentation thickness in the region varies between 0.92 cm – 1.12 cm. There are no polders in Sundarban region but resistance to flow is relatively high. By considering these two contradictory situations, sedimentation in the poldered region is likely to be in similar magnitude. In another study, it was shown that water-logging inside polders 24 and 25 is affected by sedimentation outside the poldered region (WARPO and BUET, 2019).

Land reclamation in off-shore region

Land reclamation in off-shore region is largely dictated by availability of sediments. Intervention like cross-dam (which can be considered as a specific sediment management option to reclaim land) sometimes accelerate the process, but effectiveness of cross-dam depends on sediment availability. A particular example can be shown where a cross-dam is constructed by BWDB in between char Islam and char Montaz. Cross-dam in this location is built sometime in 2010. Impact of cross-dam in this region is shown in Figure 1.2 (in year 1984 which is almost 16 years before construction of the cross-dam) and in Figure 1.3 (in year 2018 which is almost 8 years after construction of the cross-dam). The reclaimed lands are shown in Figure 1.2 by green, red, blue and yellow circles whereas, the lost land located in the south of char Kukri Mukri is shown by white circle. This example clearly shows system response when a specific sediment management option is implemented.



Figure 1.2: Land status and cross-dam location almost 16 years before the construction of the cross-dam. Cross-dam is constructed just west of red-circled zone during the year 2010.

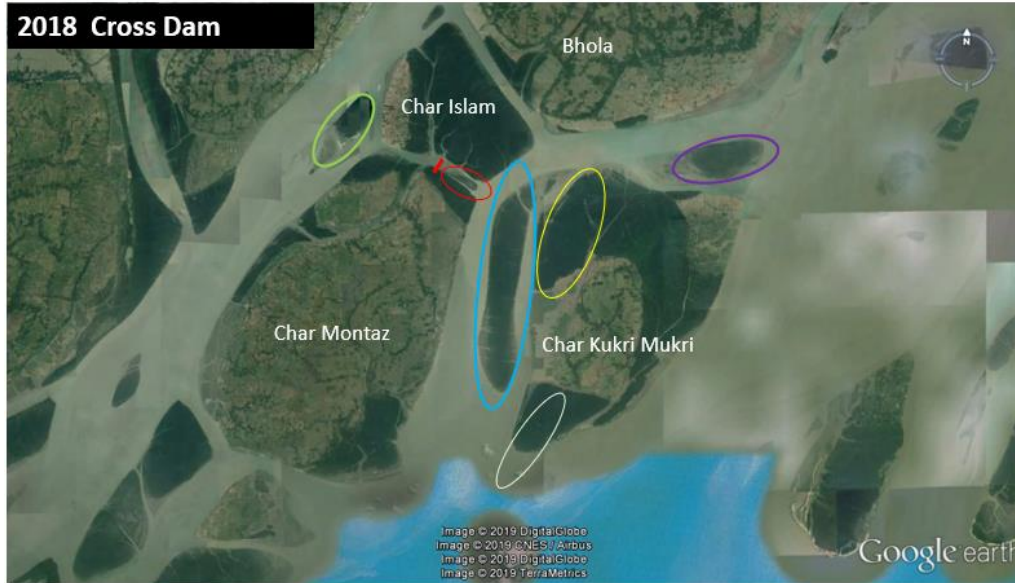


Figure 1.3: Reclaimed and eroded lands as a system response almost after 8 years due to construction of cross-dam. The green, red, blue and yellow circles show reclaimed land. The white circle south of char Kukri Mukri show the lost land. The cross dam is shown by red line in between Char Islam and Char Montaz.

1.4 Organization of the Report

After introduction (Chapter-1), chapter-2 describes the study area in detail. Chapter-3 introduces the integrated modelling framework – the Bangladesh Delta Model (BDM). In chapter-3, in addition to model domain, detail description is given about the input data, model boundary conditions, calibration and validation of the model. Chapter-4 is the result chapter describing results of different model application. This includes simulation results of tides in the Bay of Bengal, storm surge in the Bay of Bengal, different types floods in Bangladesh and sedimentations in both inland and costal floodplains all over Bangladesh. Chapter-5 summarizes the results and highlights the main findings.

CHAPTER TWO

Study Area

2.1 Introduction

The entire coastal zone comprising the south-west region including part of the Bay of Bengal within the oceanic circulation zone is considered as the study area (Figure 2.1 and Figure 2.2). It is seen that most of the lands in the study area lie within 5m contour line (Figure 2.1). The clockwise oceanic circulation driven by Coriolis force drives the sediments from Lower Meghna estuary towards the western estuarine systems (Figure 2.2). A total of 139 coastal polders in the region largely determine the pattern of coastal floodplain sedimentation. The lands inside these polders are considered as ‘protected’ and do not allow any sediments to be deposited on the floodplain (Figure 2.3).

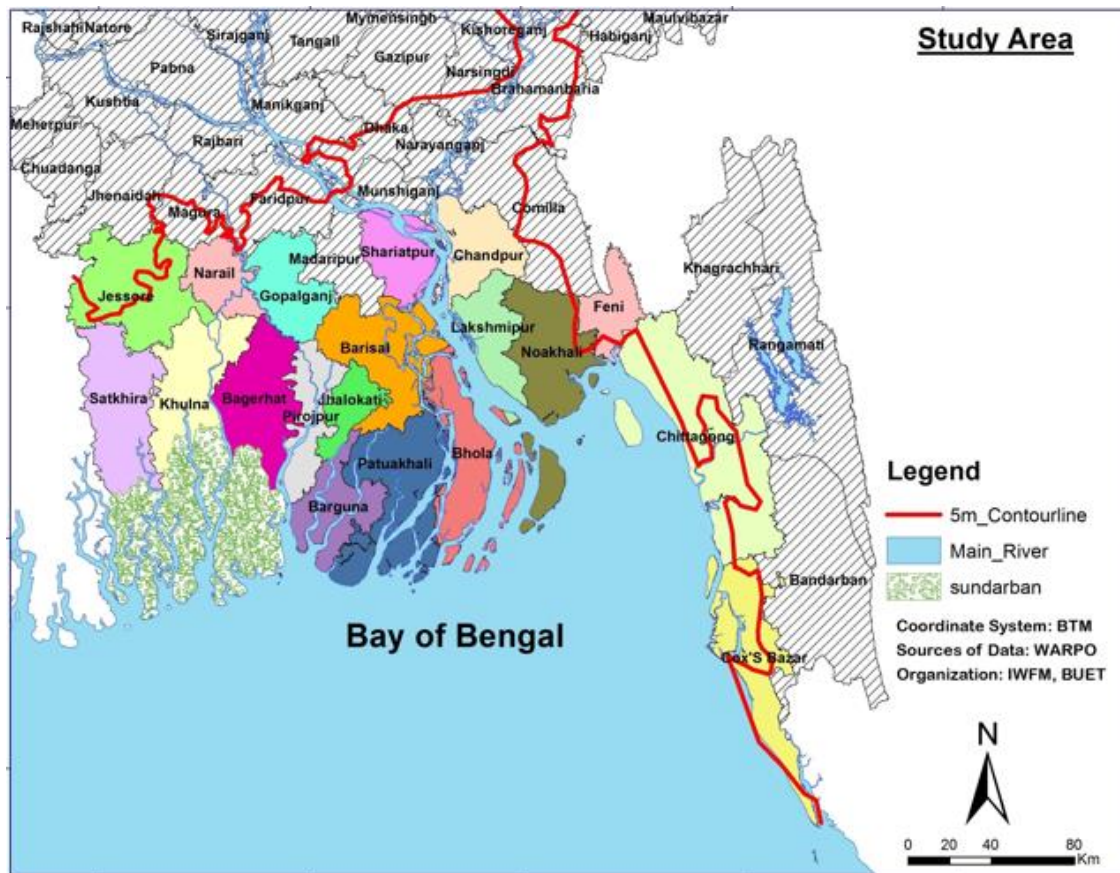


Figure 2.1: Study Area.



Figure 2.2: Oceanic circulation zone.

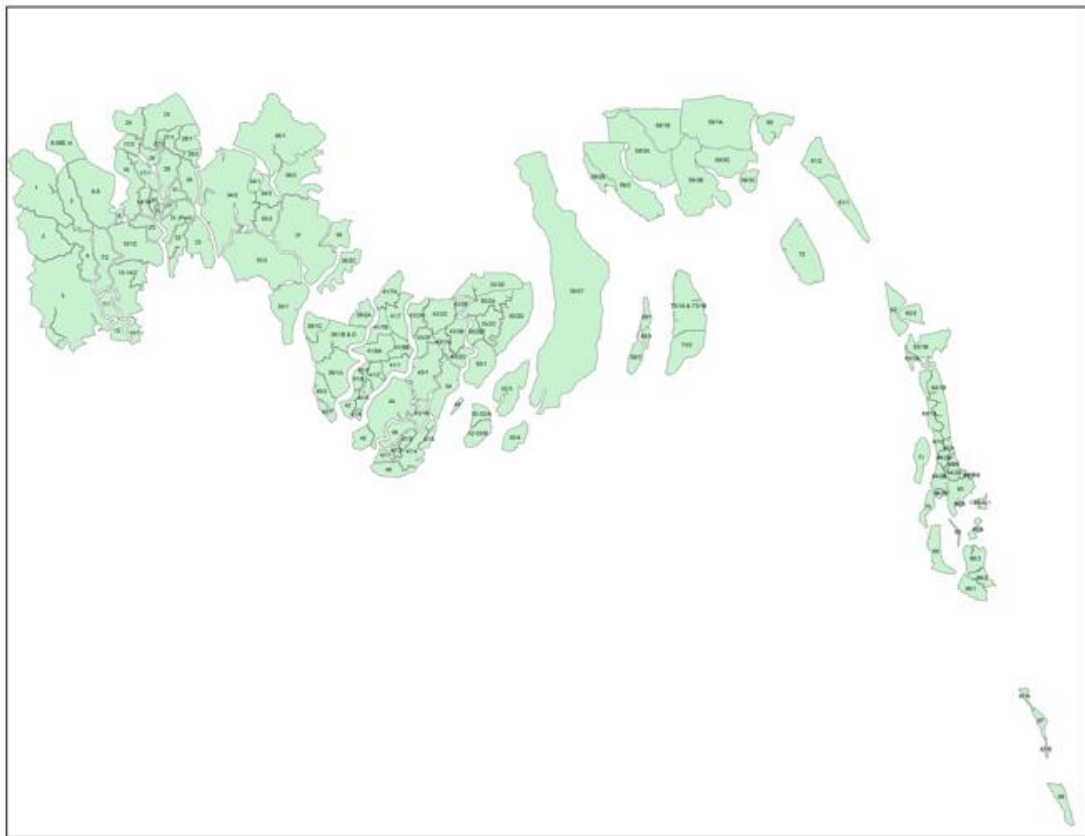


Figure 2.3: Protected land inside polders in the study area.

2.2 Estuarine Systems

As shown in [Figure 2.4](#), the discharges coming from the Ganges, Brahmaputra and Upper Meghna rivers drain through the complicated estuarine networks in the south west region of Bangladesh. The combined flows of Ganges and Brahmaputra rivers comes through the Padma river and after joining with Upper Meghna, the bulk of the combined flow discharges through the Lower Meghna estuary. The estuarine systems receive the freshwater flow from the above rivers, mix with saline water due to large tidal prism and eventually discharge into the Bay of Bengal. The eastern part of these estuarine systems is known as Eastern Estuarine System (EES), the central part is known as Central Estuarine Systems (CES) and the western part is known as the Western Estuarine System (WES). These EES, CES and WES are connected through several cross channels. The Ganges, before joining with the Brahmaputra, bifurcates as the Gorai, which is the main flow-carrying channel for the WES. In the same way, the Padma, before joining with the Upper Meghna, bifurcates as the Arial Khan river and acts as a major source of freshwater for the CES. The CES also receives water from the EES through three small spill channels. The Beel Route, a man-made canal excavated from the Arial Khan ([Rahman et al., 2014](#)), is also a major source of freshwater from the EES to the CES. Freshwater sources for the WES where the ecologically important Sundarban mangrove forest ([Rahman, 2014](#)) is located are much less. The only visible source of freshwater for the WES is the bifurcated branch of the Gorai. The Gorai itself is almost dying due to shortage of flow from the Ganges ([Islam and Gnauck, 2011](#); [Mirza, 1998](#); [Bharati, 2011](#)). The other bifurcated branch of the Gorai, named the Madhumati, is acting as a freshwater source for the CES. The other small channels of WES have lost their roles as freshwater source. Among the other estuaries, the Tetulia and Lohalia are the parts of the EES, the Bishkhali, Baleshwar and Burishwar constitute the CES and all other estuaries of the Sundarban system including the Rupsha and Pashur systems are parts of WES. Existing cross channels that connect these estuarine systems are three spill channels of Lower Meghna, Beel Route, Ghashiakhali channel and the Madhumati channel. The roles of these cross channels are vital for facilitating the exchange of flow and sediments from EES to WES. The WES receives a very small amount of freshwater flow from Gorai. On the other hand, the EES receives large amounts of fresh water from the Lower Meghna and supplies some of this to the CES through the spill channels. As there is a very small number of cross channels that connect the WES to the rest of the systems, there is a large difference of water storage among the different parts of the estuarine systems, especially between CES and WES.

The dynamics of these estuarine systems are controlled by the freshwater entering through the Gorai, Arial Khan and Lower Meghna inlets and the seawater entering through the mouths of the estuaries of EES, CES and WES. The large freshwater input and the saline water intrusion due to strong tidal force make these estuarine systems suitable for the existence of diverse ecosystem resources. In addition to the tidal force, there are seasonal variations of freshwater flows in different flooding scenarios resulting variation of water storage and its distribution among the different parts of these estuarine systems ([Haque et al., 2016](#)). The variations of the hydrodynamic

conditions cause different combinations of water balances that ultimately leads to spatial and temporal movement of the sediments within the estuarine systems (Sumaiya et al., 2015; Dasgupta et al., 2014).

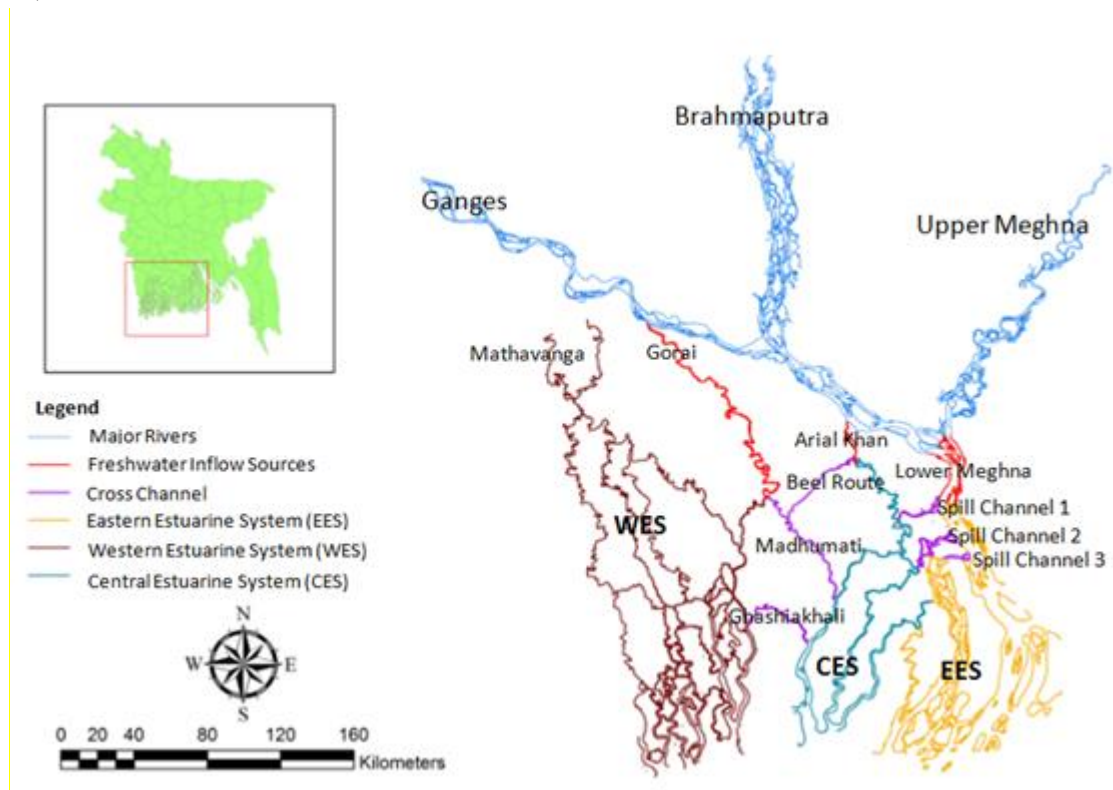


Figure 2.4: Estuarine systems of coastal zone.

2.3 Sediment Regime

The Meghna Estuary (outlet of the Ganges-Brahmaputra-Meghna (GBM) delta) (see Figure 2.5) of Bangladesh discharges the combined flow of three major river systems of the world: the Ganges, Brahmaputra, and Meghna (Hussain et al., 2014). Sediment discharge through the Meghna Estuary is the highest (Coleman, 1969) and water discharge is the third highest in the world, only after Amazon and Congo Rivers (Milliman, 1991). Rahman et al. (2018), made an extensive study to determine total amount of sediment load coming into the region. The study shows that total incoming sediments through the Ganges-Brahmaputra-Upper Meghna systems is around 500 Million Ton/year. This value is less than half the values of incoming sediments mentioned in all other earlier studies. In an earlier study (WARPO, 2016), it was found that total incoming sediments to the system is around 1050 Million Ton/year which is more the double the values calculated by Rahman et al. (2018). All these results show degrees of uncertainty still prevailing on the estimate of actual value of incoming sediments to the region. These sediments ultimately transport to the ocean mainly through the Lower Meghna estuary. The clockwise oceanic circulation of these sediments from the Lower Meghna estuary cause re-entry of sediments through the mouths of large number of western estuaries in the south-west region (Haque et al., 2016).

Goodbred and Kuehl (2000) mentioned that one third of the sediment carried by the rivers is deposited on the floodplain and tidal plain. High sediment load and several natural and anthropogenic interventions (for example climatic impacts, Farakka barrage and polderization) cause silted up of the estuaries in the south-west region.

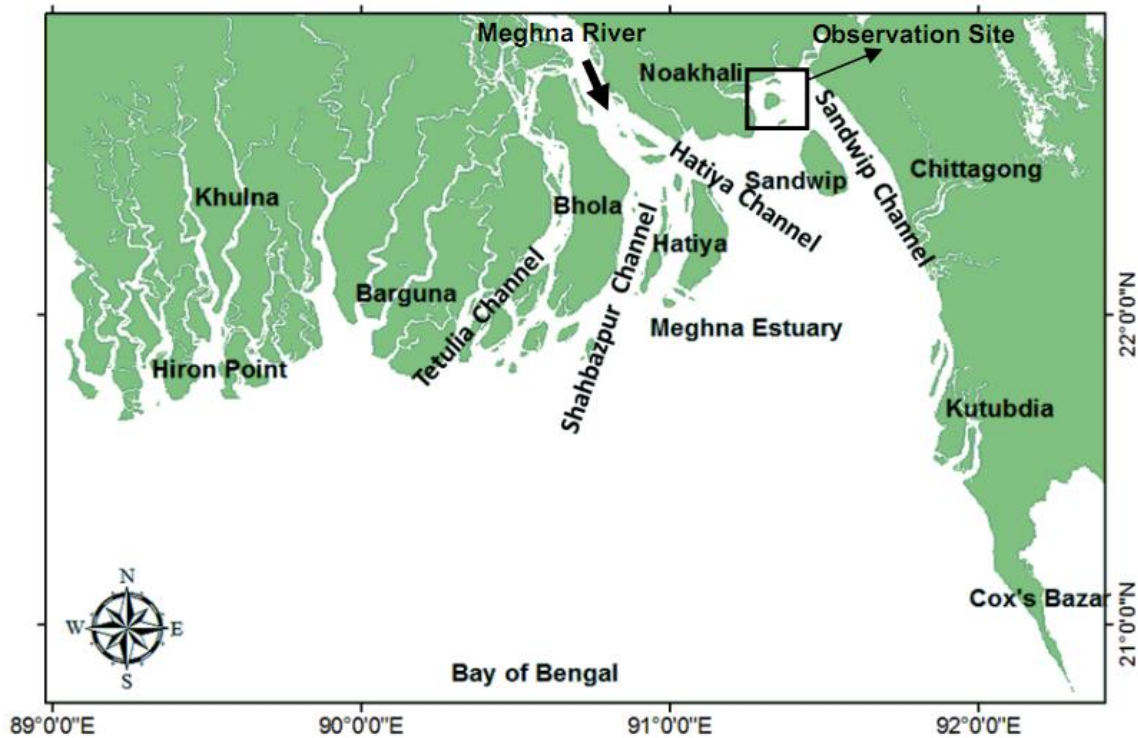


Figure 2.5: Outlet of the Ganges-Brahmaputra-Meghna (GBM) delta (Source Hussain et al., 2014).

The sedimentation problem in this region is aggravated by the construction of costal polders during the 1960s that de-linked the floodplains from the peripheral rivers. In a model simulation, WARPO and BUET (2019) shows that if polders were not present, sedimentation would happen inside the protected region of polders and would have increased the floodplain sedimentation area (see Figure 2.6). Therefore, water-logging inside polders are believed to be caused by this ‘un-managed’ sediments, although there are other factors, for example inadequate drainage routes inside polders (Tahsin et al., 2019).

With a different vision, importance of drainage route is reported in an earlier study (BWDB, 2013) where it is mentioned about the possibility of re-arranging the drainage network inside a polder. The re-arrangement of the drainage network will allow flushing of sediments from the sedimented region of smaller canals to the larger peripheral river systems. But the study did not show any specific impact of their concept. They just mentioned that further study is required to test the effectiveness of this concept.

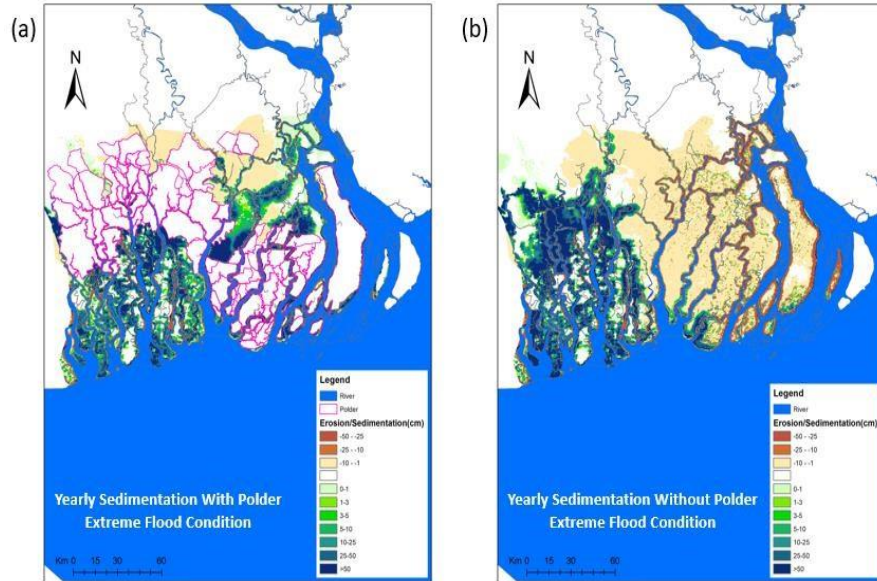


Figure 2.6: Yearly sedimentation during an extreme flood condition in the coastal zone for (a) with polder and (b) without polder condition (source: [WARPO and BUET, 2019](#)).

As mentioned in previous chapter, the clockwise oceanic circulation pattern has a significant impact on sediment distribution process in the region. This clockwise oceanic circulation patterns driven by Coriolis force, ocean current and Lower Meghna discharge is numerical simulated by applying Bangladesh Coastal Model ([WARPO and BUET, 2019](#)). The numerical model simulations are made for an average flood hydrological year covering both the dry season and monsoon. The results are shown in [Figure 2.7](#) for the dry season and in [Figure 2.8](#) for the monsoon. The results clearly show the clockwise oceanic circulation pattern makes sediments to re-enter from the ocean to the estuarine systems.

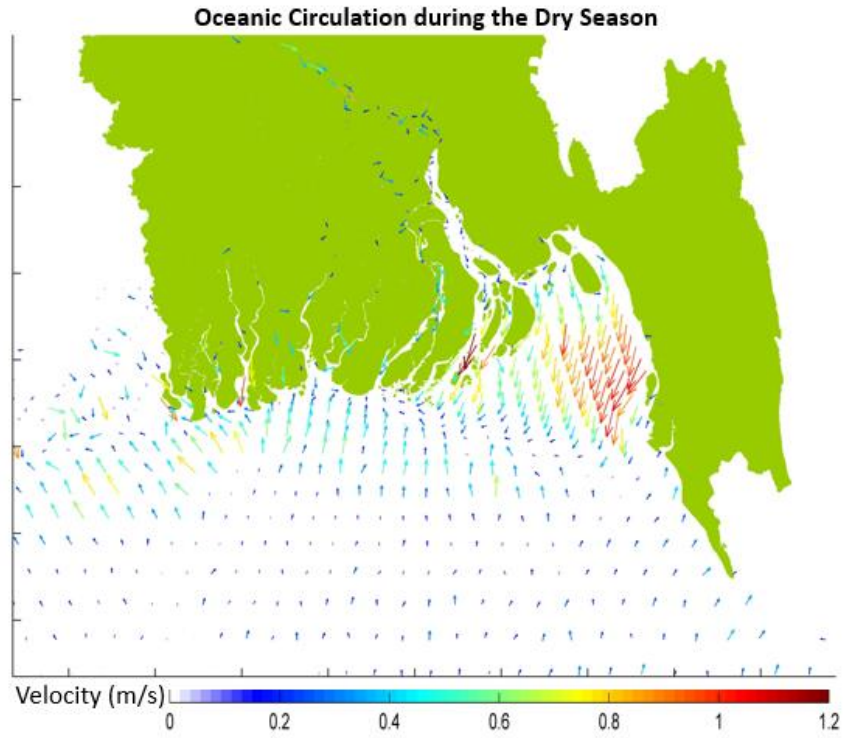


Figure 2.7: Model simulated oceanic circulation during the dry season.

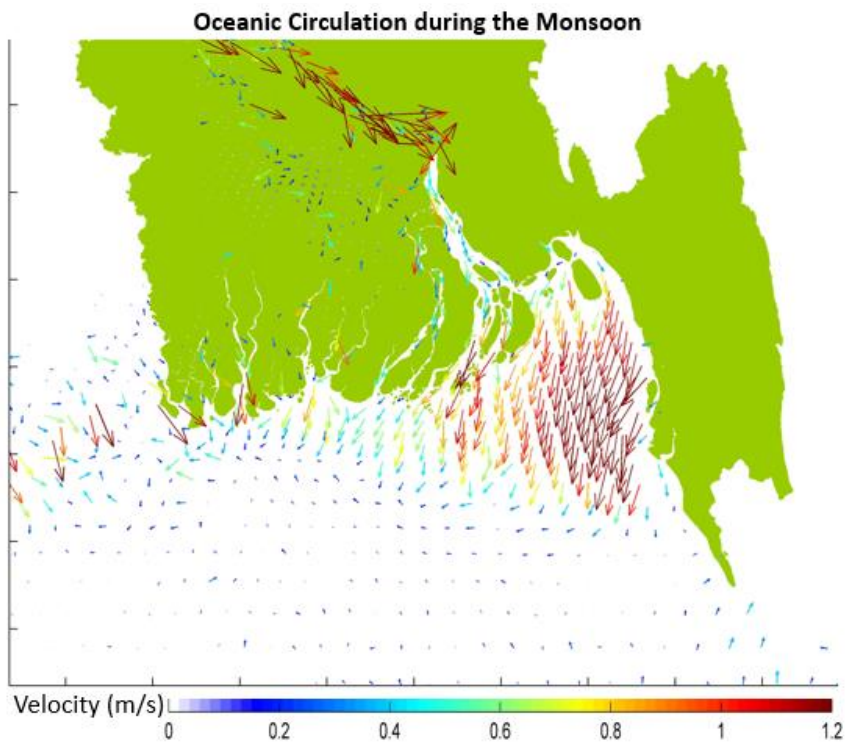


Figure 2.8: Model simulated oceanic circulation during the monsoon.

Numerical model simulation is also made to assess the resultant sedimentation and erosion throughout a hydrological year along the Meghna estuary region (Figure 2.9). Results show very little sedimentation in the oceanic part. Sedimentation is mainly observed in the southern part of Rangabali and Char Muntaj. Sedimentation is also observed at the mouth of Shabazpur channel where new chars are emerging (Figure 2.9). Several cross-dam projects are suggested in the area close to Char Muntaj and Char Kukri Mukri (EDP, 2007). The impact of these proposed cross-dams on overall sediment budget will be described in the final report of the project.

Resultant Sedimentation and Erosion during a Hydrological Year

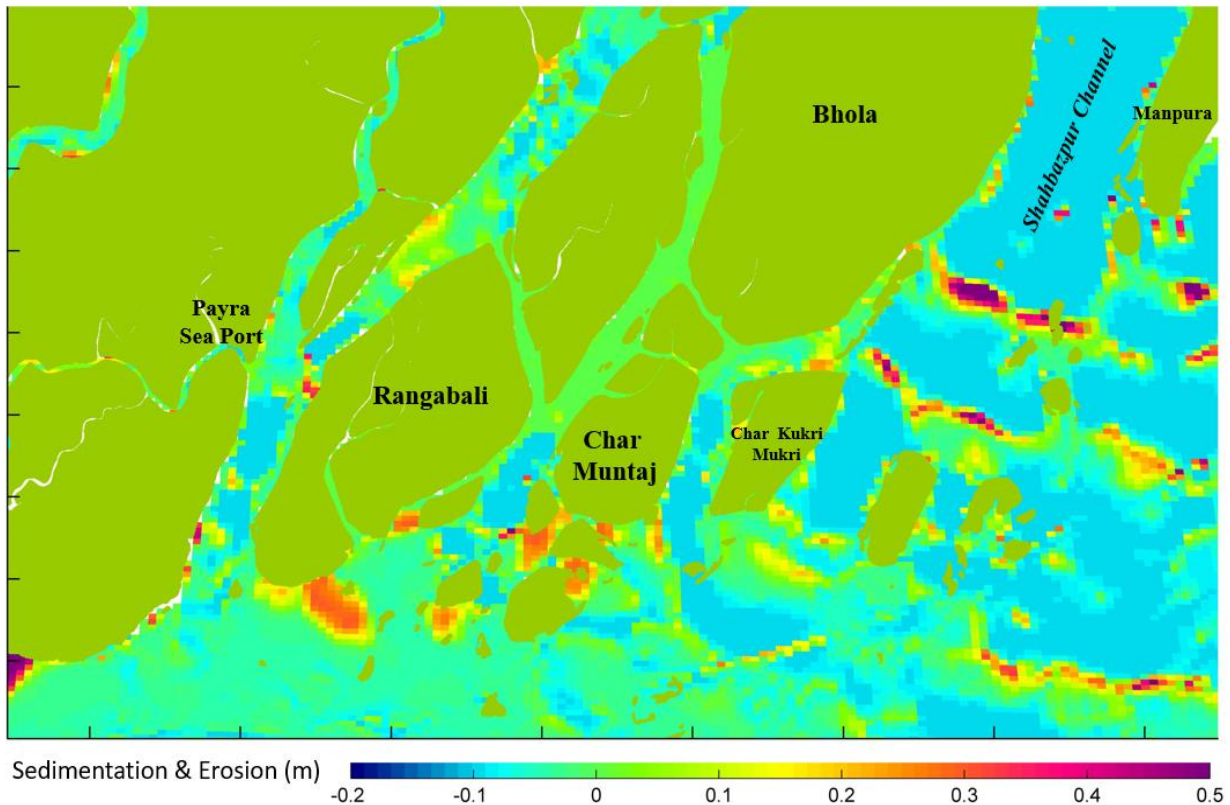


Figure 2.9: Model simulated sedimentation and erosion in the Meghna estuary region.

2.4 Existing Sediment Management Practices

The known sediment management practices in the region are (1) Dredging (2) Tidal River Management TRM (3) Cross dam

Dredging

Dredging is the most common sediment management practice in the south-west region. The impact of dredging of Hari river is studied by WARPO and BUET (2019) and the result show that sedimentation in the main river indeed increases the water-logging. Dredging in the main river

improves the water-logging condition in the area which are within the drainage zone of the river. Outside the drainage zone, dredging impact is not visible (see [Figure 2.10](#)). Except being unusually expensive, sustainability of dredging is questionable when long-term morphological time scale is considered.

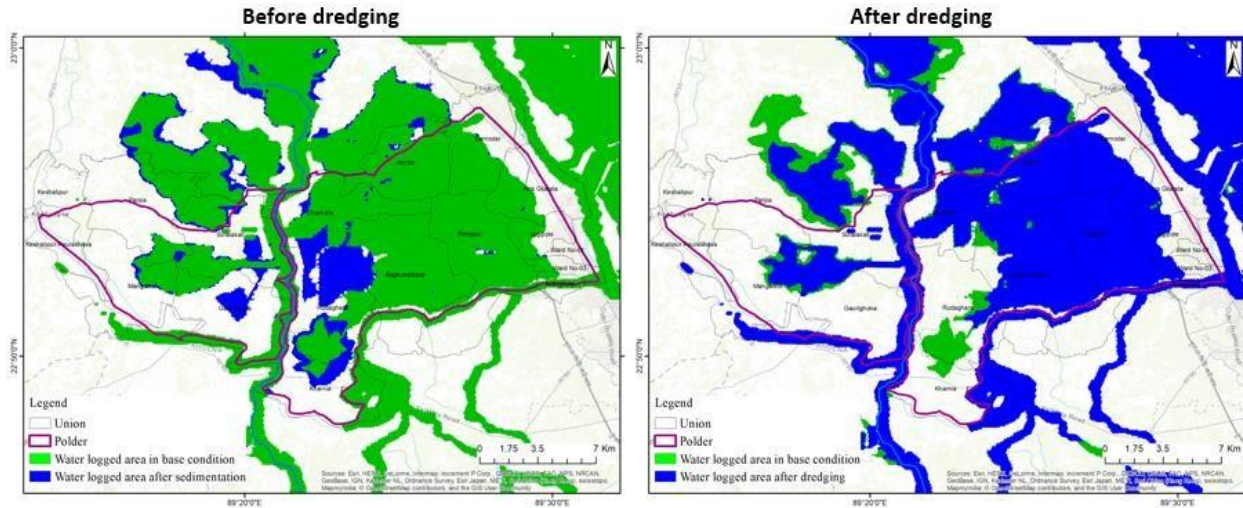


Figure 2.10: Impact of dredging of Hari river on water-logging condition inside polders 24 and 25. In the left image (before dredging) the blue areas are the additional water-logged area due to sedimentation of the Hari river. In the right image (after dredging) the green areas are free from water-logging due to dredging of Hari river (Source [WARPO and BUET 2019](#)).

TRM

To solve the long-standing problems of water-logging in the region, the Khulna-Jessore drainage rehabilitation project known as KJDRP was implemented during 1994-2002. Later, a popular concept based on generations of indigenous water management practices, formally known as Tidal River Management (TRM), was adopted. TRM allows natural movement of sediment with tidal water into a beel which is called tidal basin and allows deposition of sediment in the beel ([Figure 2.11](#)). The benefits of TRM concept was assessed by [Al Masud et. al. \(2018\)](#) by satellite data analysis and noticed that the TRM concept have reduced water-logging up to 4243 ha of land on August, 2011 compared to 2006 in Hari-Teka and Bhadra basins. Hence, the total agricultural land was increased by 3005 ha of land in 2011 (during TRM operation) as compared to 2006. The vegetation was also improved by 2851 ha of land in the floodplain.

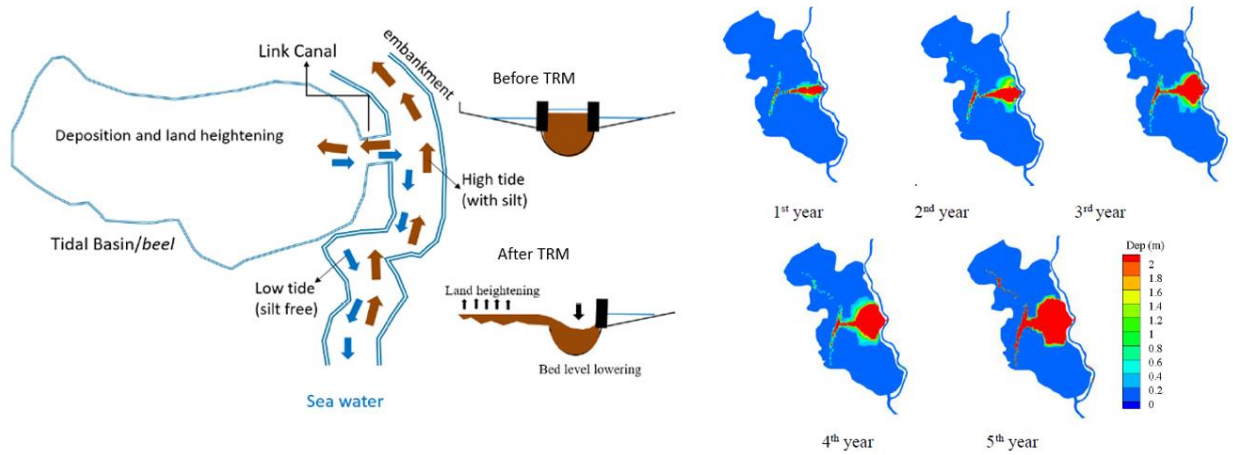


Figure 2.11: Concept of Tidal River Management TRM (Source: Rocky et al., 2020).

Although TRM is a process-based sediment management practice but its impact is dominantly local. Moreover, the implementation process of TRM creates social conflict as during TRM a certain part of the area (including the beel area) become water-logged for a long time. Amir et al. (2013) suggested an ‘embankment option’ coupled with TRM which will allow construction of embankment along both banks of the main channel and then cutting the embankment sequentially from upstream to downstream to ensure gradual sedimentation of beels. A geo-spatial analysis by Hussain et al. (2018) denoted that during TRM implementation in Pakhimara Beel at Tala upazila of Satkhira district, about 5090 acres of agricultural land and about 729 acres of homestead land was water-logged.

Cross-dam is another well-known sediment management practice which is used for land reclamation in off-shore region (EDP, 2007). BWDB proposed 18 probable cross dam locations in the coast (Figure 2.12). Impact of these cross-dams on local or overall sedimentation in the region has not yet been studied.

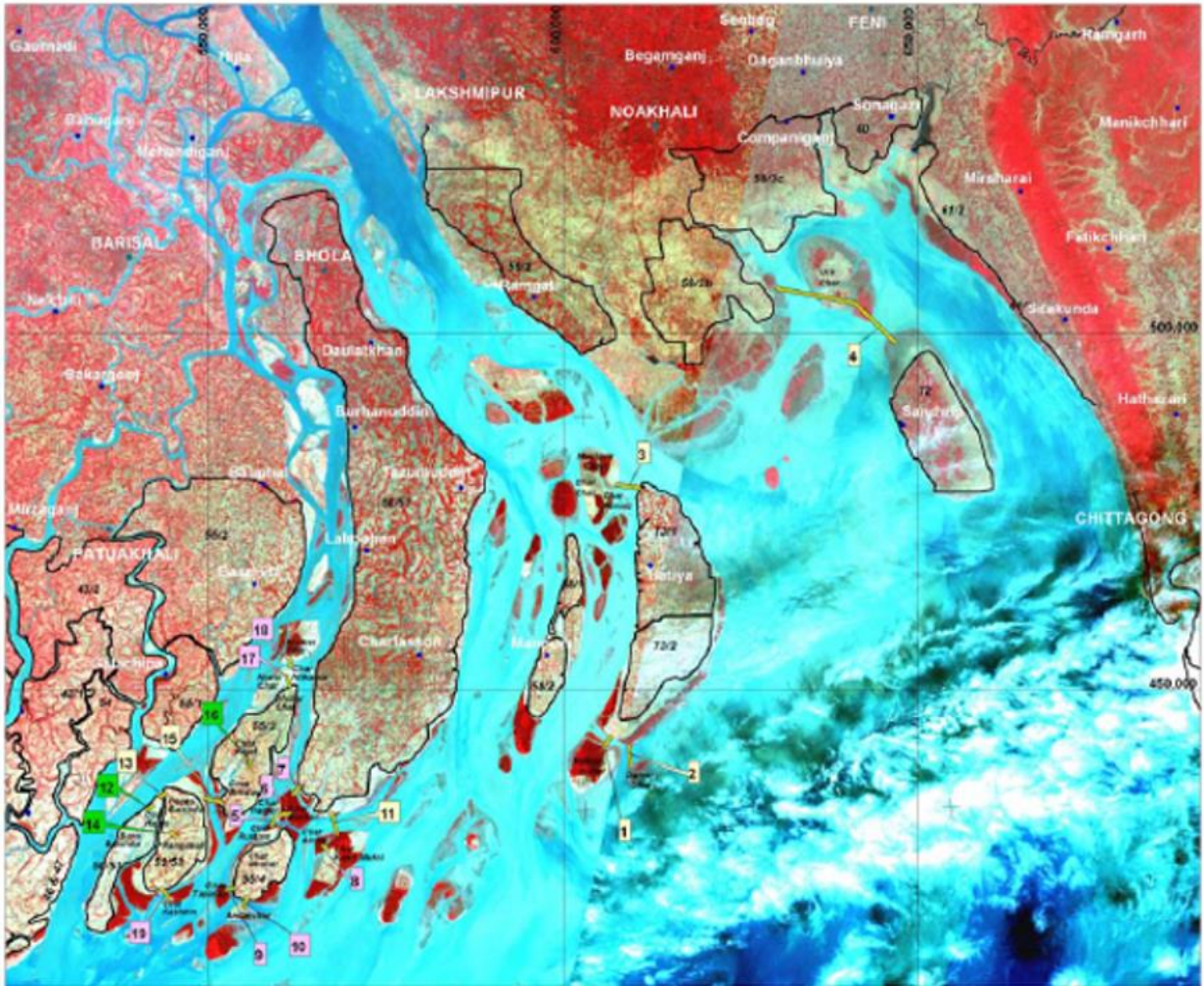


Figure 2.12: Proposed cross dam locations by BWDB (Source; EDP 2007).

CHAPTER THREE

Methodology

3.1 Introduction

This study is based on application of numerical model. The numerical model used in this study is Delft3D. Three modules of Delft3D modeling suite (Deltares, 2014) are applied in the present study. These are (a) hydrodynamic model (b) morphology model and (c) storm surge model. The Delft3D has a long track records of using in different environments, such as, oceans, coastal oceans, estuarine and river systems all over the world (Thanh et al., 2019; Sandbach et al., 2018; Hu et al., 2018; Salehi, 2018; Li et al. 2018; Bennett et al., 2018; Al Azad et al., 2018). This model has been used in many applications in Bangladesh as well (Haque, et al., 2016, for hydrodynamic model, WARPO and BUET, 2019, for morphology model, Akter et al., 2019 for salinity model and Al Azad et al., 2018 and Haque et al., 2018 for storm surge model).

3.2 Integrated Modelling Framework: The Bangladesh Delta Model (BDM)

Based on Delft3D, a new modelling framework named Bangladesh Delta Model (BDM) is developed in this study. BDM modeling framework integrates the entire processes of ocean, coast, Sundarban, polders, canal network, estuaries, inland rivers of different scales, embankments, wetlands, beels and haors. The model domain is extended southward to the Bay of Bengal down to Sri Lanka & Thailand coast and northward to the inflow points of all 54 transboundary rivers. The model domain is extended southward to the Bay of Bengal down to Sri Lanka & Thailand coast and northward to the inflow points of all 54 transboundary rivers. To capture these complicated network and processes in different scales – we have divided BDM into three categories in terms of grid resolution. These are: low resolution (BDM-L), medium resolution (BDM-M) and high resolution (BDM-H). The main reason of these divisions is to optimize the computational resources based on the objective of model application. The three categories of BDM are briefly summarized in Table 3.1.

Table 3.1: BDM integrated modeling framework

Model Name	Resolution	Description	Application
BDM-L	Grid resolution coarse. 40-layer model.	Captures BoB, Islands & Chars, All Major, Intermediate and Minor river/estuarine systems, Polders.	Macro level study. Can be applied to resolve ocean processes, coastal and inland flooding, storm surge.

BDM-M	Grid resolution medium. 40-layer model.	Captures BoB, Islands & Chars, All Major, Intermediate and Minor river/estuarine systems, Polders, Inland embankments, Road networks, Few canals inside polders.	Micro level study. Application in addition to BDM-L : flooding inside polders, major river processes, river and floodplain sedimentation, salinity intrusion.
BDM-H	Grid resolution high. 40-layer model.	Captures BoB, Islands & Chars, All Major, Intermediate and Minor river systems, Polders, Inland embankments, Road networks, Small canals inside polders, Haor and Beel systems.	Micro level study. Application in addition to BDM-M : impacts of canal and road networks inside polders, beel and haor processes.
Model output for all model resolutions are: water level, water depth, velocity, discharge, salinity concentration, temperature, cyclone wind speed, surge depth, surge velocity, sediment concentration, sedimentation & erosion thickness and sedimentation volume in river-beds & floodplains and bank erosion.			

Model Grid

Model entire model grid is shown in [Figure 3.1](#). The zoomed view of different parts of the grid are shown separately in [Figures 3.2a – 3.2h](#). Relatively coarser grids are used in the ocean (12km x 35km) compared to the coast (200m x 300m). As the tidal wave scale in the Bay of Bengal is several hundred kilometers, we do not need fine grid in the ocean part. Instead, the high-resolution model can capture a canal of width 5m or in few places, even less. The bathymetry of the Bay of Bengal is adopted from the global source of 2019 General Bathymetric Chart of the Ocean (GEBCO) data (<https://www.gebco.net/>). Model bathymetry is shown in [Figure 3.2](#).

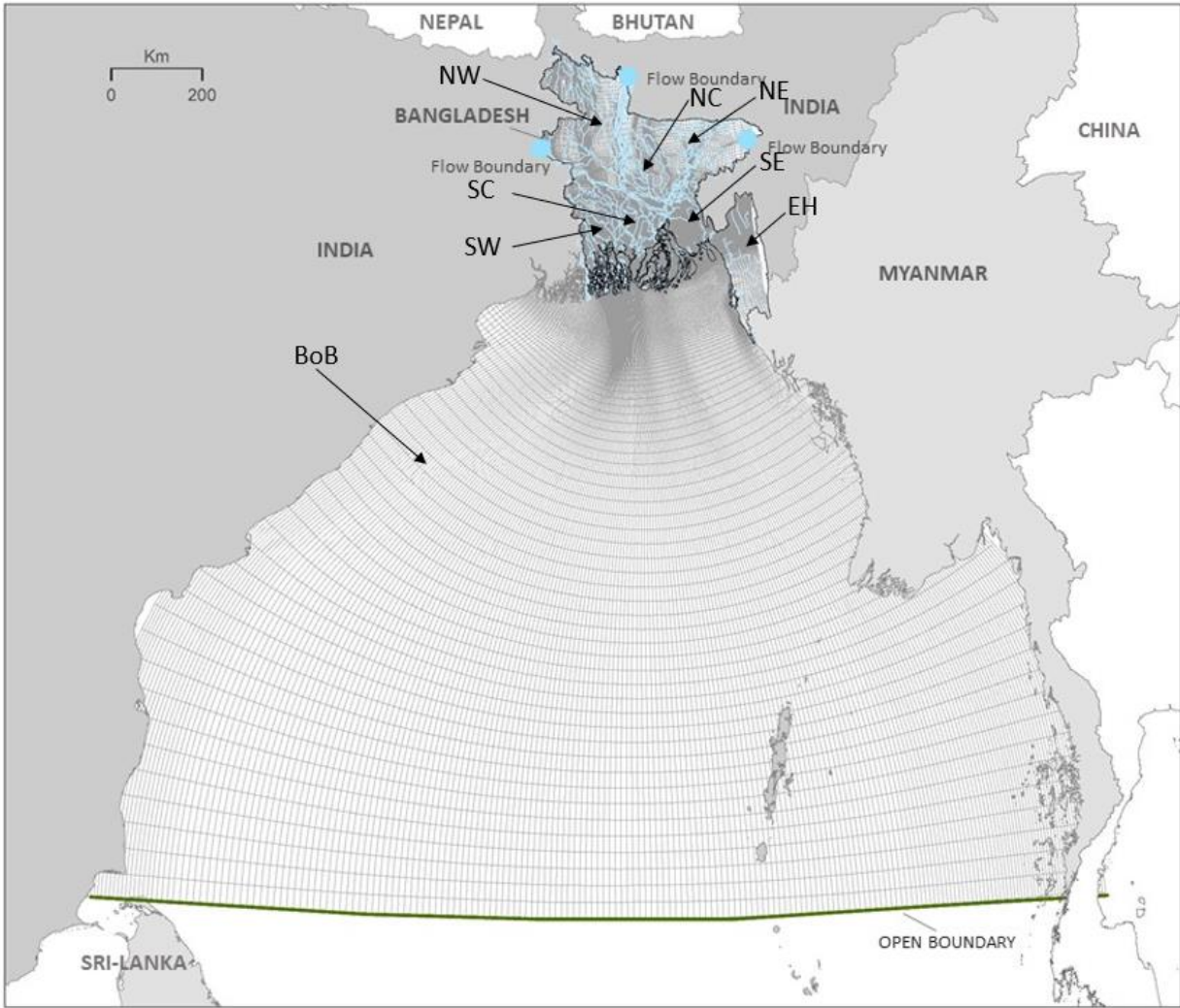


Figure 3.1: Model domain and grid of Bangladesh Delta Model (BDM). The figure also shows locations of different hydrological zones and the Bay of Bengal. These zones are (1) South West (SW) (2) South Central (SC) (3) South East (SE) (4) Eastern Hills (EH) (5) North West (NW) (6) North Central (NC) (7) North East (NE) (8) Bay of Bengal (BoB).

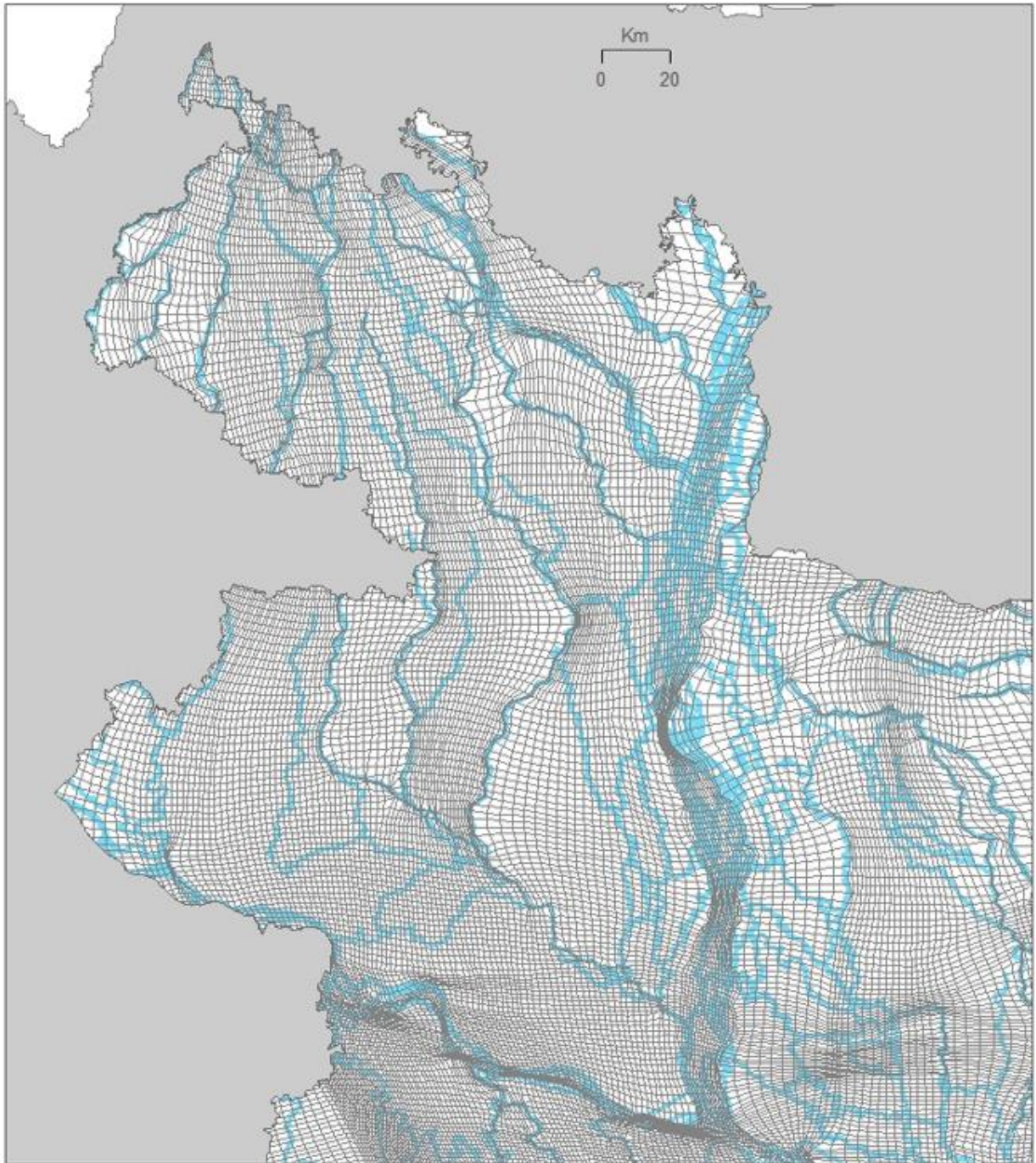


Figure 3.2a: Model grid for North East (NE) region.

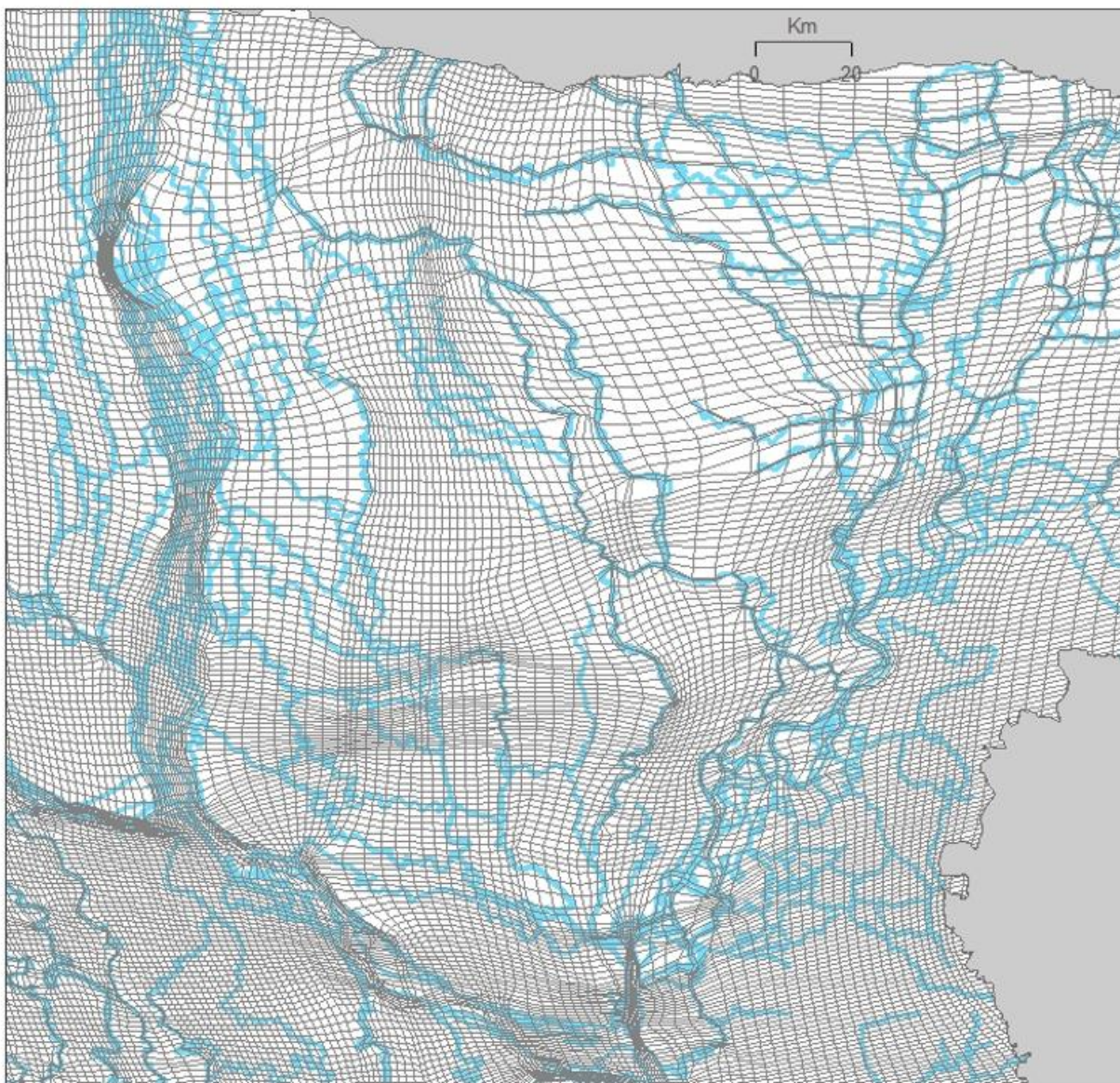


Figure 3.2b: Model grid for North Central (NC) region.

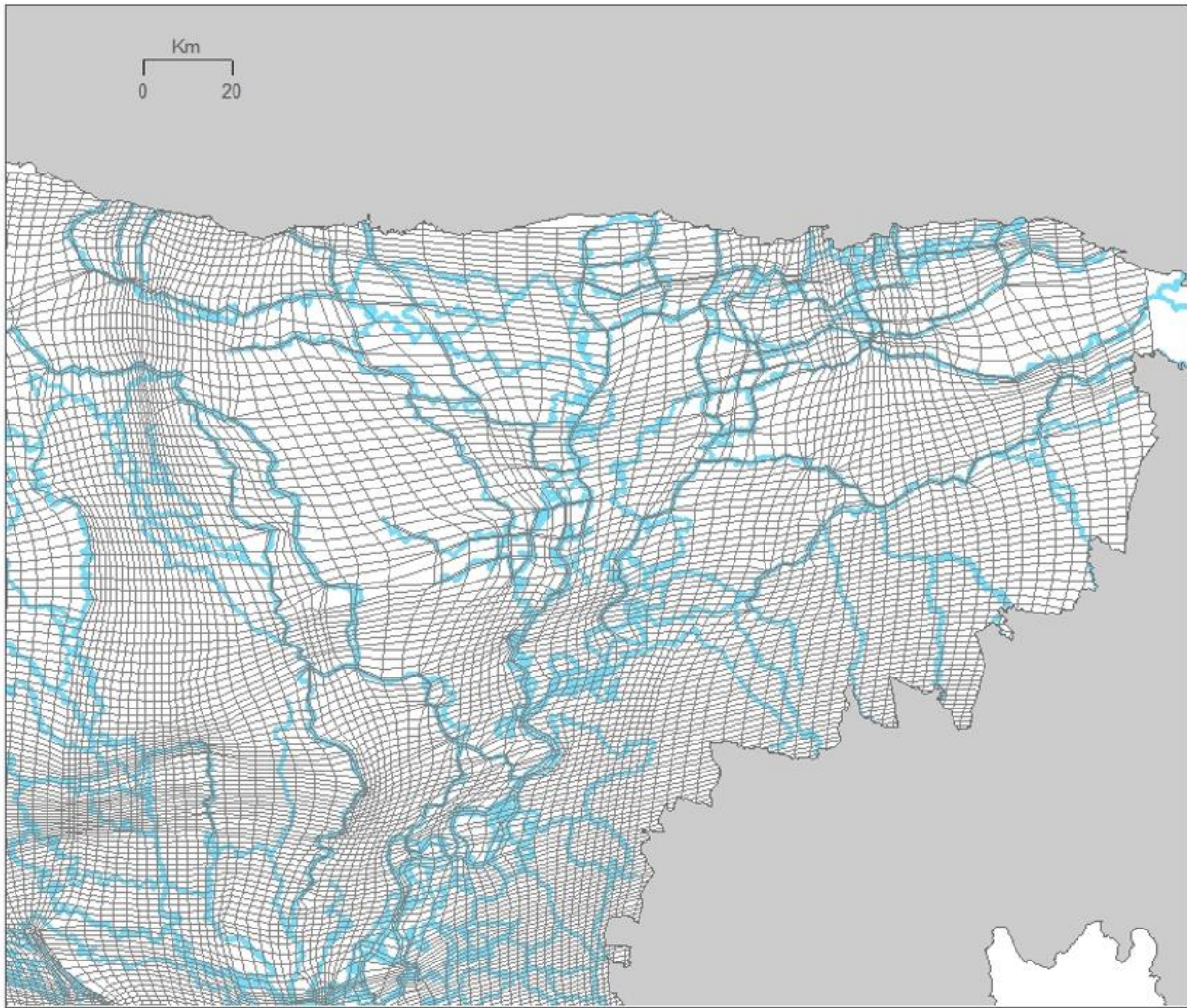


Figure 3.2c: Model grid for North East (NE) region.

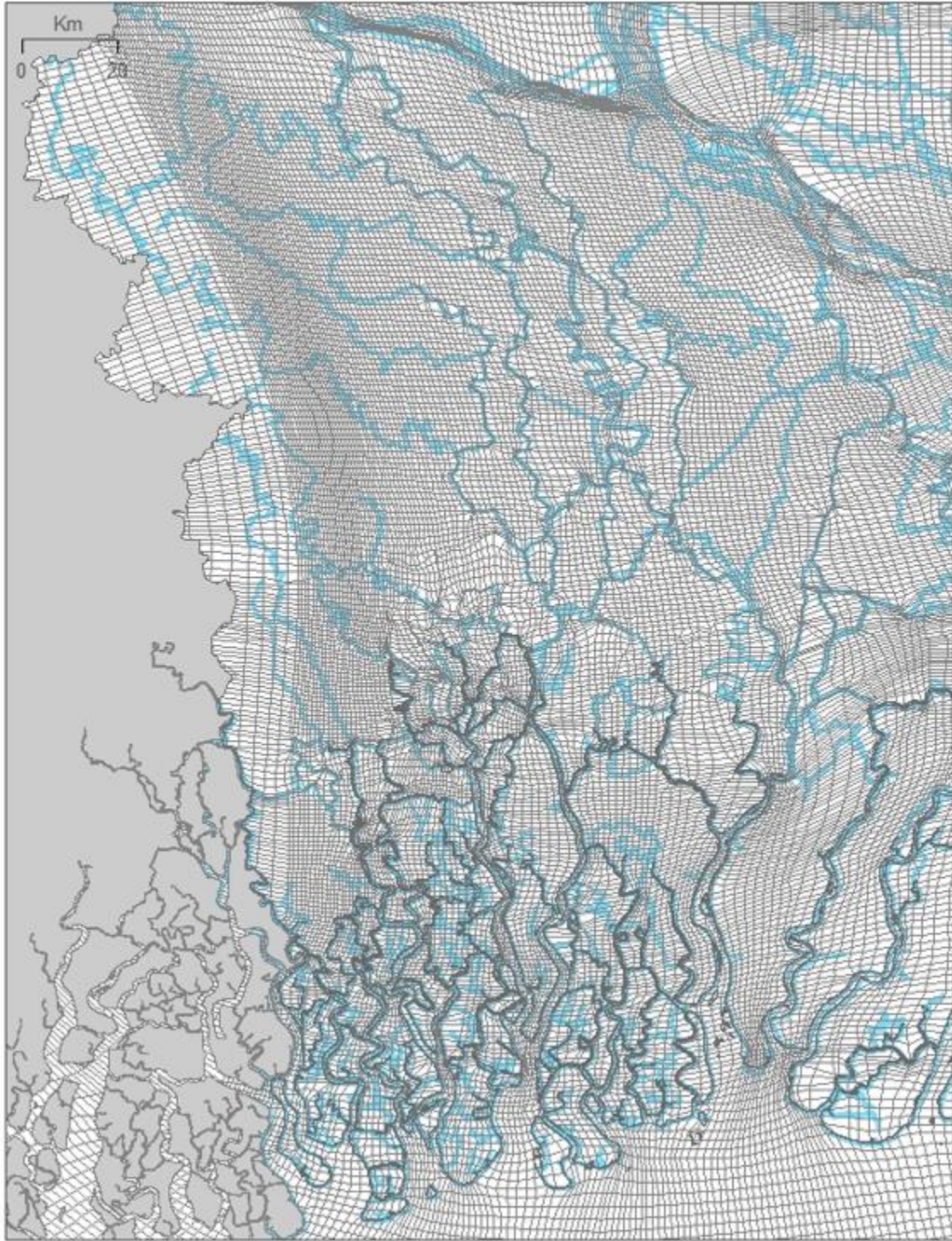


Figure 3.2d: Model grid for South West (SW) region.

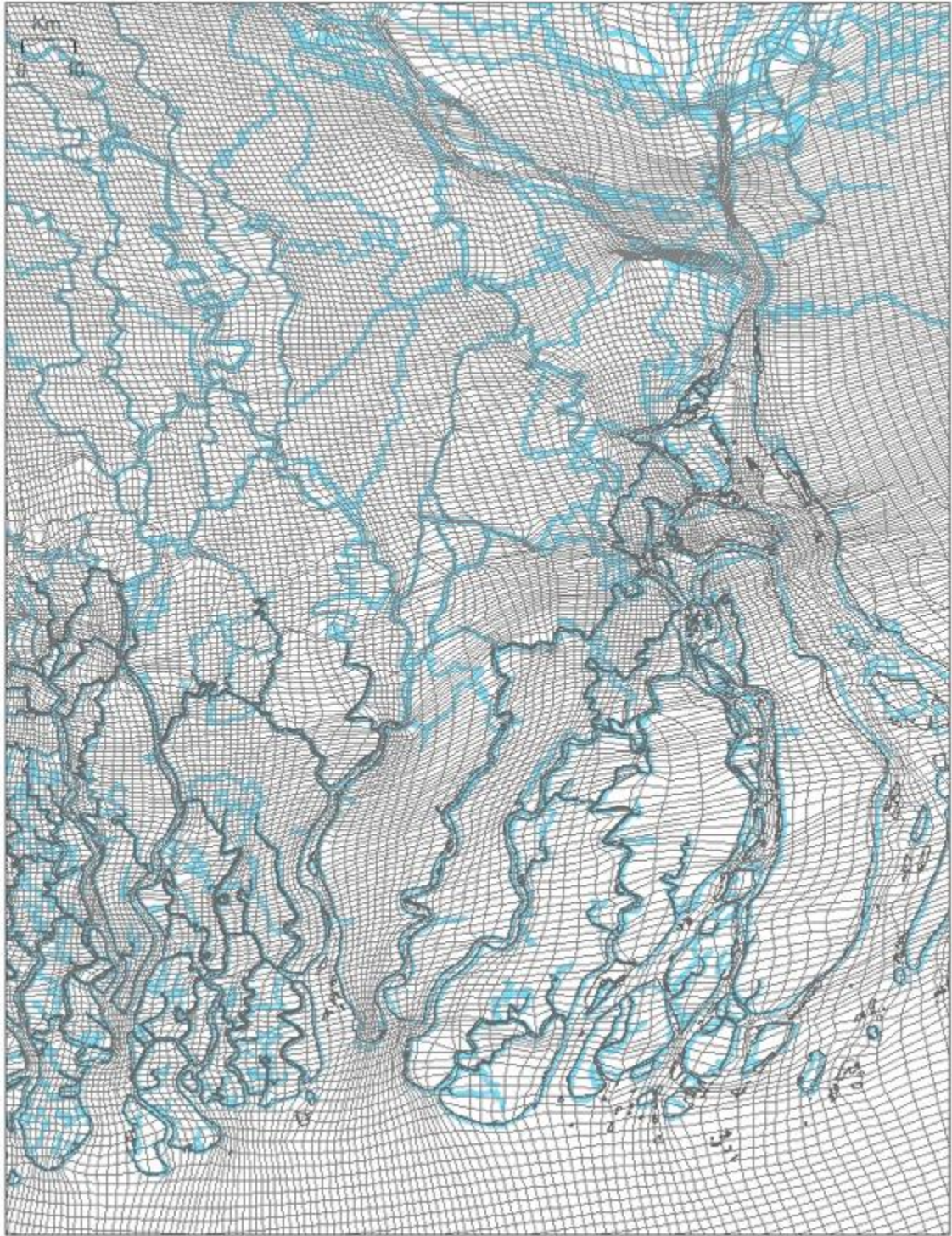


Figure 3.2e: Model grid for South Central (SC) region.

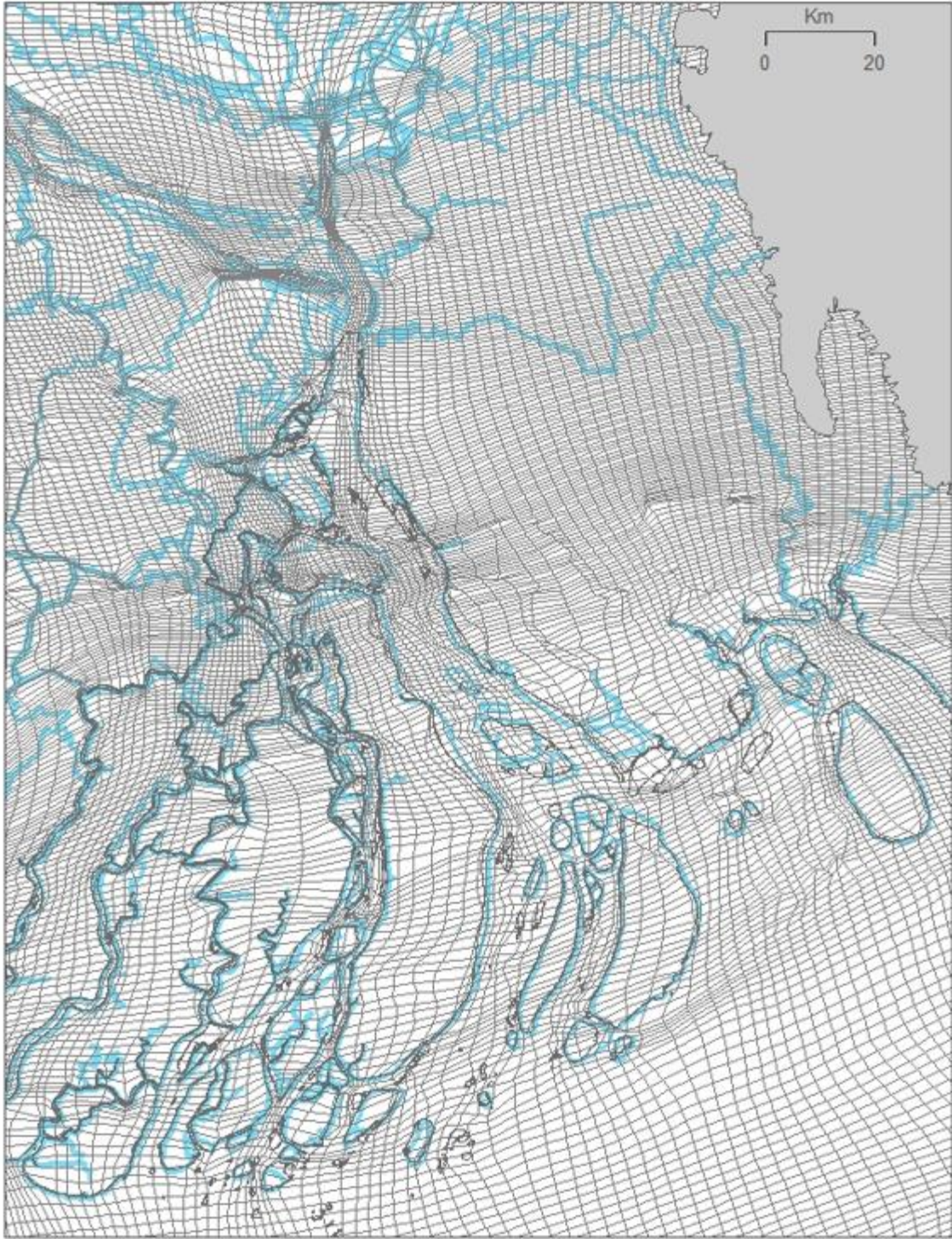


Figure 3.2f: Model grid for South East (SE) region.

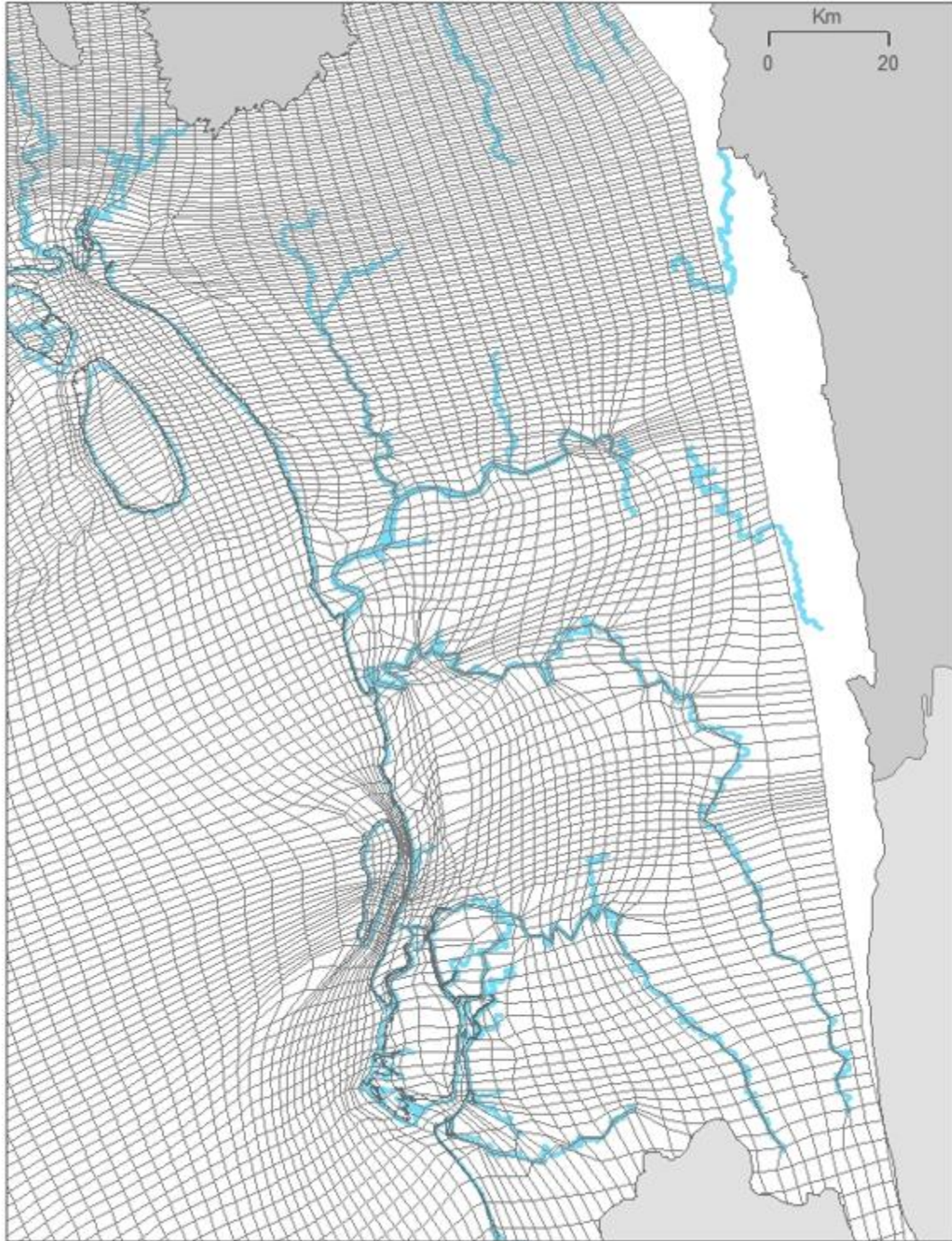


Figure 3.2g: Model grid for Eastern Hill (EH) region.

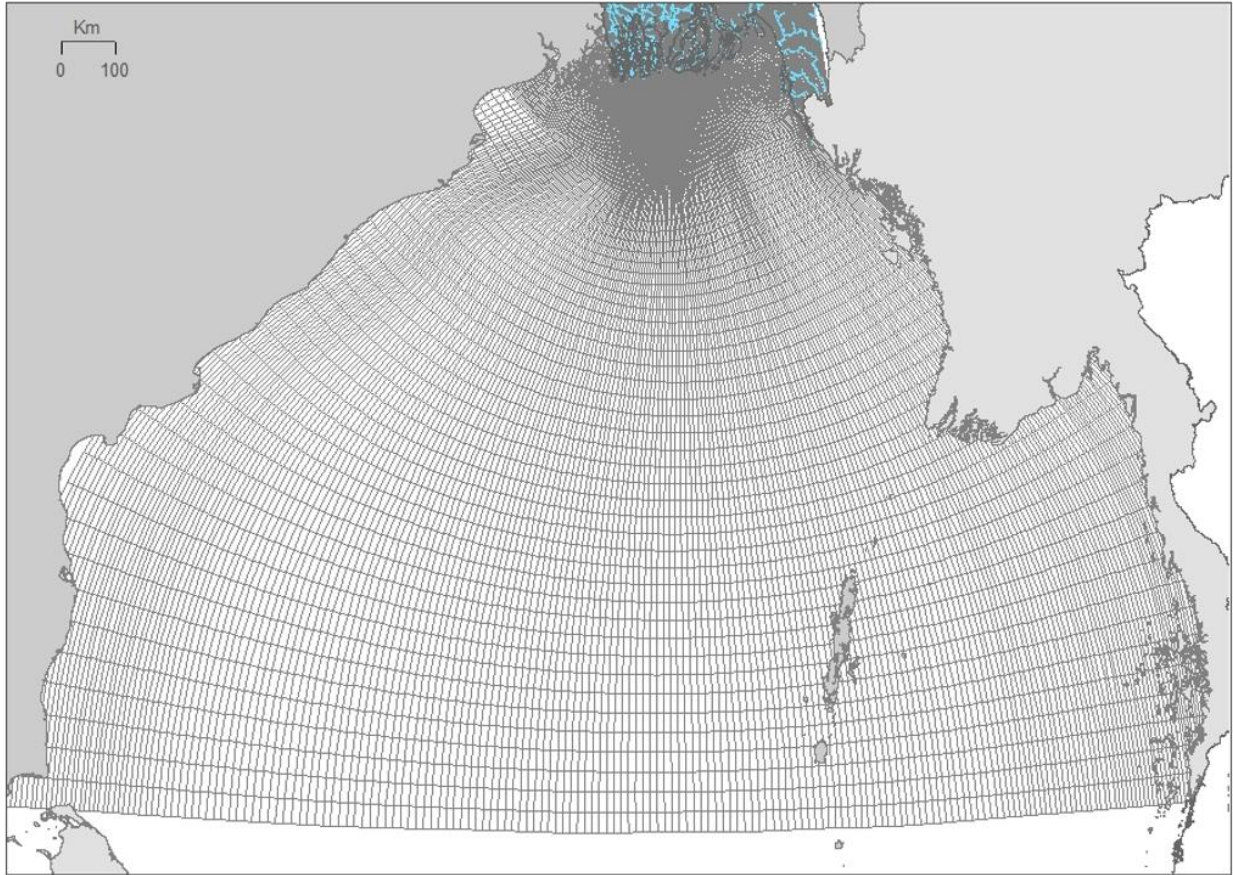


Figure 3.2h: Model grid for Bay of Bengal (BoB) region.

Model Bathymetry and Topography

The bathymetry of the Bay of Bengal is adopted from the global source of 2019 General Bathymetric Chart of the Ocean (GEBCO) data (<https://www.gebco.net/>). Bay of Bengal bathymetry used in the model is shown in Figure 3.3.

For model topography, the DEM available at WARPO for the entire Bangladesh is used (Figure 3.4). For bathymetry of rivers and estuaries, measured data from various secondary sources are used.

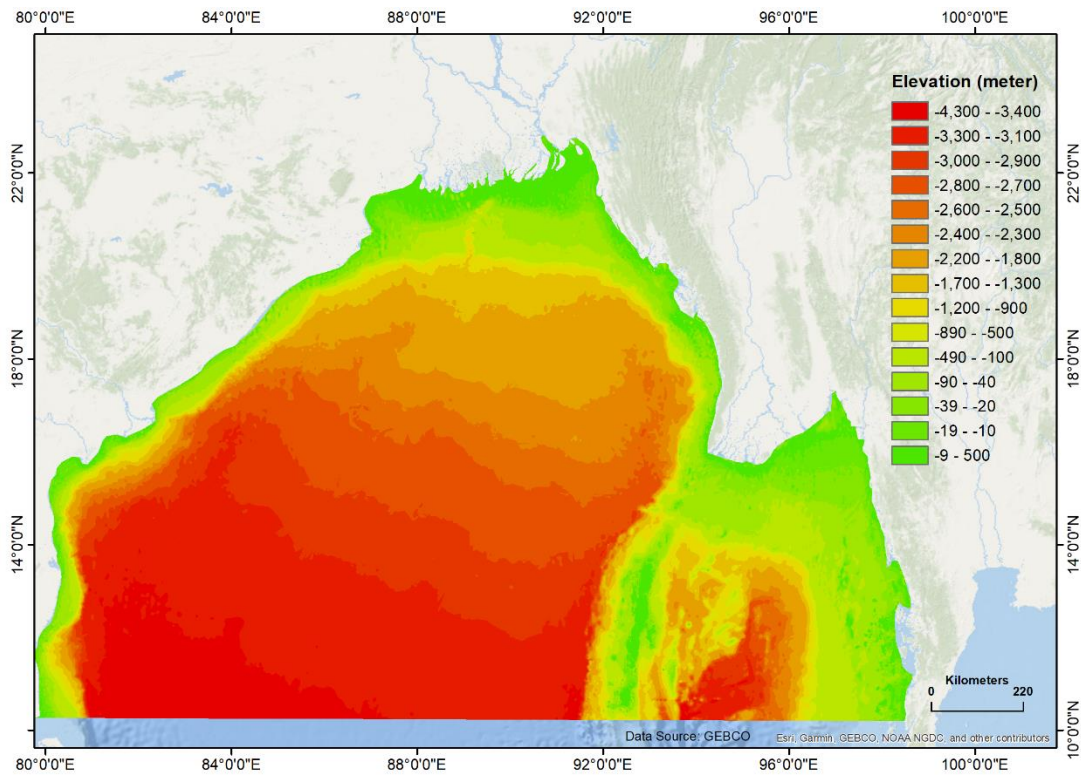


Figure 3.3 : GEBCO bathymetry of Bay of Bengal used in the model.

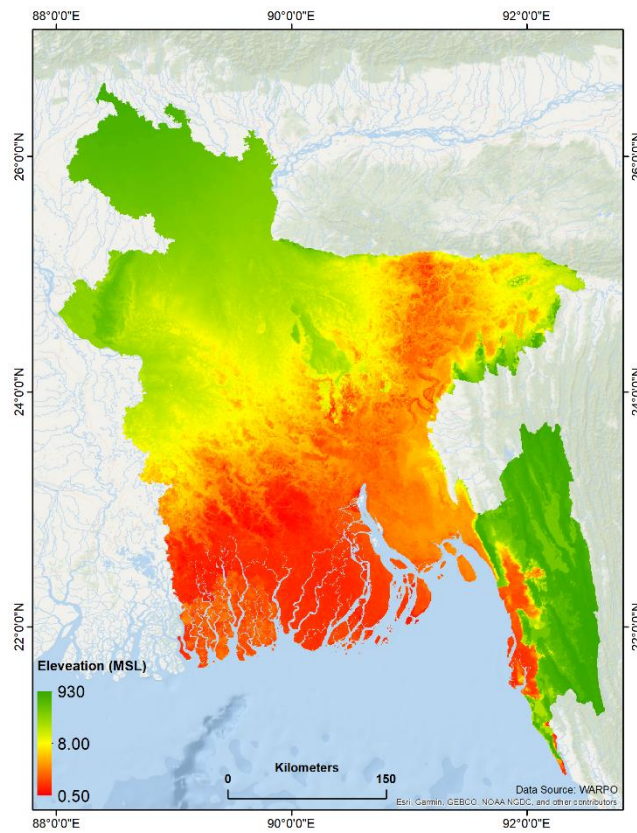


Figure 3.4 : WARPO DEM for Bangladesh used as model topography.

Boundary Conditions

Two types of boundaries are used in the model. Open boundary at the southern end of the model domain where temporal variation of water level is imposed and river flow input at the northern end of the model domain. Western coast of the open boundary is Sri Lanka and eastern coast is Thailand. These southern boundary locations are selected to encompass the genesis of cyclones in the Bay of Bengal. For river boundaries, inflows of rivers from all the inlets are provided. These include discharges from all major rivers and all transboundary river flows.

For Sri Lanka coast, time series of water level is provided at water level station Colombo and for Thailand coast, time series of water level is provided at water level station Ko Taphao Noi (see [Figure 3.1](#) for these boundary locations). The time series data of these water levels are collected from global source (<https://uhslc.soest.hawaii.edu/>). Snapshots of time series at two open boundary locations are shown in [Figure 3.5](#).

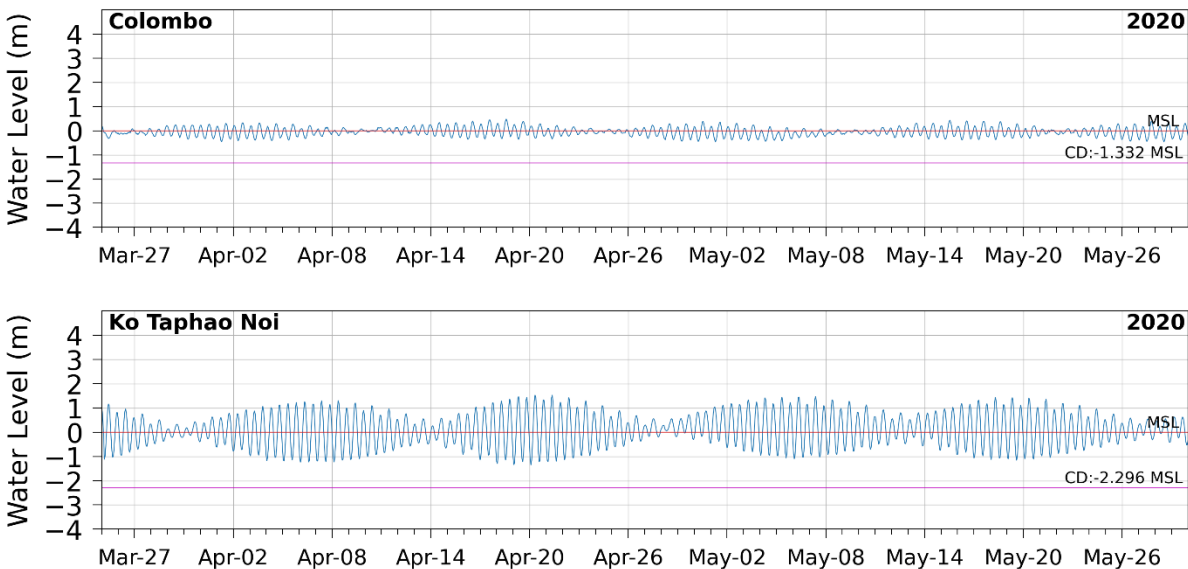


Figure 3.5: Water level data at two open boundary locations Colombo of Sri Lanka and Ko Taphao Noi of Thailand. Data are shown for March to May in 2020.

3.3 Model Calibration and Validation

Calibration

Model is calibrated against measured water level data at five water level station during the period from May 19 to June 21, 2017. These locations are shown in [Figure 3.6](#). Sources of these data are BIWTA and Bangladesh Navy. During calibration and validation, wind fields are generated in the

model domain by using measured wind data of BDM. Locations of wind stations which are used in different stages of model calibration, validation and application are shown in [Figure 3.7](#). Results of model calibration is shown in [Figure 3.8](#).



[Figure 3.6](#) : Calibration and validation locations of BDM.

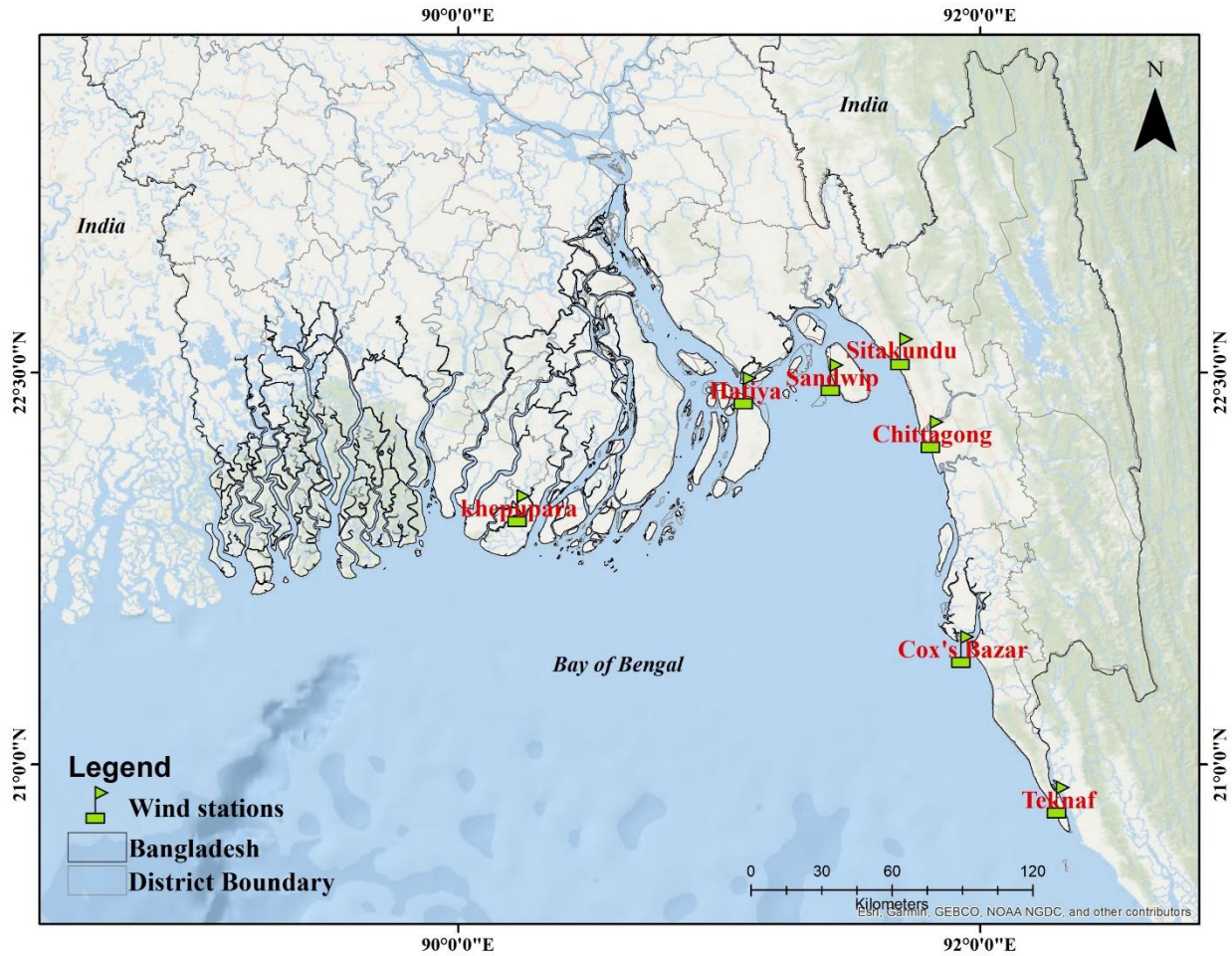
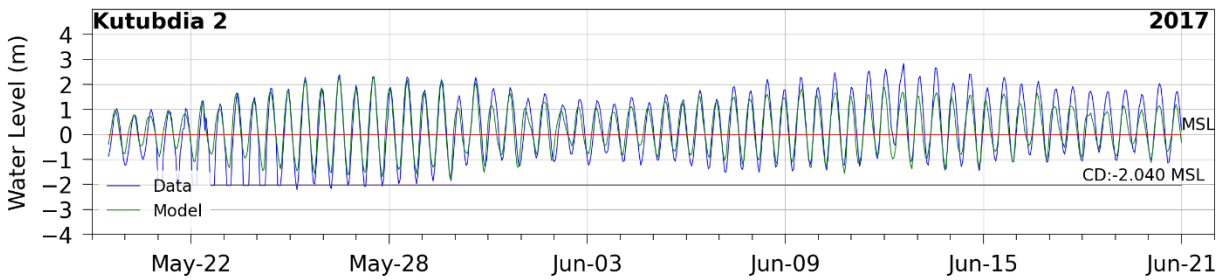
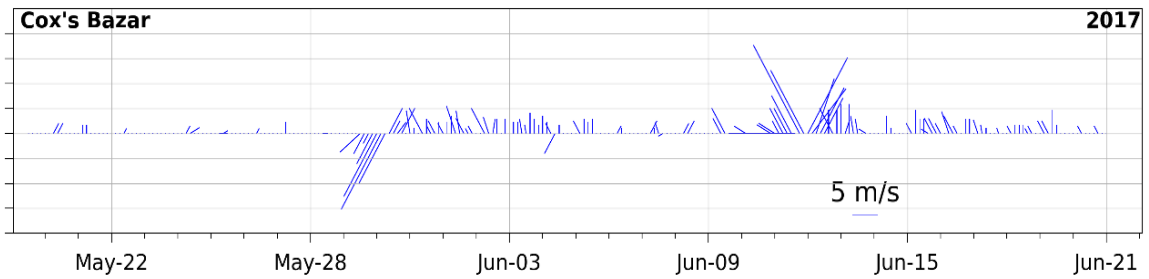
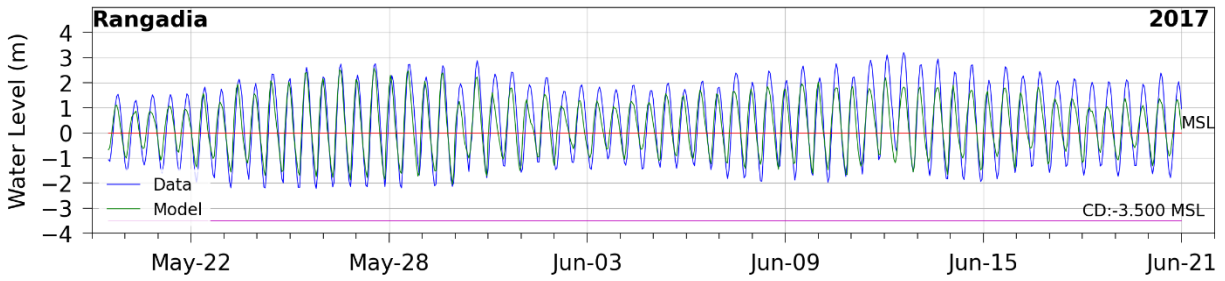
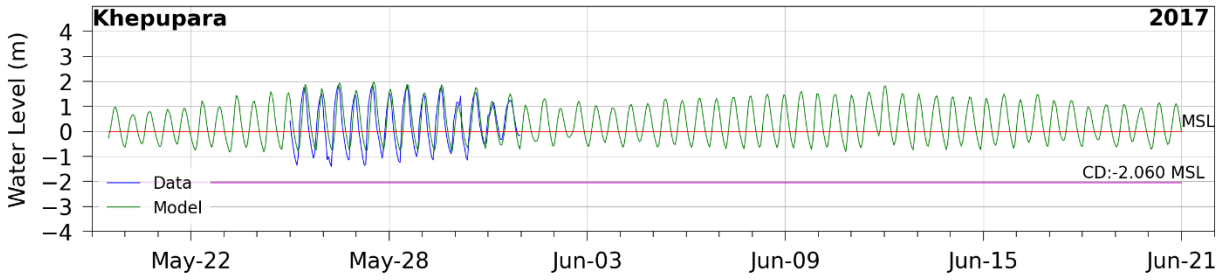
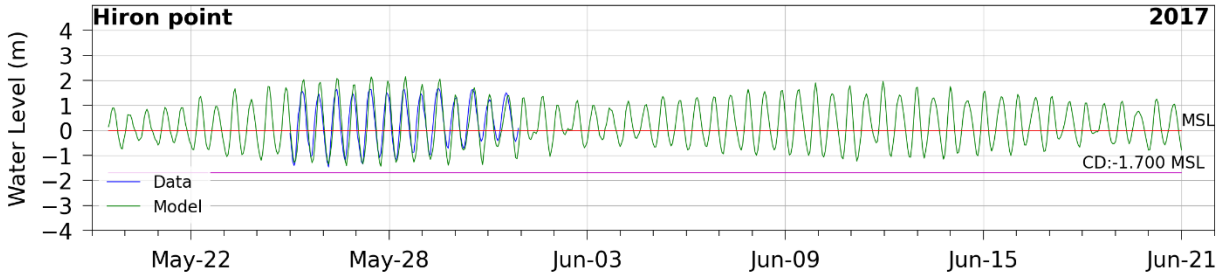


Figure 3.7: Wind station locations maintained by BMD. Data from these stations are used during different phases of model calibration, validation, and application. Note that all wind stations are land-based stations.



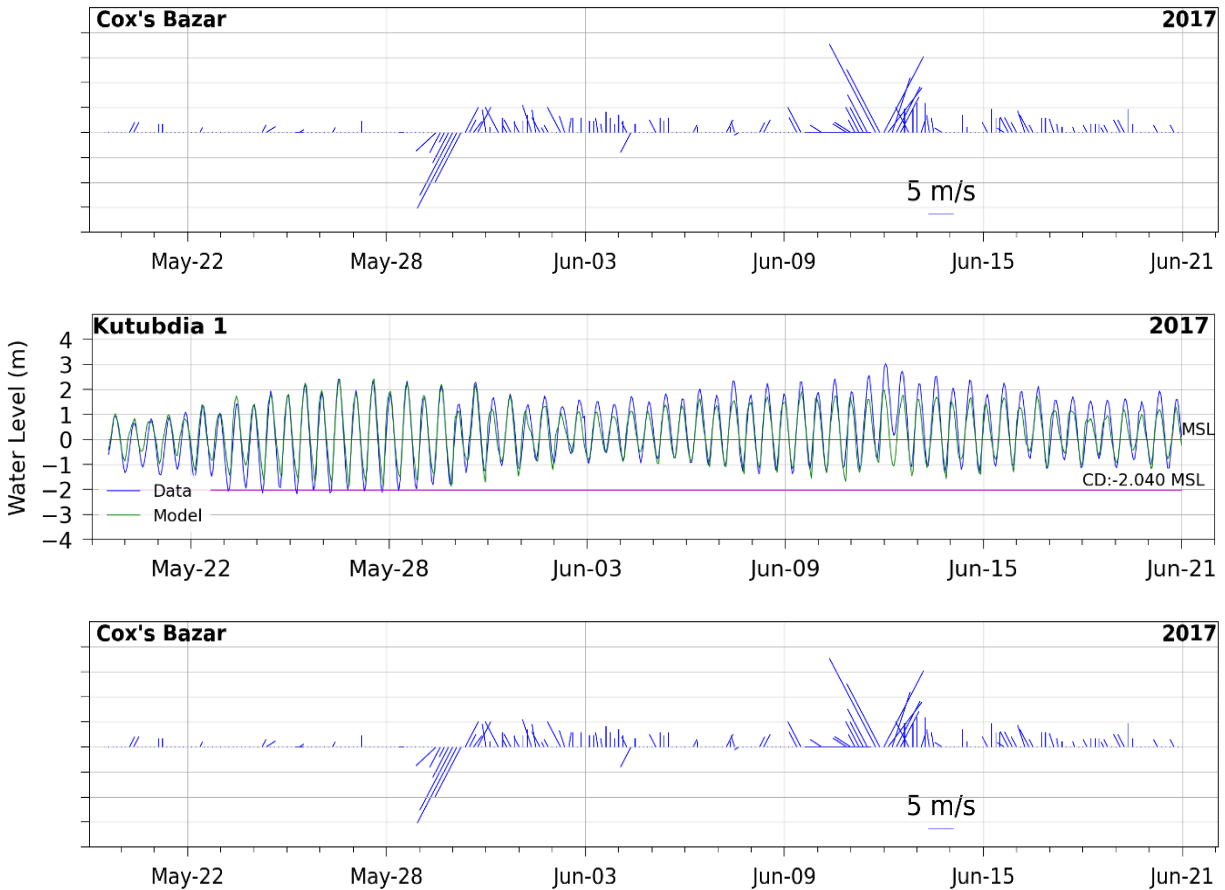


Figure 3.8: Results of model calibration at different water level stations. Calibration results are supplemented by wind stick diagrams at nearest wind station to show the wind effects on resultant water levels.

To explain the model calibration performance, two stations (Kutubdia-1 and Kutubdia-2) are selected where results are shown for the following: (1) simulated water level with the measured water level (2) 34-Hour Low Pass filter (34 HLP) which is the residuals and (3) 34-Hour High Pass filter (34 HHP) which is the tidal signals. Results for Kutubdia-1 station is shown in [Figure 3.9](#) and Kutubdia-2 station is shown in [Figure 3.10](#).

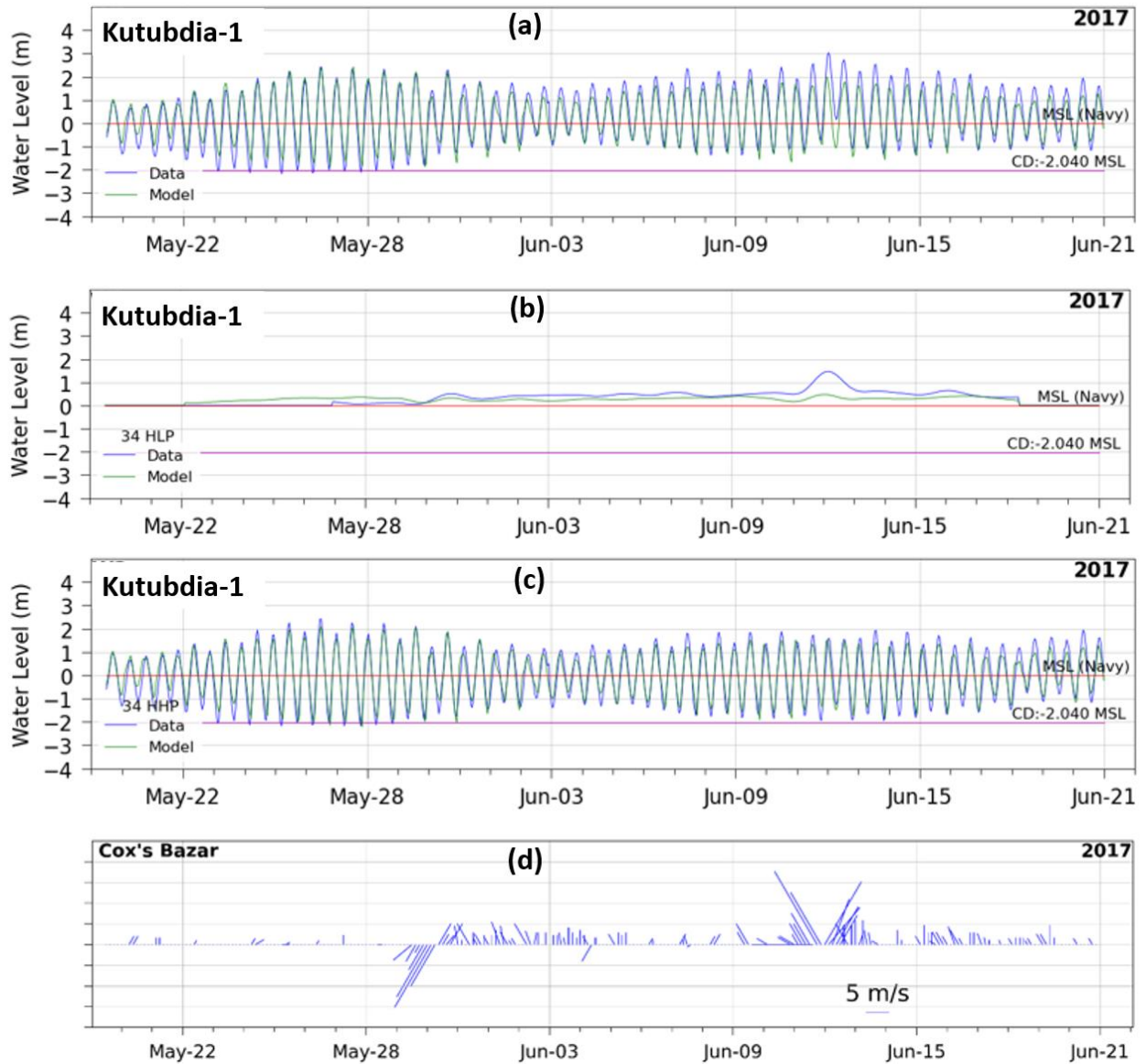


Figure 3.9: Synthesis of calibration result at Kutubdia-1 station. From top to bottom (a) comparison between model and measured water level (b) 34 HLP (c) 34 HHP and (d) wind stick diagram at Cox's Bazar station.

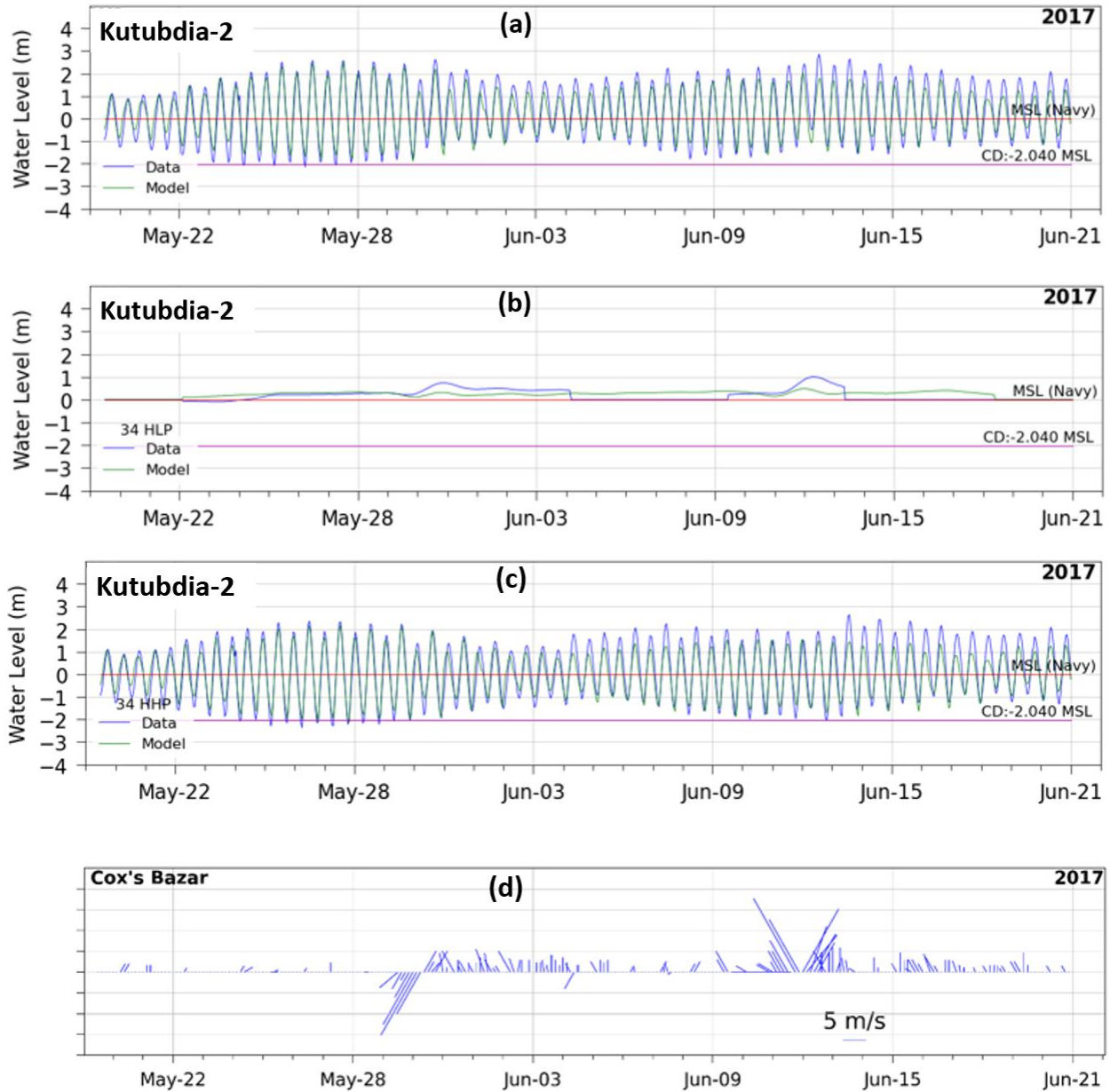


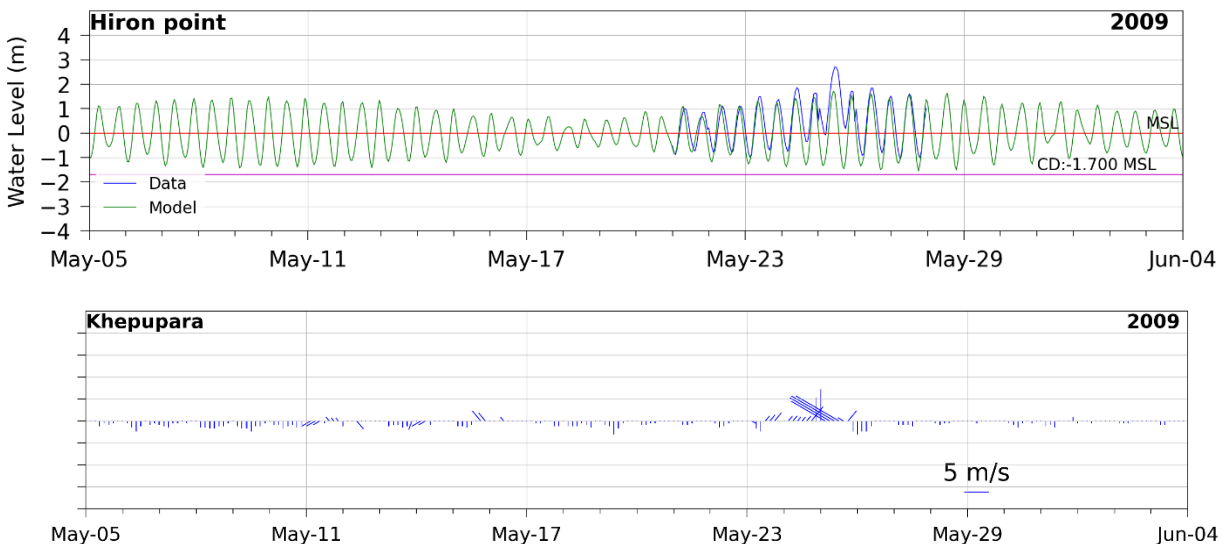
Figure 3.10: Synthesis of calibration result at Kutubdia-2 station. From top to bottom (a) comparison between model and measured water level (b) 34 HLP (c) 34 HHP and (d) wind stick diagram at Cox's Bazar station.

In general, the model simulation slightly overestimates the measured water level during the third week of May but underestimate during the second to the beginning of 3rd week of June (the larger part is underestimated). The reason of this discrepancies can be explained with the help of 34 HLP (figure (b) for each station) and wind stick diagram (figure (d) for each station). The 34 HLP plots represents water level variations which have a period greater than 34 hours which means there are no tides in these plots. Therefore, these plots represent residuals in the water levels where tides are filtered out. Underestimation and overestimation of water levels of the model compared to the

measurements are associated with the underestimation and overestimation of residuals. Residuals in these applications are largely dominated by wind stresses exerted on the water surface. The winds in these calibration simulations are represented by the wind data at the Cox’s Bazar station. All the wind station data that can be used in the model are land-based stations. The wind stress on the sea surface is due to the winds blowing over the ocean. Therefore, the discrepancies between the model water levels and measured water levels are mainly due to inappropriate representation of winds in the model. This is further stressed in the 34 HHP plots (figure (c) in each stations). 34 HHP plots represent water levels which have a period less than 34 hours and are mainly represented by the dominant tides in the area. The model performs far better when only tides are considered. Therefore, it is expected that the model calibration against observed water level can be significantly improved if the buoy based observed wind in the Bay of Bengal are used in the modeling framework, rather than the land based wind data. In the subsequent application of the model, wind fields will be provided by using wind data from global source, for example data from Cross-Calibrated-Multi-Platform (CCMP) <https://climatedataguide.ucar.edu/climate-data/ccmp-cross-calibrated-multi-platform-wind-vector-analysis>.

Validation

Model validation is made at two water level stations, Hiron point and Rangadia (see Figure 3.6 for the locations). Validation time is selected as May 5 to June 4, 2009. Validation of model results is shown in Figure 3.11. It is noted here that cyclone Aila made landfall in the Indian Sundarban coast on May 25, 2009. The wind stick diagram at Khepupara captured the cyclone signal correctly. But the model results show underprediction in both the stations during the cyclone landfall time. The reason of this underprediction is the absence of synoptic wind fields in the model which is explained before. Application of synoptic wind fields from CCMP data will certainly improve the model result. CCMP data also captures the cyclone signals.



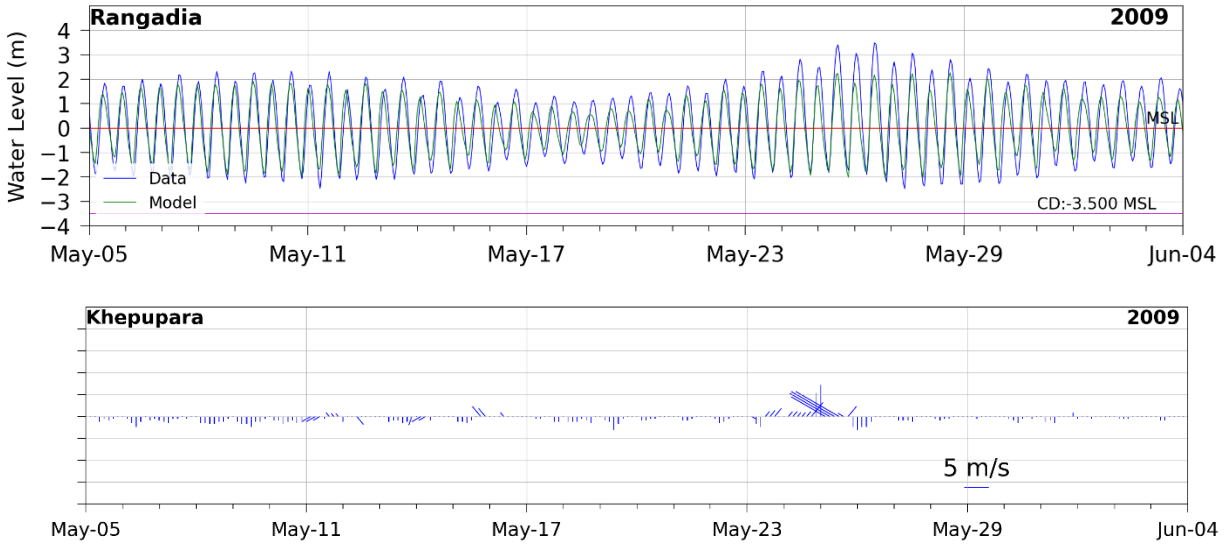


Figure: 3.11: Results of validation for BDM. To show the wind effects, the results also show wind stick diagram at Khepupara wind station of BMD.

Quantification of model calibration and validation performance

Model calibration and validation performance is quantified through several statistical indicators. Statistical indicators determining the model calibration and validation performance is shown in [Table 3.2](#). Evaluating different statistical indicators, overall model performance during calibration is found as ‘Very Good’. For validation, results are mixed. For Rangadia station, model evaluation is ‘Very Good’. But for Hiron Point station, model evaluation is ‘Unsatisfactory’. As mentioned before, model could not capture the impact of cyclone Aila properly due to absence of synoptic wind field in the model domain. Only cyclone wind cannot solve the problem. This will be resolved in subsequent application of the model.

Table 3.2: Statistical indicators along with performance evaluation criteria that determines the model calibration and validation performance.

Model Calibration							Model Validation						
Station	Statistical Indicators					Calibration Performance	Station	Statistical Indicators					Validation Performance
	RMSE	MAE	NSE	RSR	R ²			RMSE	MAE	NSE	RSR	R ²	
Kutubdia 1	0.53	0.42	0.80 (VG)	0.45(VG)	0.82 (VG)	Very Good	Rangadia	0.67	0.56	0.77 (VG)	0.49 (VG)	0.78 (G)	Very Good
Kutubdia 2	0.43	0.34	0.85 (VG)	0.38 (VG)	0.87 (VG)	Very Good							
Rangadia	0.67	0.57	0.77 (VG)	0.48 (VG)	0.79 (G)	Very Good	Hiron Point	0.71	0.55	0.35 (U)	0.81 (U)	0.66 (S)	Unsatisfactory (Poor)
Hiron Point	0.35	0.29	0.85 (VG)	0.39 (VG)	0.91 (VG)	Very Good							
Khepupara	0.59	0.51	0.60 (S)	0.63 (S)	0.63 (S)	Satisfactory (Fair)							
Qualitative Evaluation of Statistical Indicators													
Statistics	Very Good		Good		Satisfactory (Fair)		Unsatisfactory (Poor)		Reference				
R ²	0.80 < R ² ≤ 1		0.70 < R ² ≤ 0.80		0.60 < R ² ≤ 0.70		R ² ≤ 0.60		(Duda et al. 2012)				
NSE	0.75 < NSE ≤ 1.00		0.65 < NSE ≤ 0.75		0.50 < NSE ≤ 0.65		NSE ≤ 0.50		(Moriassi et al. 2007)				
RSR	0.00 ≤ RSR ≤ 0.50		0.50 < RSR ≤ 0.60		0.60 < RSR ≤ 0.70		RSR > 0.70		(Moriassi et al. 2007)				

CHAPTER FOUR

Results from BDM

4.1 Introduction

This chapter presents some preliminary results of low-resolution version of BDM, the BDM-L. Most of the objectives of this project is achieved by application of BDM-L. Few of the scenarios needs output from BDM-M. Following sections present simulation results from BDM-L by describing tide propagation in the Bay of Bengal, distribution of freshwater plume, vertical stratification structure of freshwater in the ocean, cyclone wind distribution in the Bay of Bengal, simulation of several past cyclones, effect of cyclone wind on tidal current, inundation during monsoon flood in Bangladesh, inundation during storm surge flood in the coast, sediment movement path along the coast and sedimentation in the floodplains. All these processes are relevant to study the impacts of different sediment management practices in the coast.

4.2 Simulation of Tide in the Bay of Bengal

BDM is applied to simulate different process of tides in the Bay of Bengal. Tide propagation and distribution of freshwater plume is simulated by applying depth averaged 2D version of the model while vertical structure of freshwater is simulated with the 3D version of the model.

4.2.1 Tide propagation in the Bay of Bengal

Tide propagation is simulated from the southern most boundary of the model (Sri Lanka-Thailand region) to the coast of Bangladesh. Simulated flood and ebb tides in the Bay of Bengal towards the Bangladesh coast is shown in [Figure 4.1a](#) and [Figure 4.1b](#). The figures also show location of Swatch-of-No-Ground in the Bay.

The results show that tides arrive almost at the same time along the coast ([Figure 4.1a](#)). Flood tide slows down along the Lower Meghna estuary due to the impact of freshwater. Relatively higher velocity along the mouth of the estuaries of the western coast during the flood tide causes ocean sediments to enter inside the western estuarine systems. Sources of these ocean sediments are Lower Meghna estuary which propagates along the continental shelf during the ebb tide ([Figure 4.1b](#)) and later re-enter into the system during the flood tide ([Figure 4.1a](#)). Just at the beginning of the ebb tide in the ocean, there is a flow disaggregation line and a zone of stagnation occurs. This zone has significant impact on the sedimentation all along the estuary mouths.

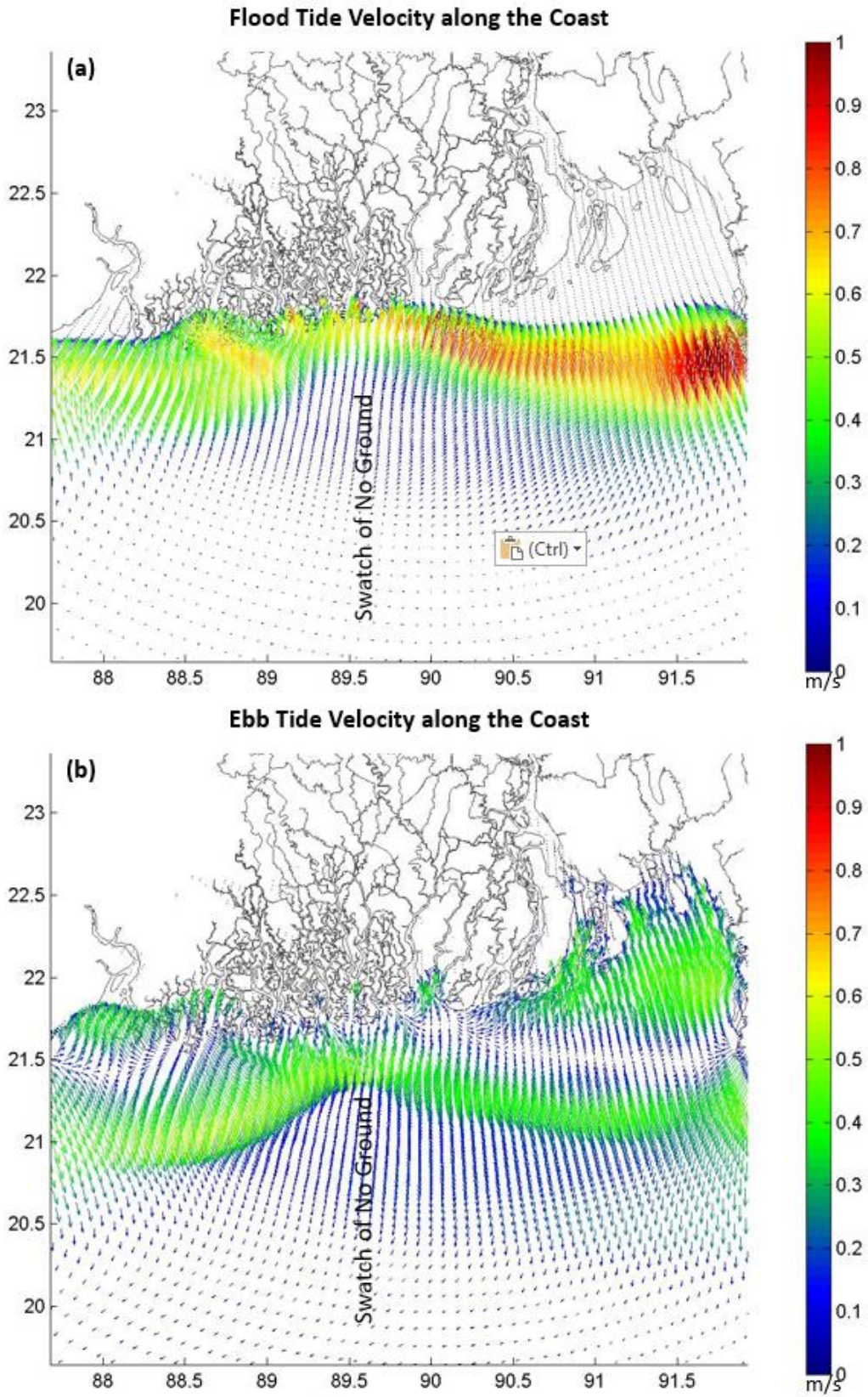


Figure 4.1: Simulated (a) flood and (b) ebb tides in the Bay of Bengal.

Swatch-of-no-ground is a submarine canyon in the ocean floor (Figure-4.2). It spans around 1738 km². The floor is about 5km to 7km wide with a southward continuation of about 2,000 km. At the edge of the shelf, the depth is about 1200m. Both the flood and ebb currents move faster along the Swatch-of-no-Ground (Figures 4.1a and 4.1b). The Swatch-of-no-ground acts like a fast flowing channel and divides the entire oceanic circulation into two distinct patterns – eastern circulation and western circulation. Eastern circulation is dominated by the Lower Meghna flow and the western circulation is dominated by the western estuarine systems and flows from the West Bengal coast. Due to this fast-moving flow separation line, it appears that the sediments from the Lower Meghna system may not be able to deposit in the Swatch-of-no-ground – which is a popular hypothesis these days. But this needs further analysis.



Figure 4.2: Location of Swatch-of-no-ground in the Bay of Bengal.

4.2.2 Distribution of freshwater plume

Distribution pattern of the freshwater plume from the Lower Meghna system is simulated by allowing the freshwater to enter inside a saline environment of the ocean. Following the dilution line of saline zone, freshwater plume movement zone is demarcated (Figure 4.3).

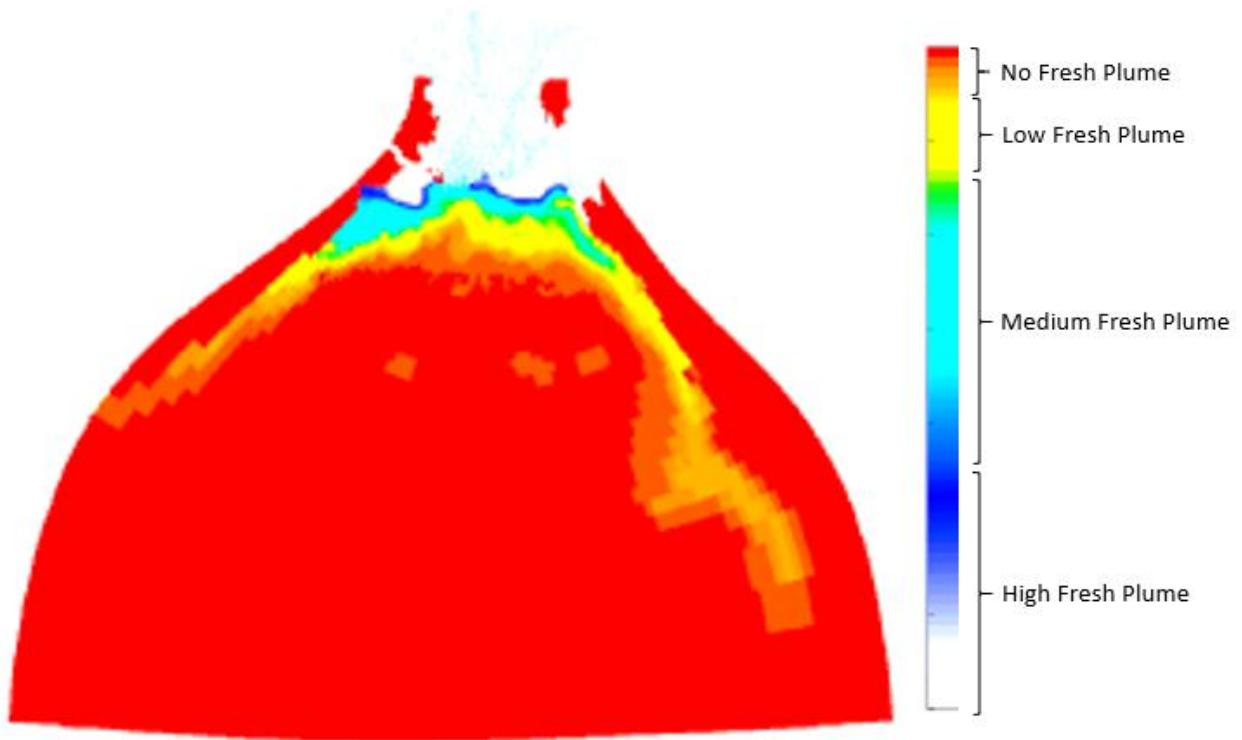


Figure 4.3: Distribution of freshwater plume from the Lower Meghna estuary.

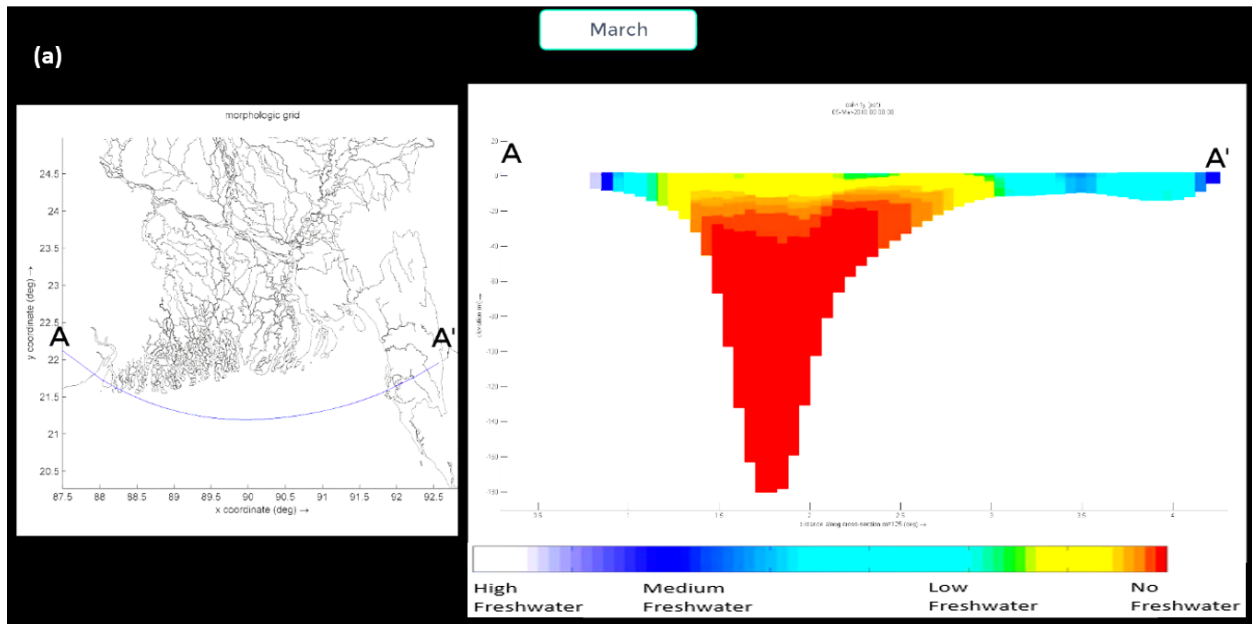
The results show that freshwater plume is concentrated along the continental shelf. If we take freshwater plume as a proxy of sediment-laden water, the sediments from the Lower Meghna estuary is mainly distributed along the continental shelf. There is hardly any freshwater plume goes into the deep ocean. This means that sediment concentration in the deep ocean is low. This also shows that assumption of a low sediment concentration in the deep ocean is valid (WARPO and BUET, 2019). Freshwater plume from Lower Meghna propagates a long distance up to the coast of Thailand. This simulation does not consider all the freshwater sources from India, Sri Lanka, Myanmar, and Thailand.

4.2.3 Vertical stratification

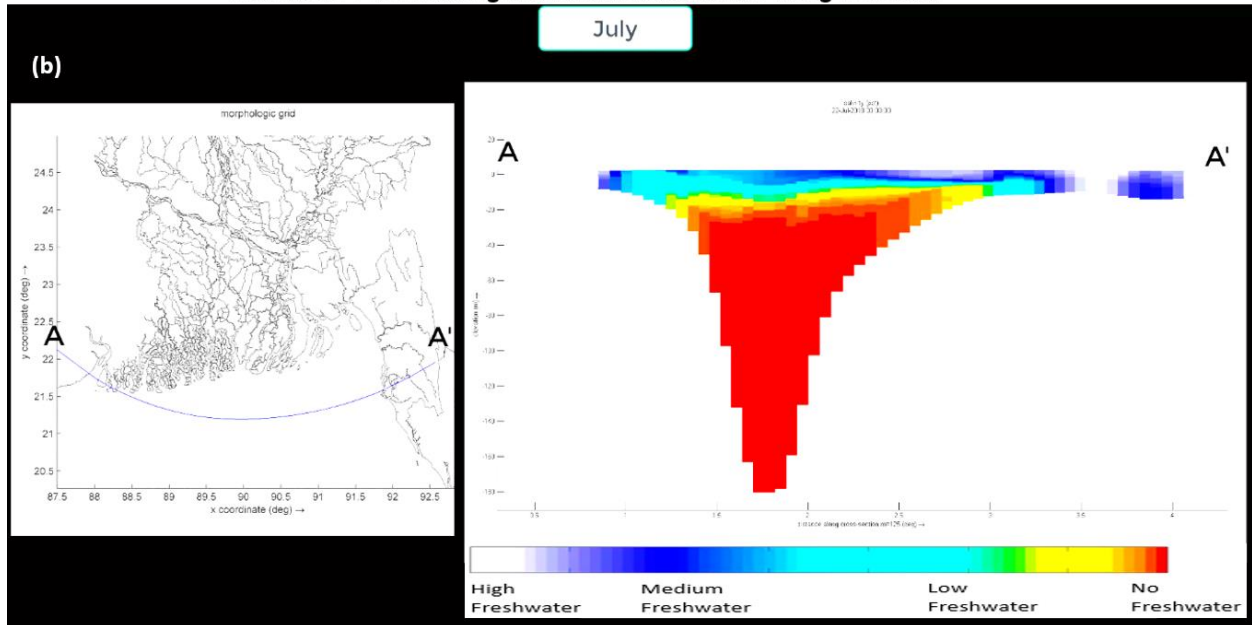
Vertical profile of cross section and longitudinal section along the coast during dry season and monsoon is shown in Figures 4.4a to 4.4d. These sections are prepared from the 3D model simulation. Salinity is used as a proxy variable to create a stratified condition. High saline water (no freshwater as red color in the figures) represents a denser fluid and no saline water (high freshwater as white color in the figures) represents a lighter fluid. The most significant physical feature in the cross sections (Figures 4.4a and 4.4b) is the existence of *swatch of no ground* (see Figure 4.2). The vertical distribution inside *swatch of no ground* shows that the entire canyon is filled with denser fluid both in dry season and in monsoon. This means there is no vertical infiltration of freshwater inside the canyon even during the monsoon. The sediments are mainly carried in suspension by freshwater from the estuarine system. This sediment laden freshwater

cannot enter inside the canyon, rather it is distributed within the first 50m zone from MSL. This shows that the popular belief of “*all the sediments in the system ultimately deposits in the swatch of no ground*” may not be true. If vertical profile of freshwater plume is taken as a proxy of density stratification, it is seen that stratification exists along the east coast throughout the year. Longitudinal section along the coast (Figures 4.4c and 4.4d) shows dominant influence of Meghna flow in vertical flow structure particularly during the monsoon.

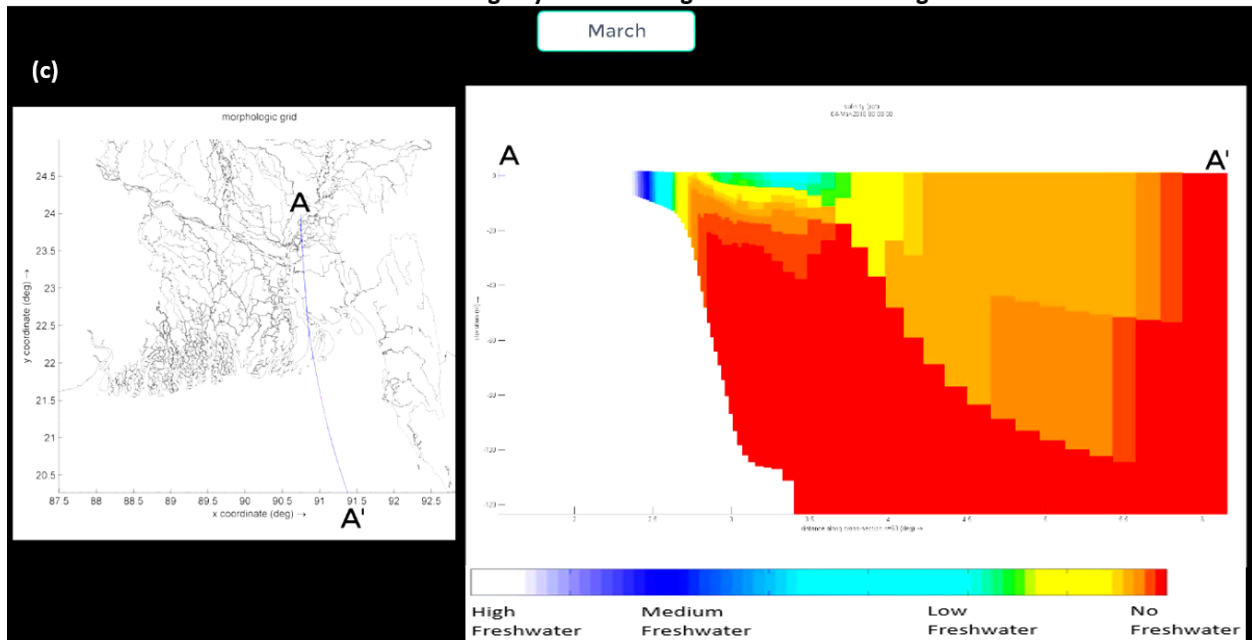
Freshwater Plume during Dry Season: Cross Section along the Coast



Freshwater Plume during Monsoon: Cross Section along the Coast



Freshwater Plume during Dry Season: Longitudinal Section along the Coast



Freshwater Plume during Monsoon: Longitudinal Section along the Coast

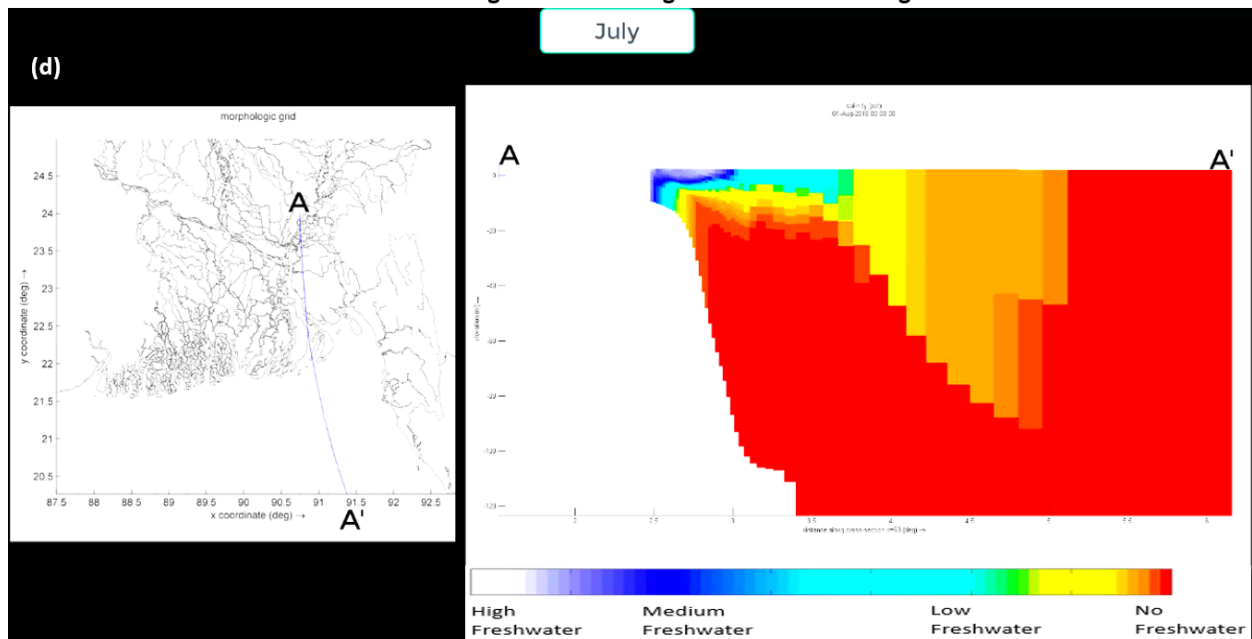


Figure 4.4: Vertical distribution of freshwater plume (a) cross section during dry season (b) cross section during monsoon (c) longitudinal section during dry season (d) longitudinal section during monsoon.

4.3 Simulation of Storm Surge in the Bay of Bengal

Cyclone generated surge in the ocean acts as a hydrodynamic shock and re-distributes the sediments in the ocean. This also drives the oceanic sediments inside the estuarine systems. So, it is extremely important to simulate cyclone and storm surge events in the Bay of Bengal.

4.3.1 Cyclone model

It is observed during model calibration that model performance deteriorates when synoptic wind field is not specified all along the model domain. To examine the model performance, wind fields are generated from 3 different approaches (a) Delft-dash-board (d) direct application of Holland's equation (c) CCMP data. Following relation is used for Holland's equation:

$$V_g(r) = \sqrt{\left(\frac{R_w}{r}\right)^B V_{max}^2 \exp\left(1 - \left(\frac{R_w}{r}\right)^B\right) + r^2 \frac{f^2}{4} - \frac{rf}{2}} \quad (1)$$

Where

$V_g(r)$ is the geostatic wind velocity (km/hr)

R_w is the radius of maximum wind (km)

r is the distance from center of the cyclone (km)

V_{max} is the maximum wind speed (km/hr)

f is the Coriolis parameter

B is the parameter in Holland's equation

We have experimented the wind field by using different B values for a particular cyclone size (R_w). For 1991 cyclone, the cyclone size used is 63 km (As Salek, 1998). A comparison of cyclone wind field generated from Delft Dashboard, Holland's equation and CCMP data for 1991 cyclone is shown in Figure 4.5. CCMP data merges observed winds and simulated winds from various sources. We are still experimenting by using wind fields computed by different methodologies. We expect to present the conclusive results in the Final report.

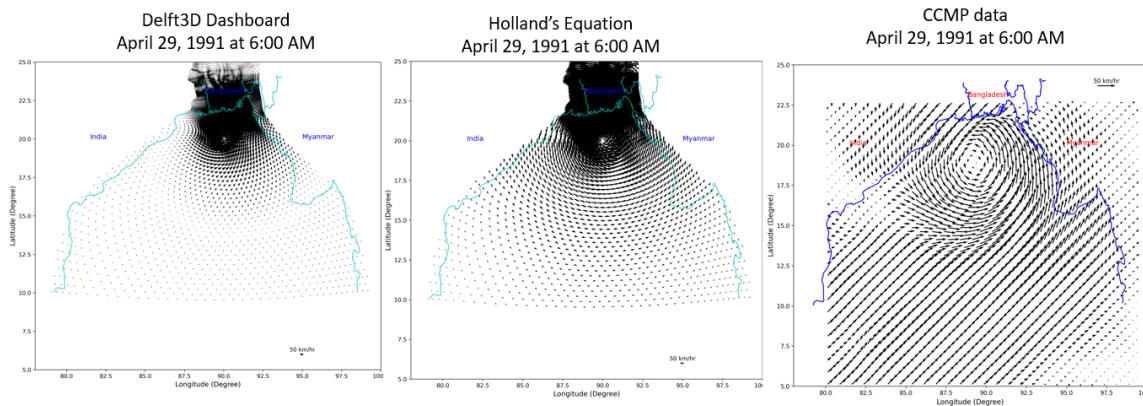


Figure 4.5 : Comparison of cyclone wind field generated from Delft3D Dashboard, Holland's equation and CCMP data.

4.3.2 Past cyclone scenarios

Total 12 past cyclonic events in the last 30 years (1990 – 2020) are simulated. For each of the simulations, results are presented for cyclone wind field, sea surface elevation and water level time series in a specific location (here in Kutubdia-1, see [Figure 3.6](#) for location of Kutubdia-1). Out of 12 simulated events, 9 cyclones made landfall on Bangladesh coast. Among these cyclones, 1991 cyclone was the strongest one, with a wind speed of 235 km/hour. 1991 cyclone crosses the Chittagong coast on April 29, 1991 during the time when tidal phase was spring tide high water in landfall location. SIDR was another strong cyclone with a wind speed of about 213 km/hour which made landfall on Khulna-Barishal coast on November 15, 2007.

Normally wind speed of a cyclone is the maximum before the landfall of the cyclone when it is still in the ocean. To show the maximum impact on the sea, snapshots of wind fields and water level fields are shown during the time when wind speed of the cyclone is the maximum over the ocean. This is the instant when sediment transport in the ocean is expected to be maximum also. The time series of water level shows that maximum water level largely depends on the landfall location of the cyclone and tidal phase in that location. For example, out of 12 past cyclones, maximum water level at Kutubdia-1 location occurs only for 1991 Chittagong cyclone, cyclone MORA and cyclone AMPHAN.

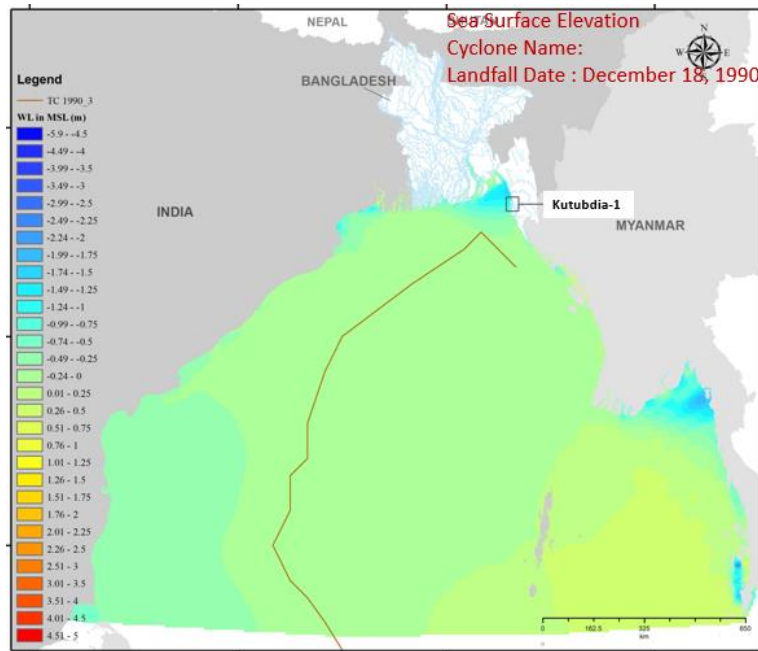
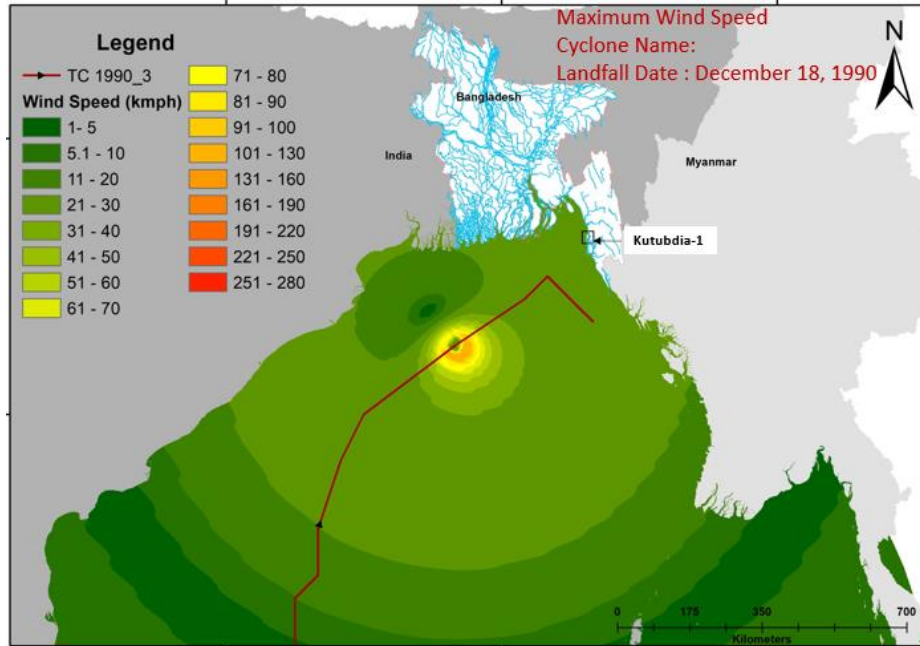


Figure 4.6: Cyclone wind speed (top), sea surface elevation (middle) and water level variation at Kutubdia-1 station during unnamed cyclone which made landfall on December 18, 1990.

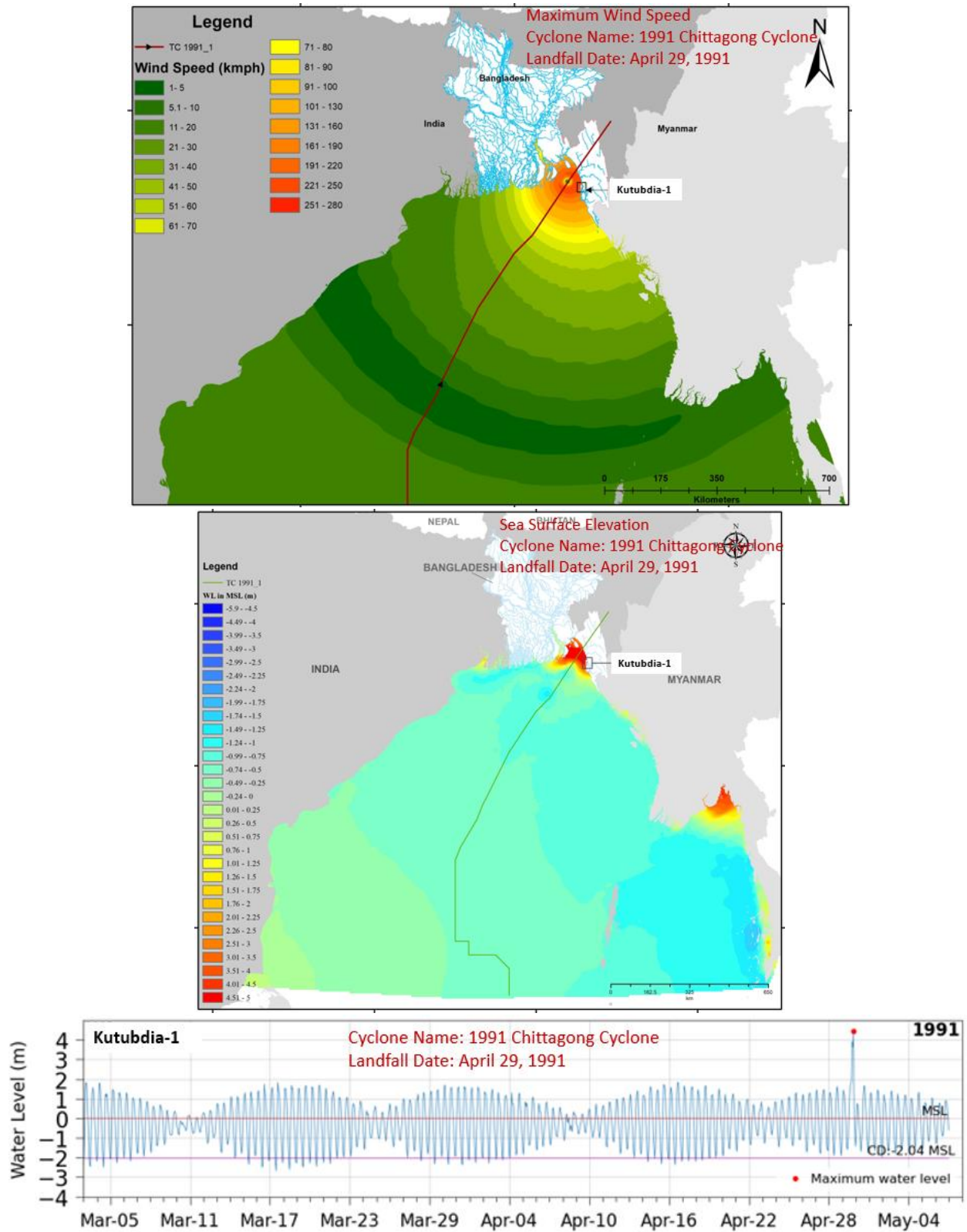


Figure 4.7: Cyclone wind speed (top), sea surface elevation (middle) and water level variation at Kutubdia-1 station during 1991 Chittagong cyclone which made landfall on April 29, 1991.

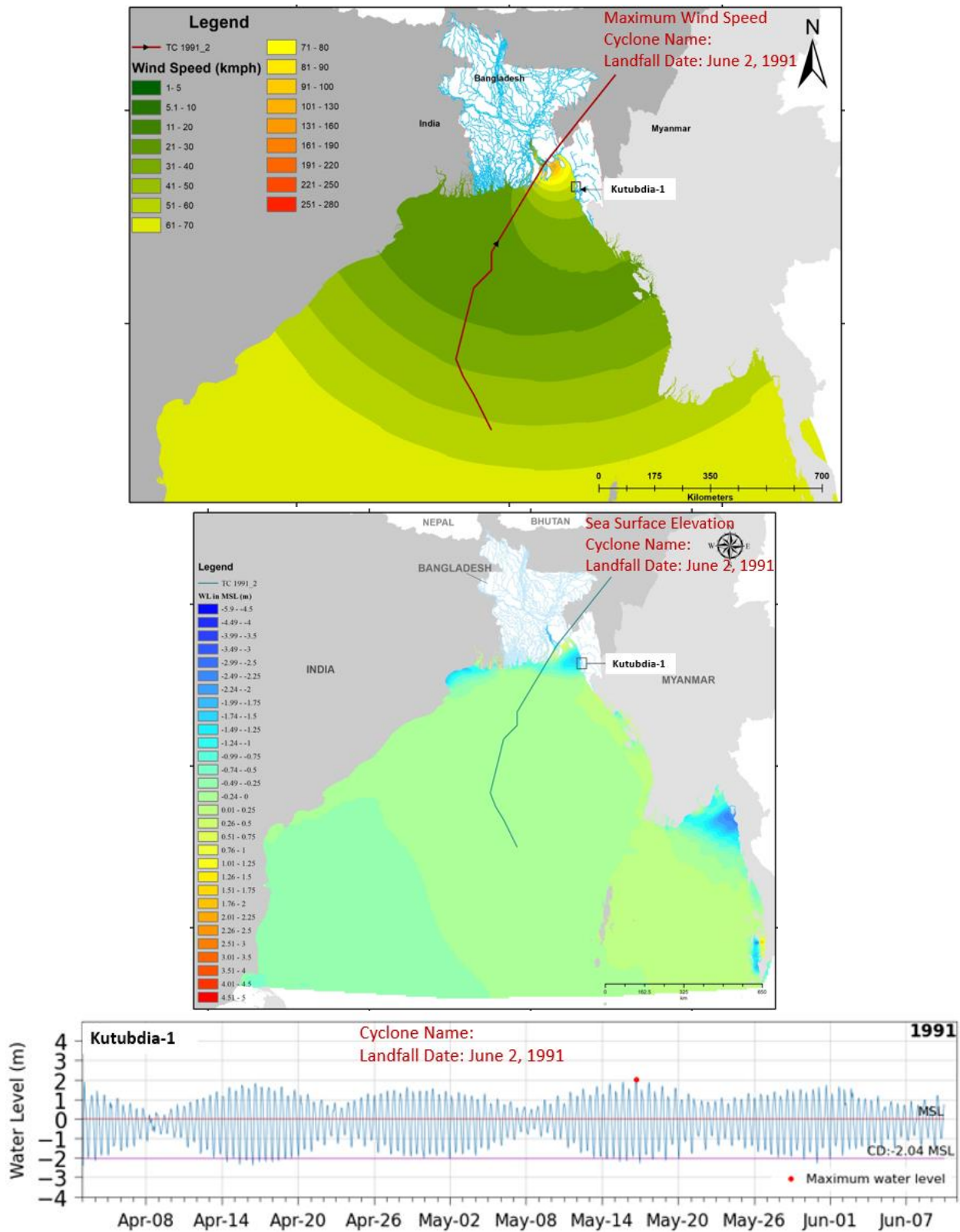


Figure 4.8: Cyclone wind speed (top), sea surface elevation (middle) and water level variation at Kutubdia-1 station during unnamed cyclone which made landfall on June 2, 1991.

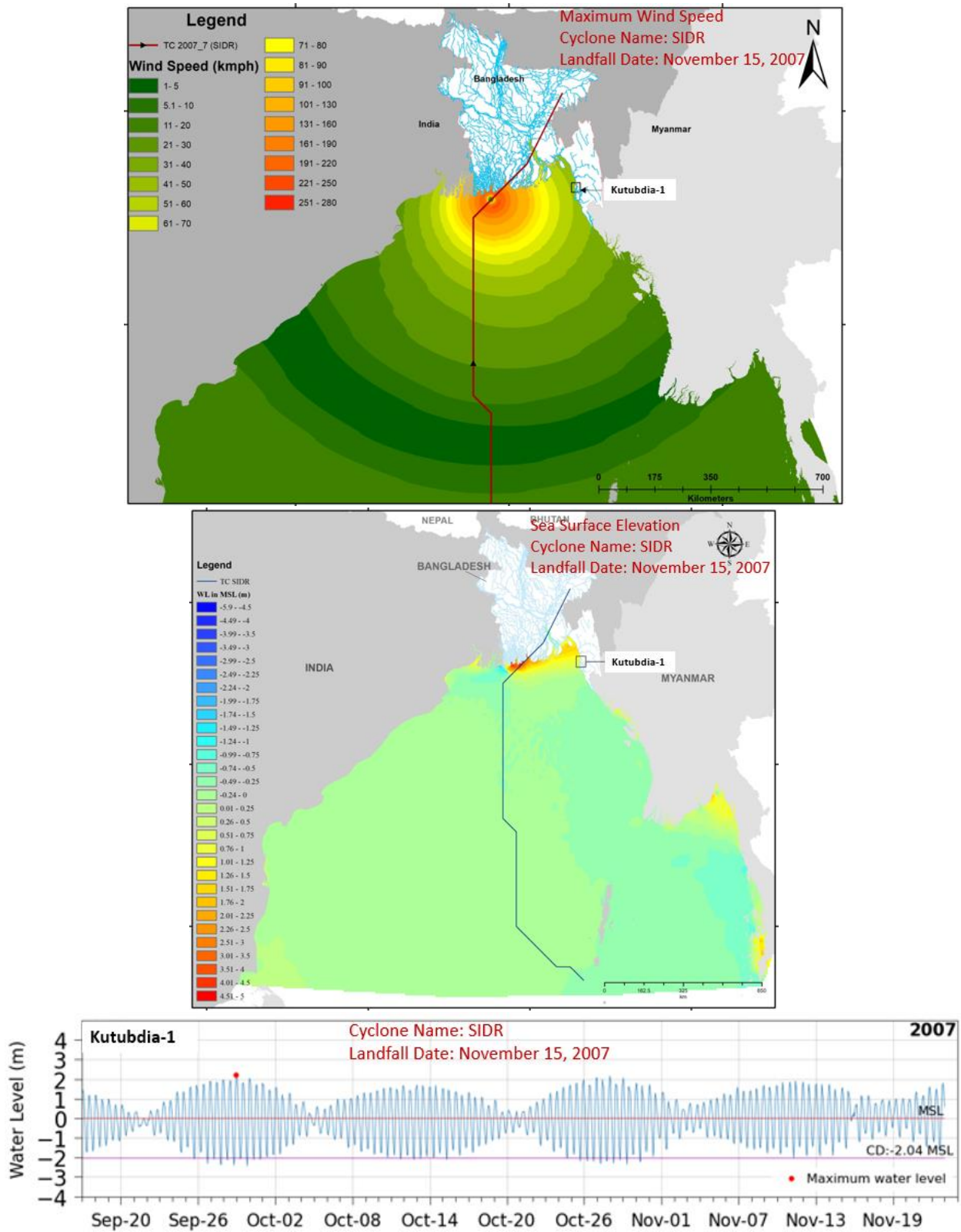


Figure 4.9: Cyclone wind speed (top), sea surface elevation (middle) and water level variation at Kutubdia-1 station during cyclone SIDR which made landfall on November 15, 2007.

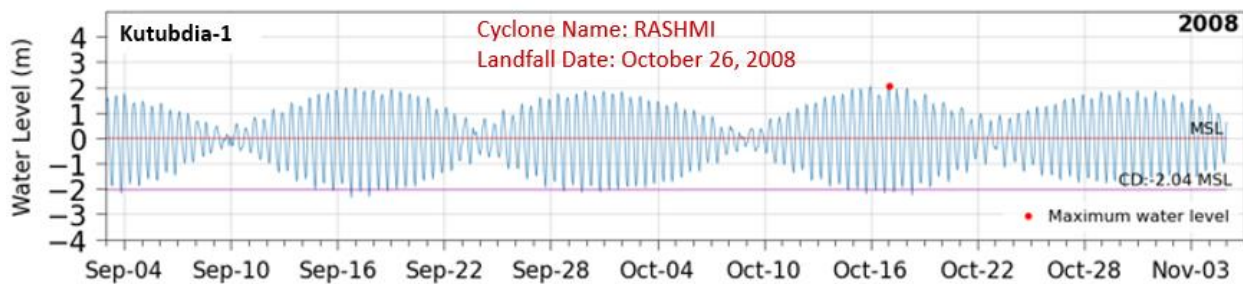
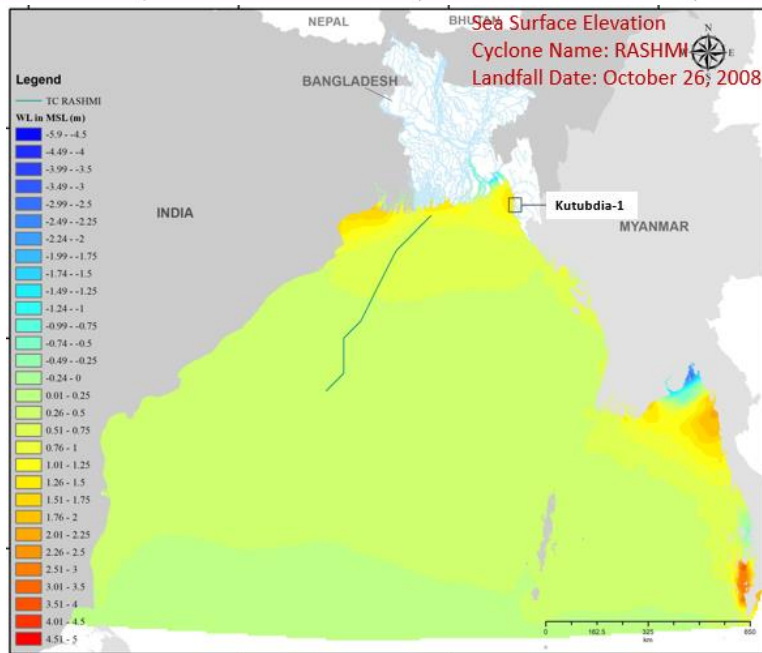
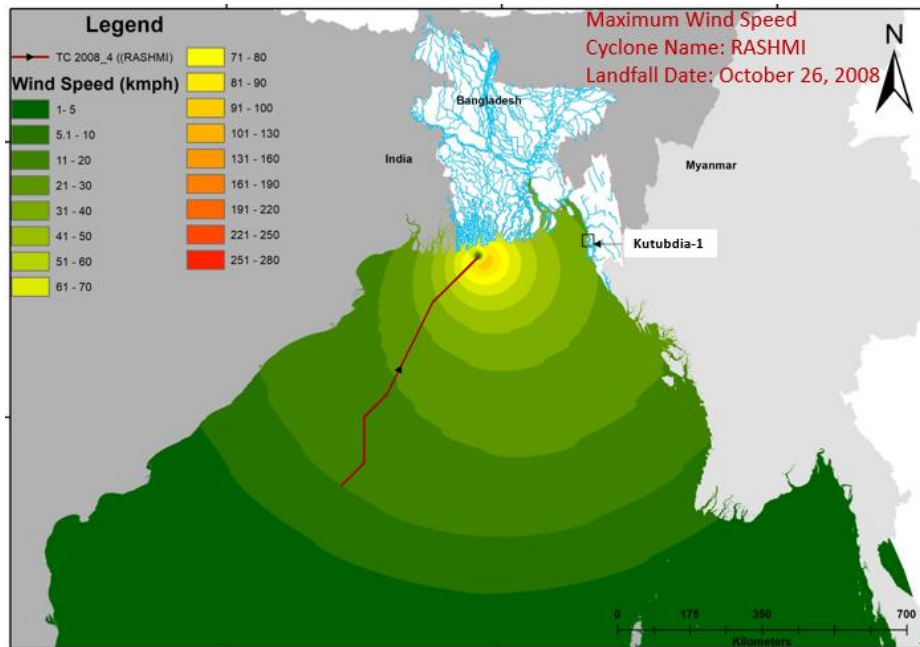


Figure 4.10: Cyclone wind speed (top), sea surface elevation (middle) and water level variation at Kutubdia-1 station during cyclone RASHMI which made landfall on October 26, 2008.

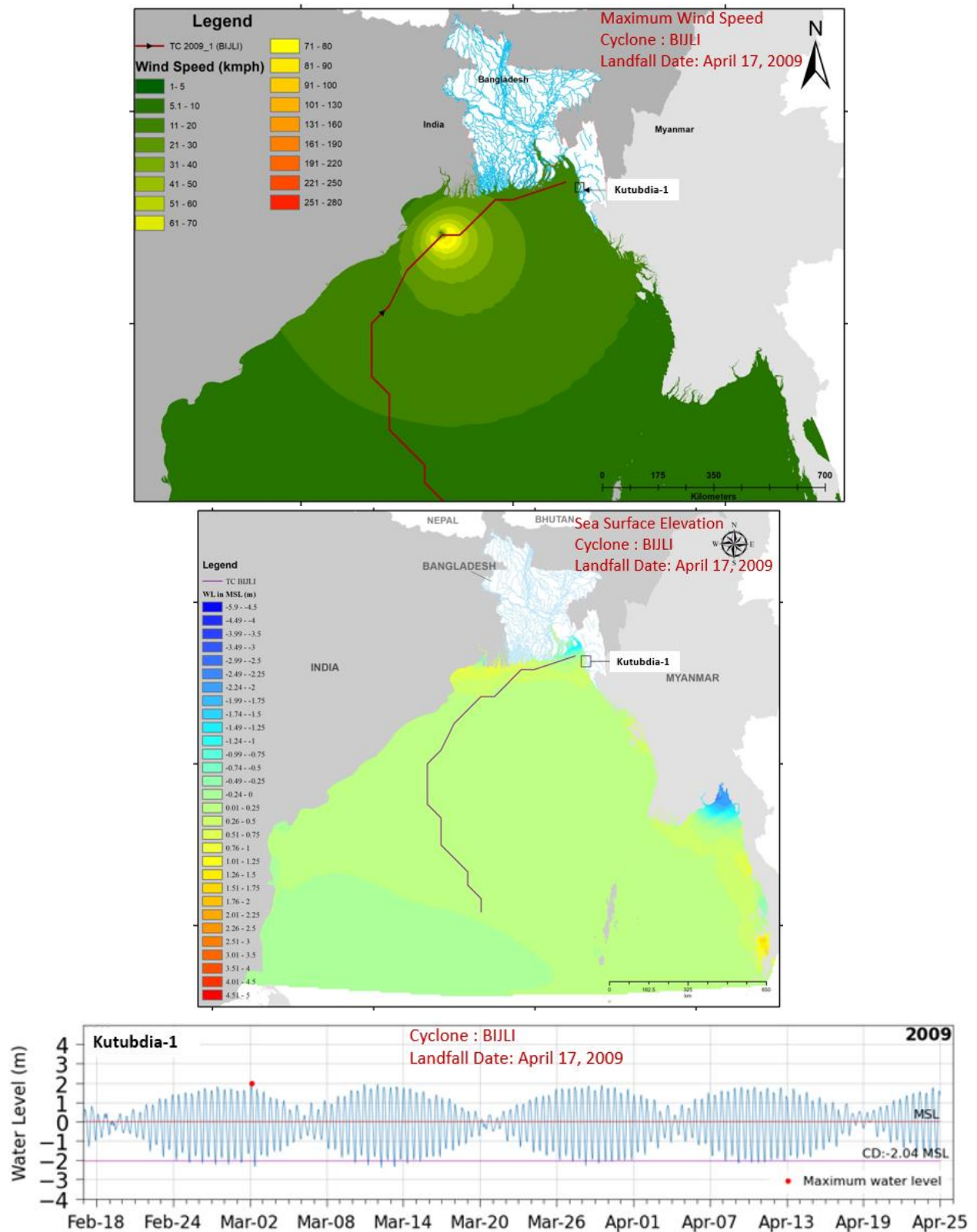


Figure 4.11: Cyclone wind speed (top), sea surface elevation (middle) and water level variation at Kutubdia-1 station during cyclone BIJLI which made landfall on April 17, 2009.

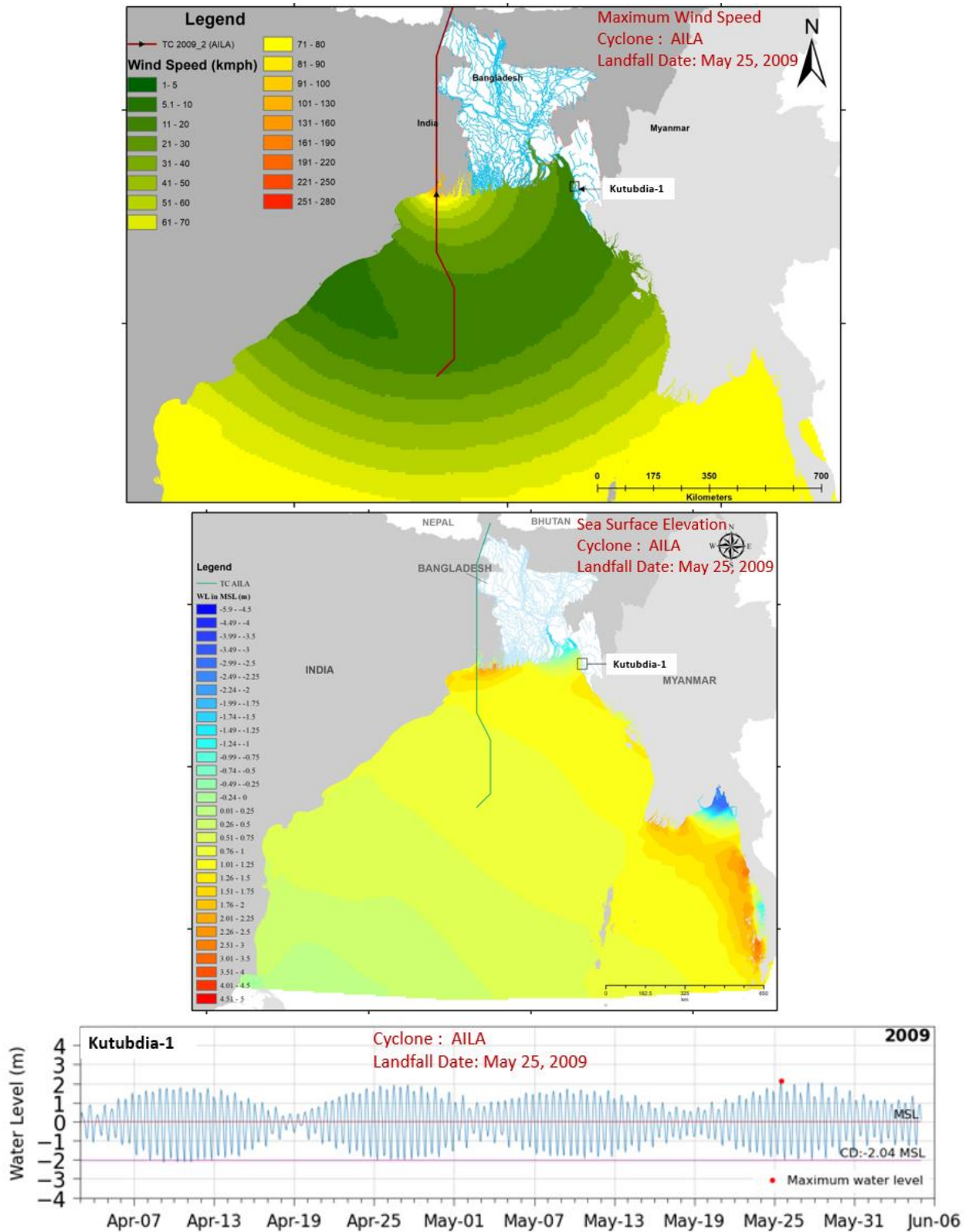


Figure 4.12: Cyclone wind speed (top), sea surface elevation (middle) and water level variation at Kutubdia-1 station during cyclone AILA which made landfall on May 25, 2009.

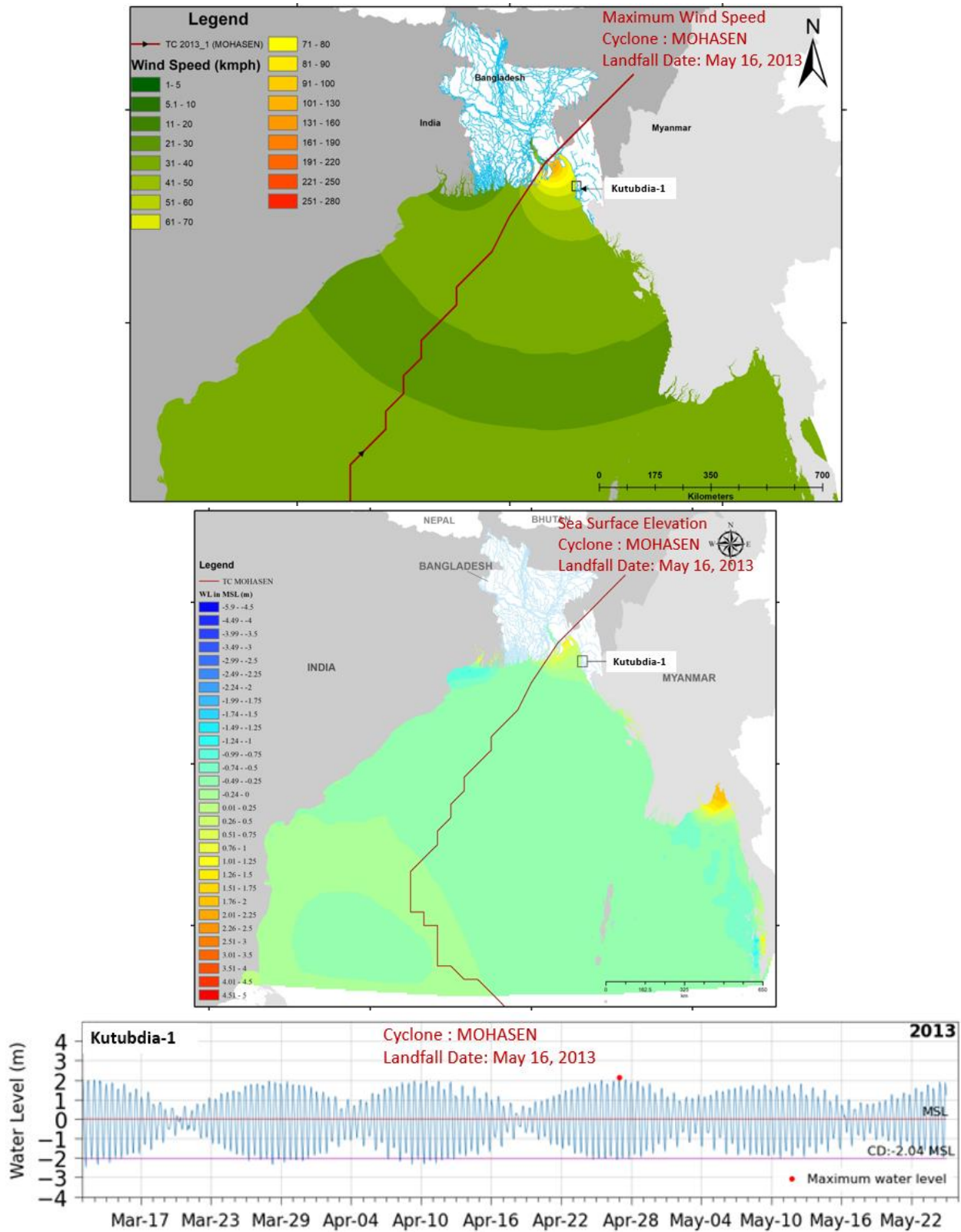


Figure 4.13: Cyclone wind speed (top), sea surface elevation (middle) and water level variation at Kutubdia-1 station during cyclone MOHASEN which made landfall on May 16, 2013.

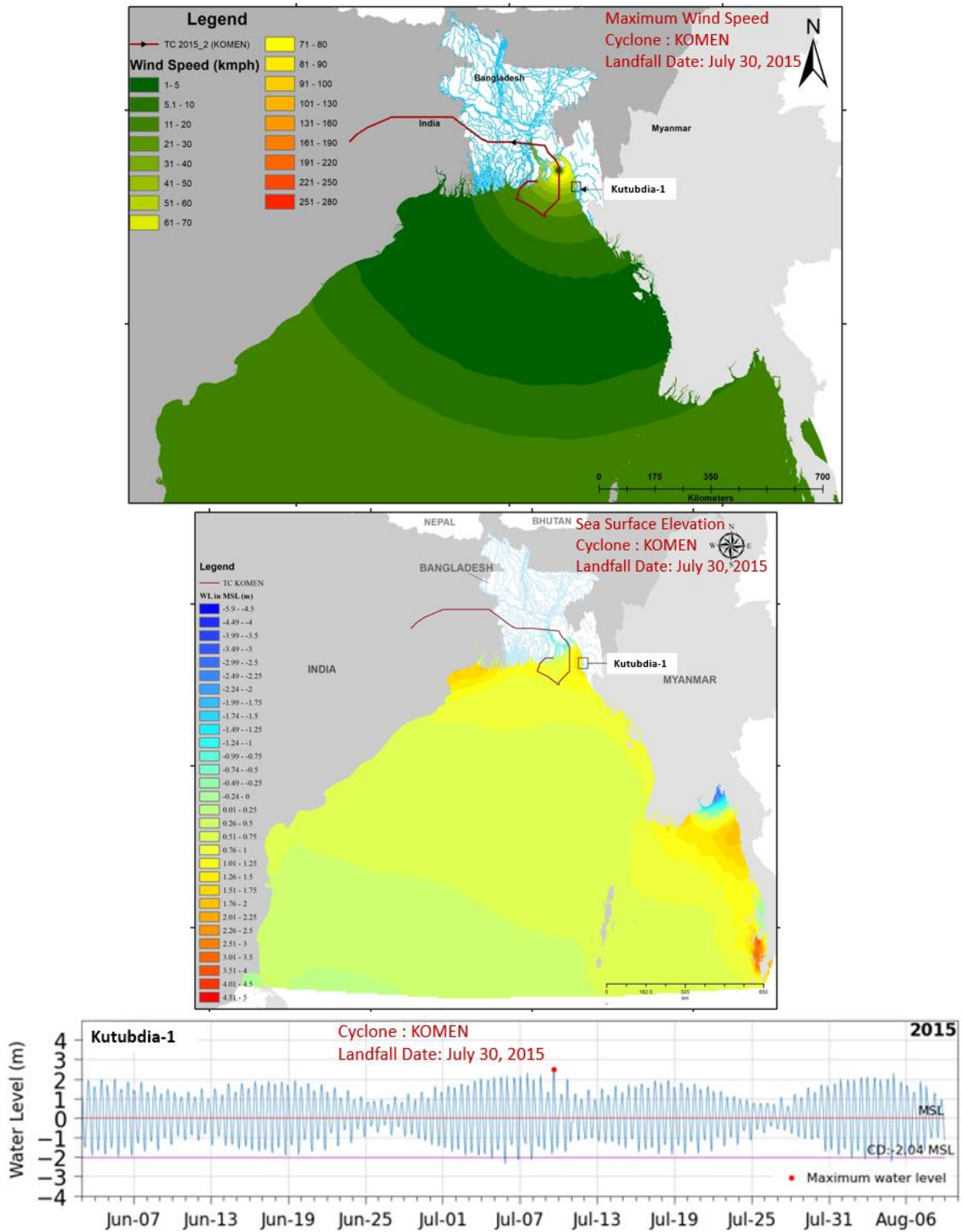


Figure 4.14: Cyclone wind speed (top), sea surface elevation (middle) and water level variation at Kutubdia-1 station during cyclone KOMEN which made landfall on July 30, 2015.

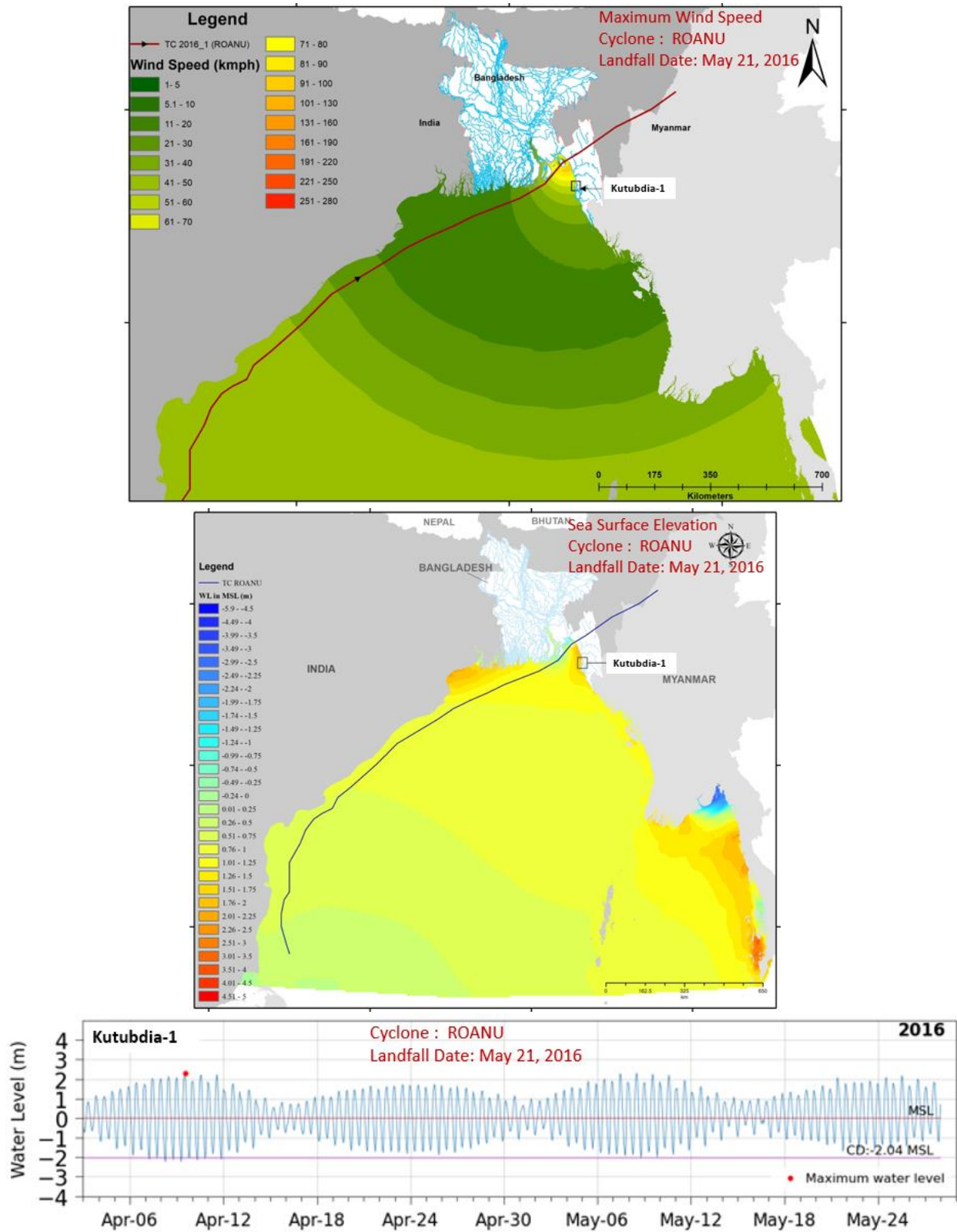


Figure 4.15: Cyclone wind speed (top), sea surface elevation (middle) and water level variation at Kutubdia-1 station during cyclone ROANU which made landfall on May 21, 2016.

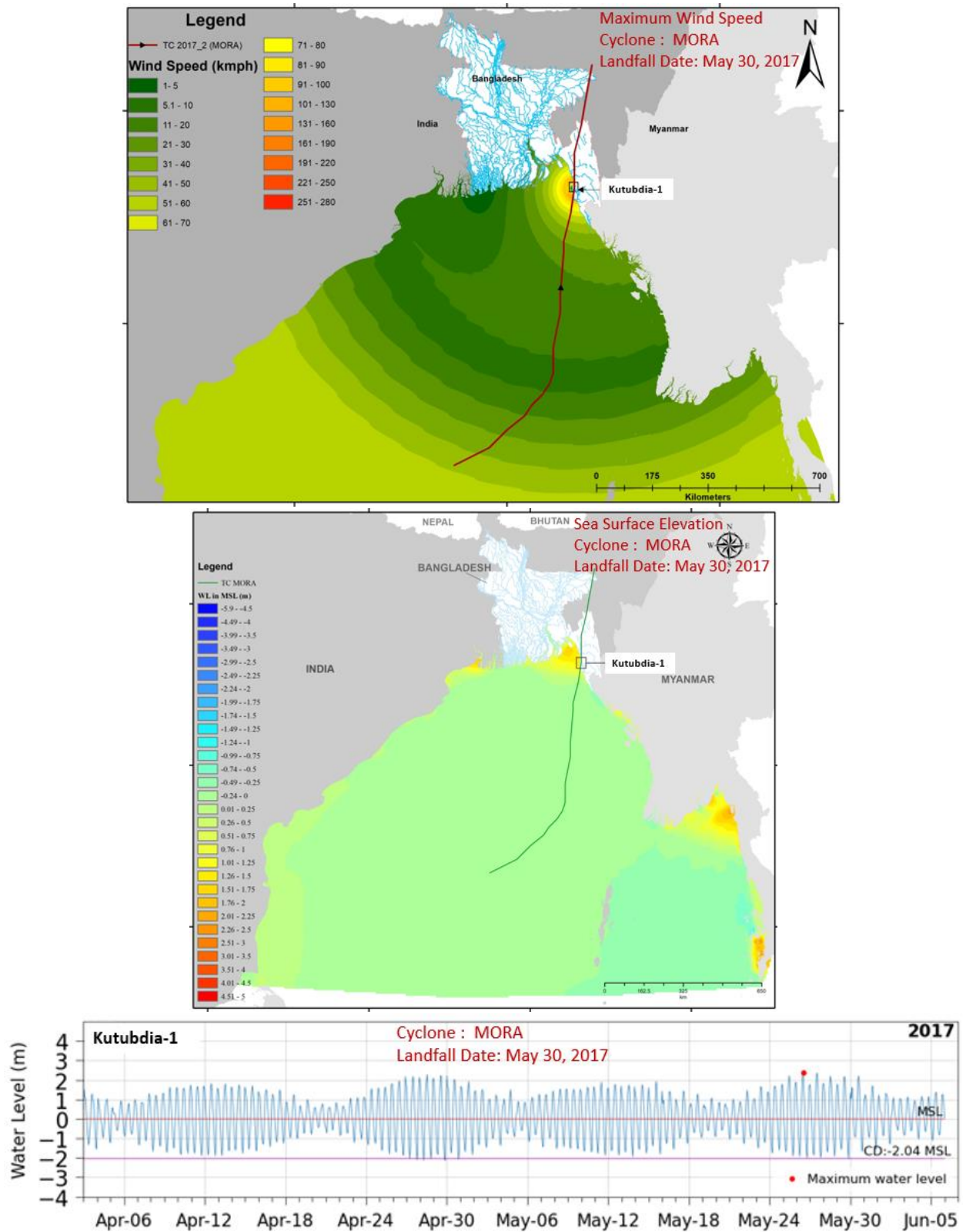


Figure 4.16: Cyclone wind speed (top), sea surface elevation (middle) and water level variation at Kutubdia-1 station during cyclone MORA which made landfall on May 30, 2017.

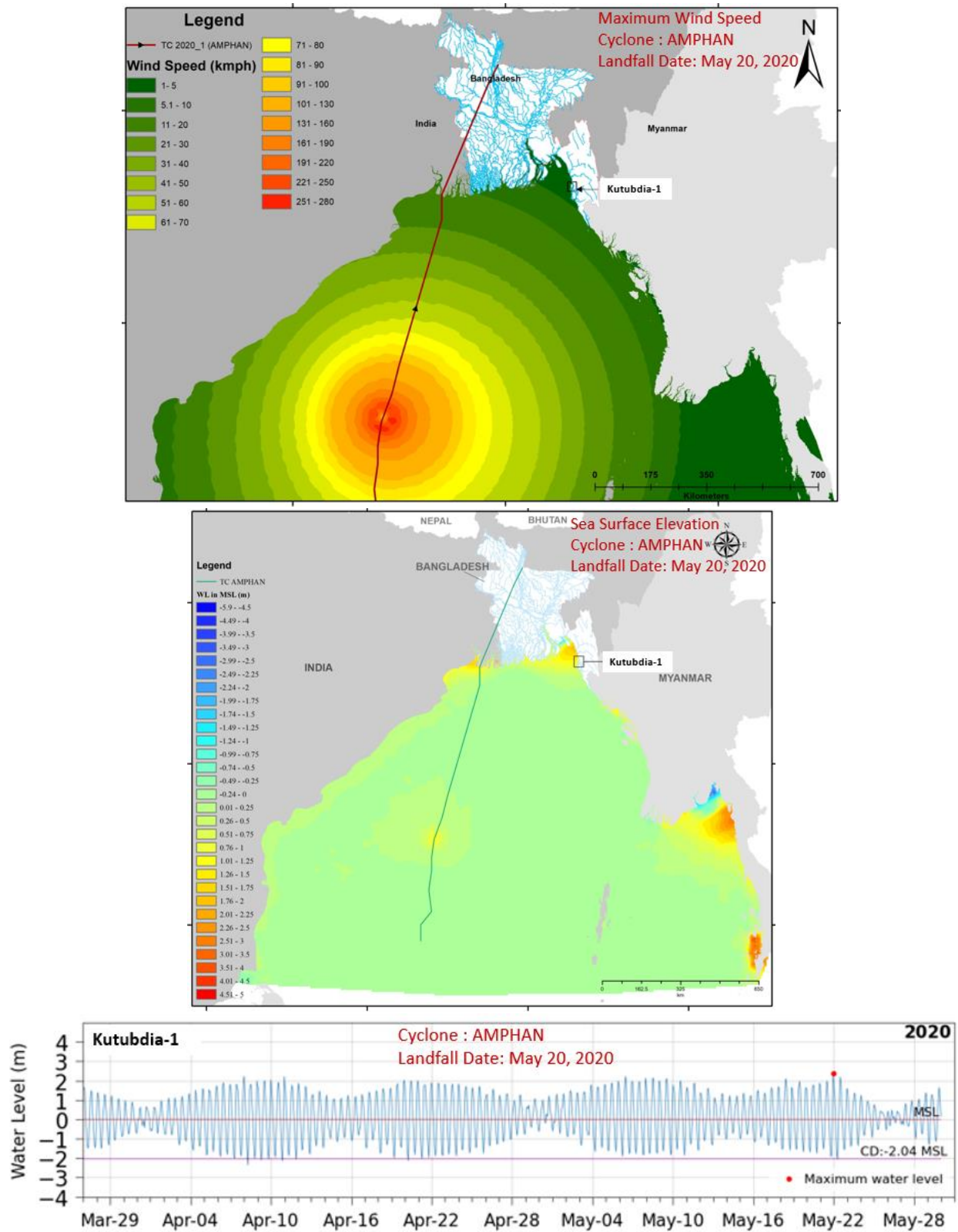


Figure 4.17: Cyclone wind speed (top), sea surface elevation (middle) and water level variation at Kutubdia-1 station during cyclone AMPHAN which made landfall on May 20, 2020.

4.3.3 Effect of cyclone wind on tidal current

Cyclones create a hydrodynamic shock (sudden increase of velocity) in the system. It is generally believed that large volume of sediments re-enter into the estuarine systems during a cyclonic event. To investigate this, a numerical experiment is conducted where two scenarios are created with model simulation (Figure 4.18) – the one *without* cyclone and the other *with* cyclone by keeping all other physical and hydrodynamic parameters same. The selected cyclone for this experiment is cyclone SIDR. The figures show velocity fields all along the coast. The results show that cyclonic wind suddenly increase the flood flow velocity (hydrodynamic shock) compared to *without cyclone* scenario. As sediment flux is related to water velocity, increased water velocity creates increased sediment flux for the same sediment concentration. So, for a similar sediment regime, cyclonic event creates increased sediment flux. This will drive increased volume of sediments to re-enter into the estuarine systems through increased flood flow velocity created by cyclone. This proves that the general belief of impact of cyclones on increased sediment flow into the system is correct.

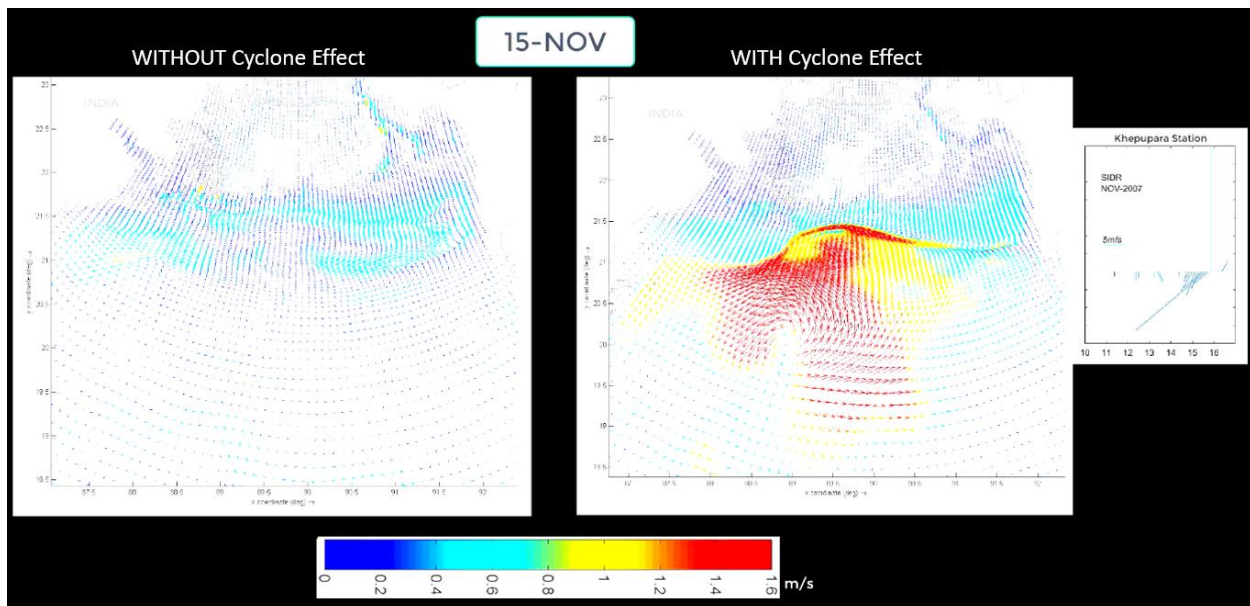


Figure 4.18: Cyclone effect on water velocity in the Bay of Bengal. The example shown here is for cyclone SIDR. The left figure shows the case without cyclone and the right figure shows the case with cyclone. The right figure is supplemented by a wind stick diagram at Khepupara wind station of BMD.

Flux is compared along four estuarine mouths by generating three hydrodynamic forcing: (1) Wind and Tide (2) Tide only (3) Cyclone SIDR. The results (Figure 4.19) show that the maximum increase of flux occurs along the Lower Meghna mouth during cyclone SIDR. This increased flux will drive increased amount of sediments through the Lower Meghna mouth. The location and amount of sediment flux depends on the cyclone landfall location and cyclone strength.

Flux Across Selected Sections along the Coast

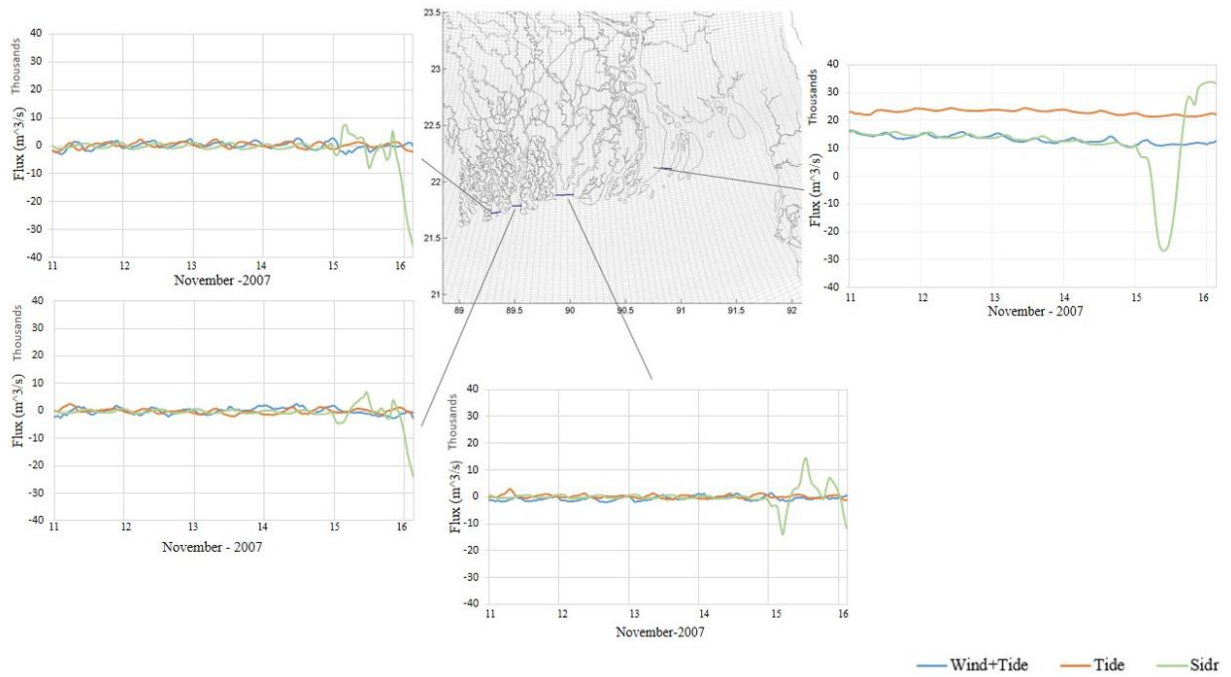


Figure 4.19: Flux along selected sections along the coast for three different hydrodynamic forcing: wind and tide, tide only and cyclone.

Effects of these hydrodynamic forcing on the bed shear stress of entire ocean and estuarine mouths are shown in Figure 4.20. The results show gradual increase of bed shear stress along the estuarine mouths when the forcing increases from tide, tide & wind, and cyclone depicting the increased sediment flux during cyclonic events.

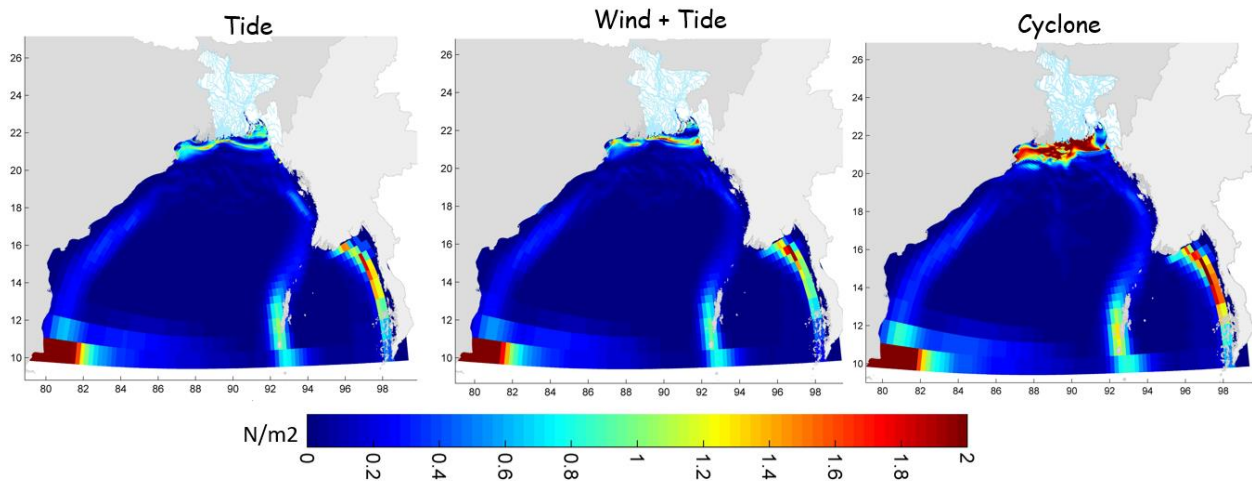


Figure 4.20: Variation of bed shear stress along the ocean and estuarine mouths during three different hydrodynamic forcing: tide, tide & wind, and cyclone.

4.4 Simulation of Land Inundation during Monsoon Flood in Bangladesh

BDM is applied to simulate 1998 flood for the entire country. Comparison between flood extent of model simulation and satellite image is shown in Figure 4.21. The result shows that model can simulate basic flooding pattern very well. The flooding by the major river systems are well reproduced. Flooding is observed in the north-eastern haor systems in the Sylhet region and the central part of the country by Brahmaputra-Jamuna system. In the coastal region, fluvial flooding is observed in the central part of unprotected region. We are still refining to resolve few issues and expecting to get a better model result. The final result will be presented in the final report of the project.

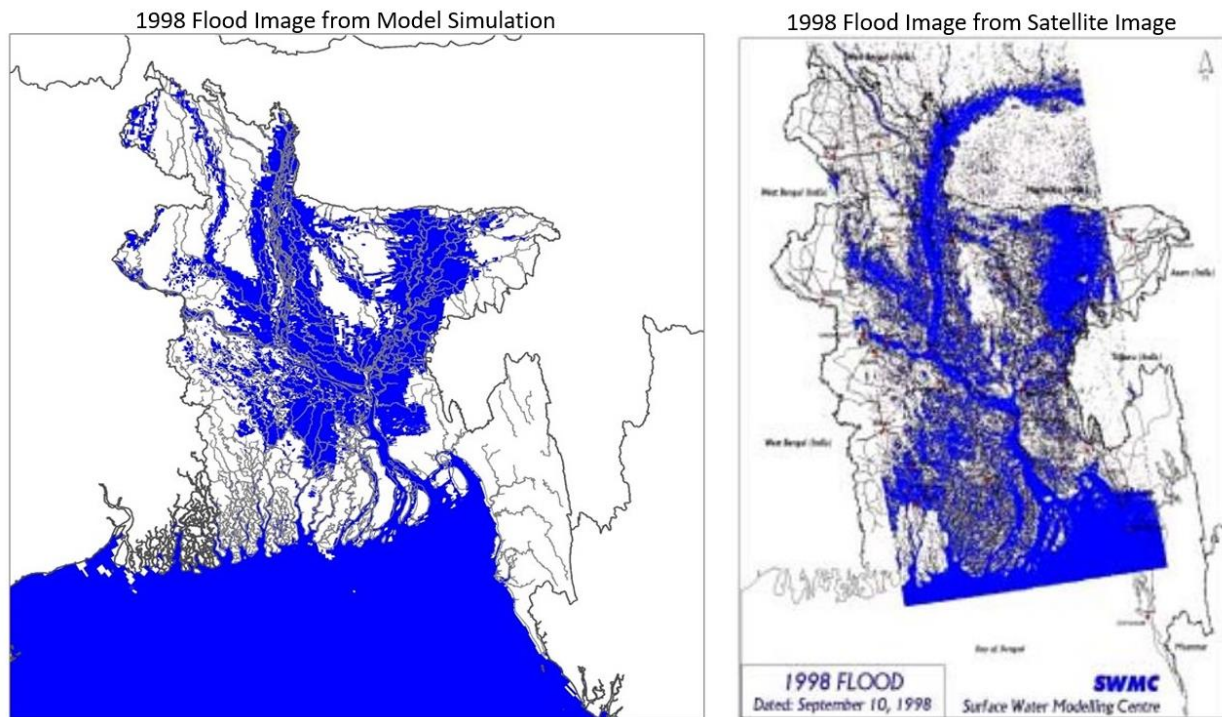
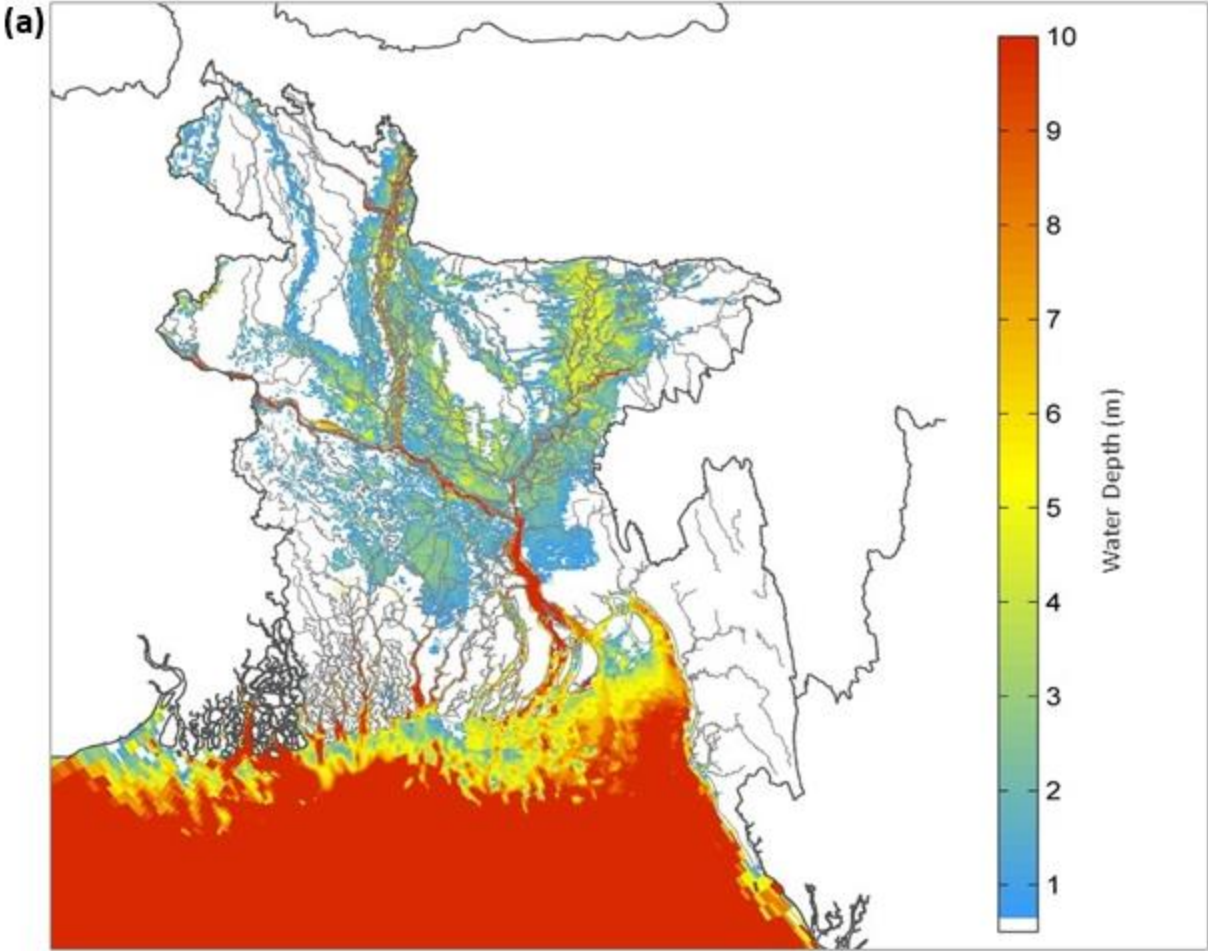


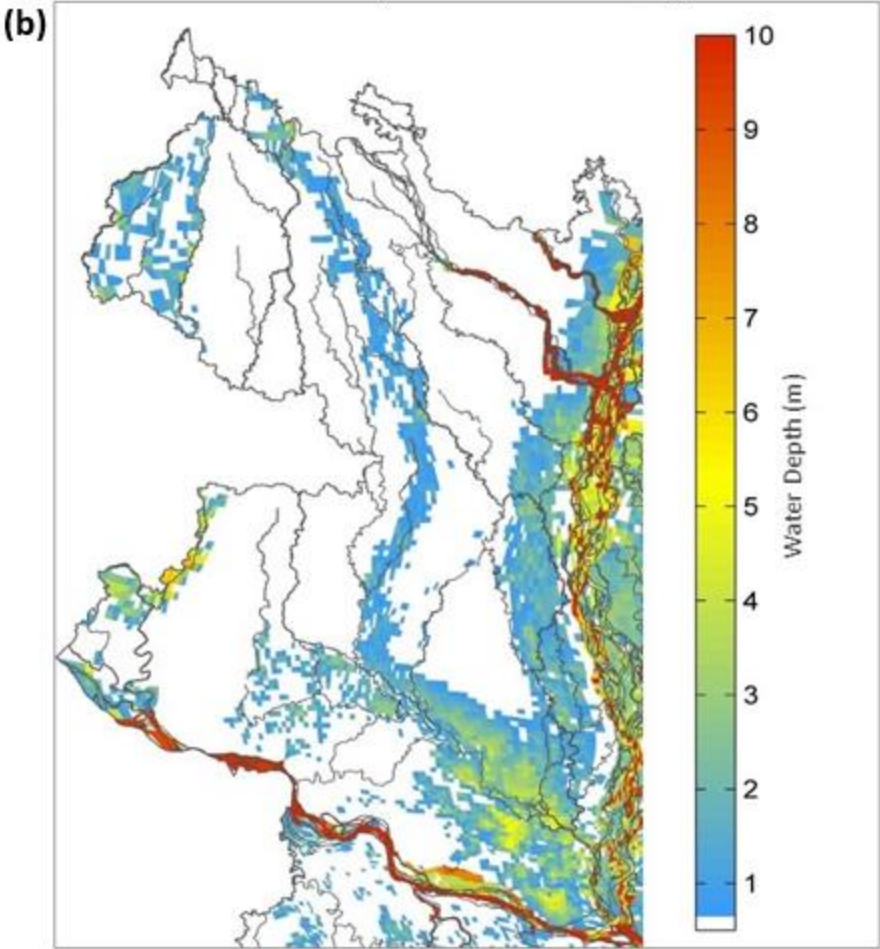
Figure 4.21: Comparison of 1998 flood extent between model simulation (left) and satellite (right).

Model simulated 1998 flood depth maps for the entire country and for 7 different regions are shown in Figures 4.22 (a-h).

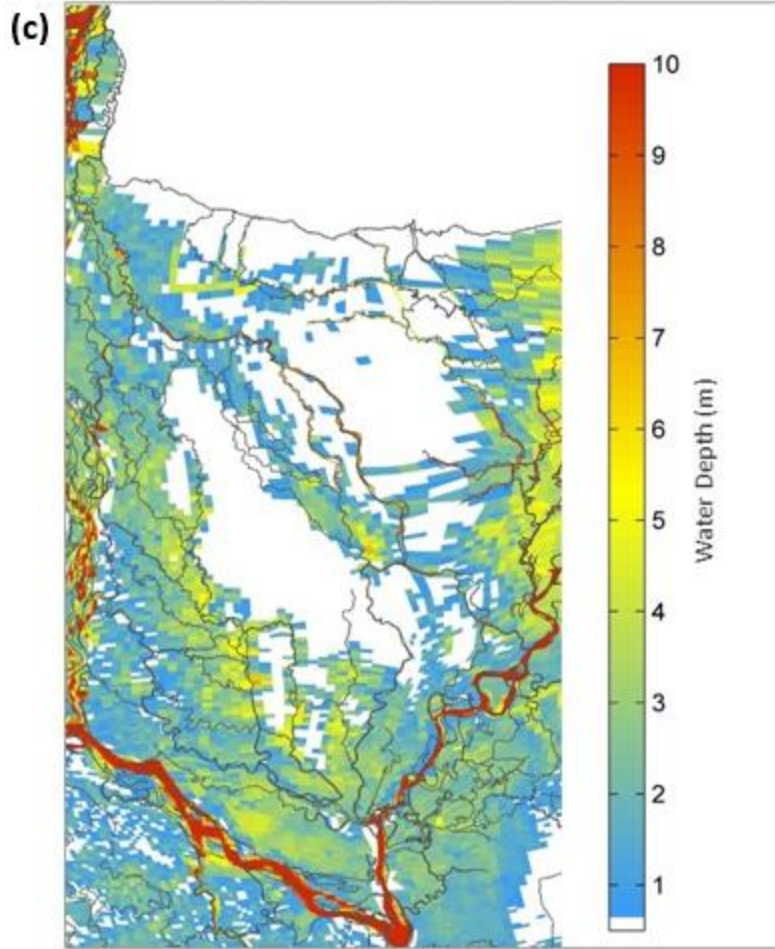
Flood Depth in entire Bangladesh



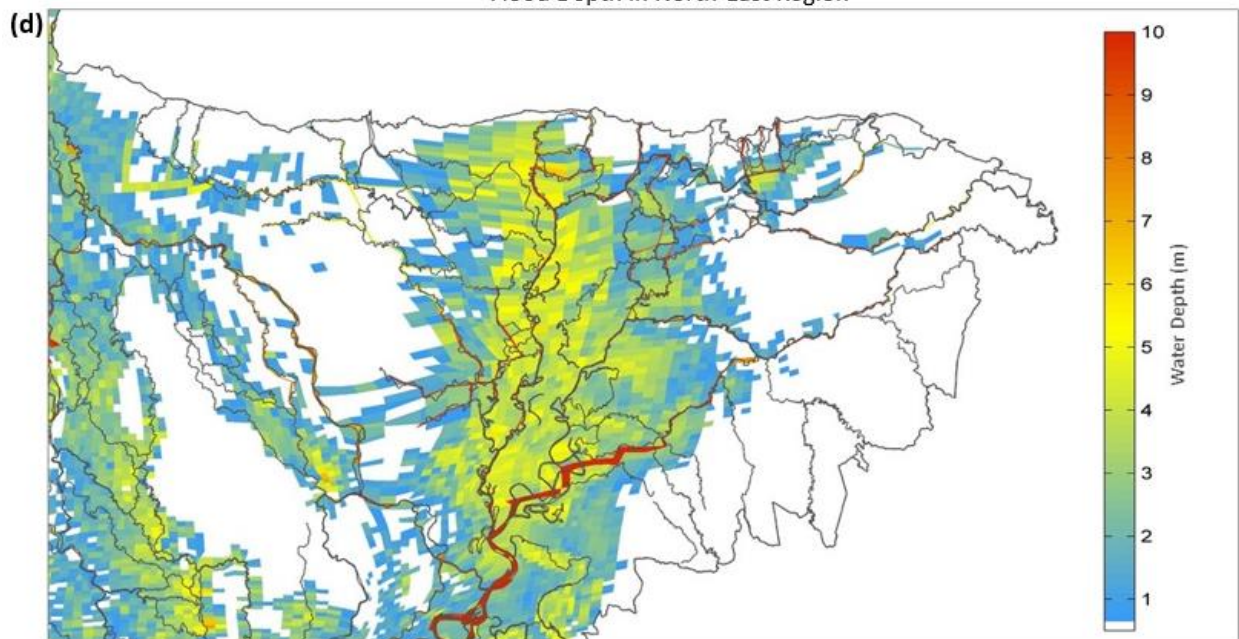
Flood Depth in North-West Region



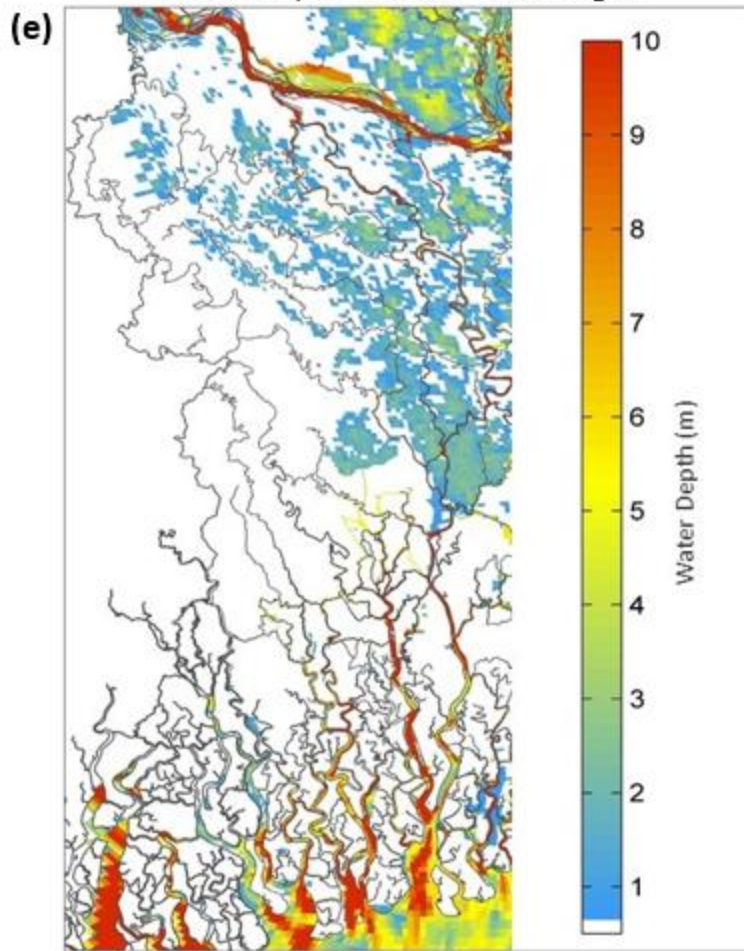
Flood Depth in North-Central Region



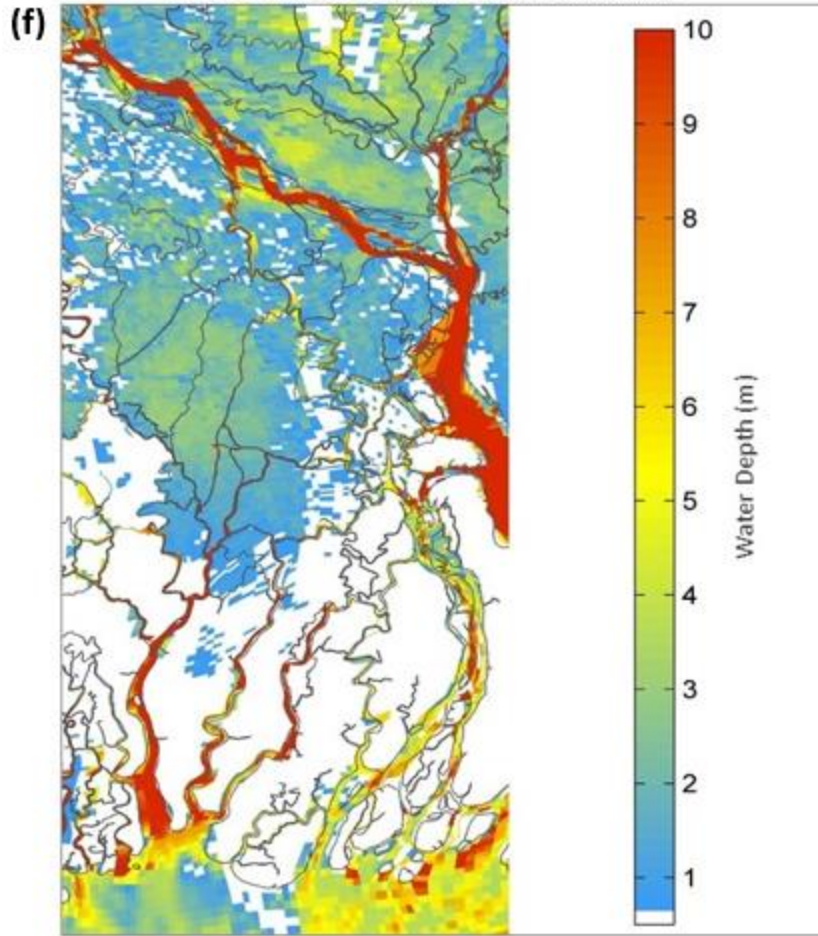
Flood Depth in North-East Region



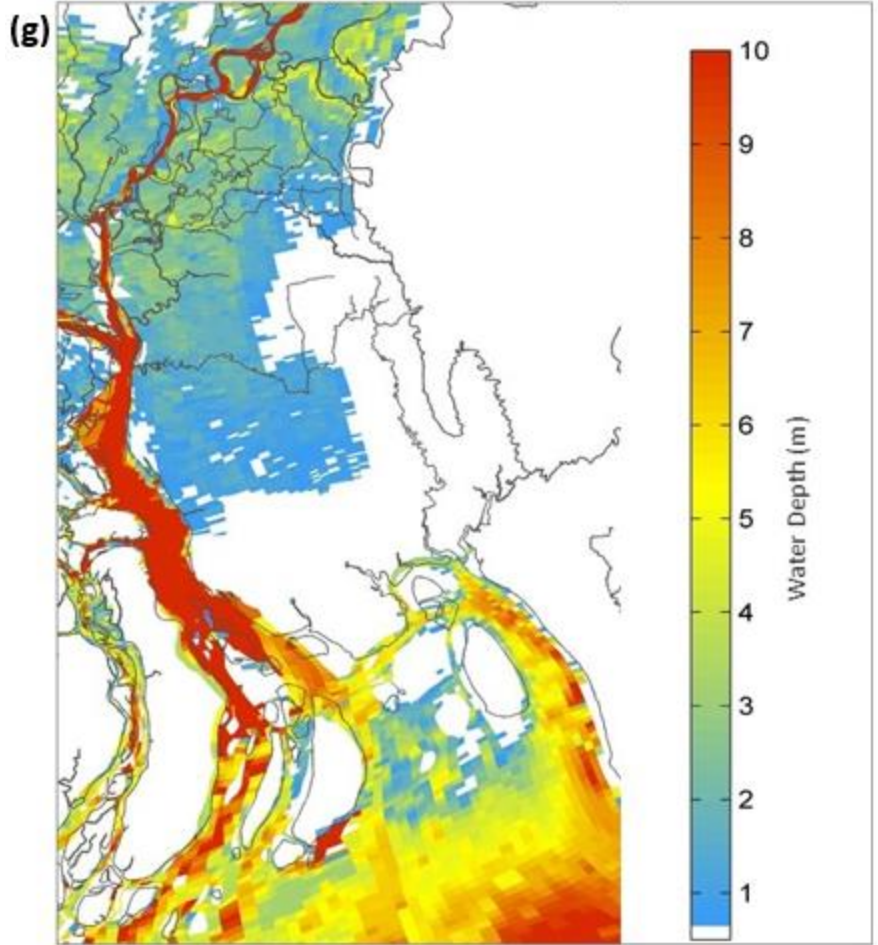
Flood Depth in South-West Region

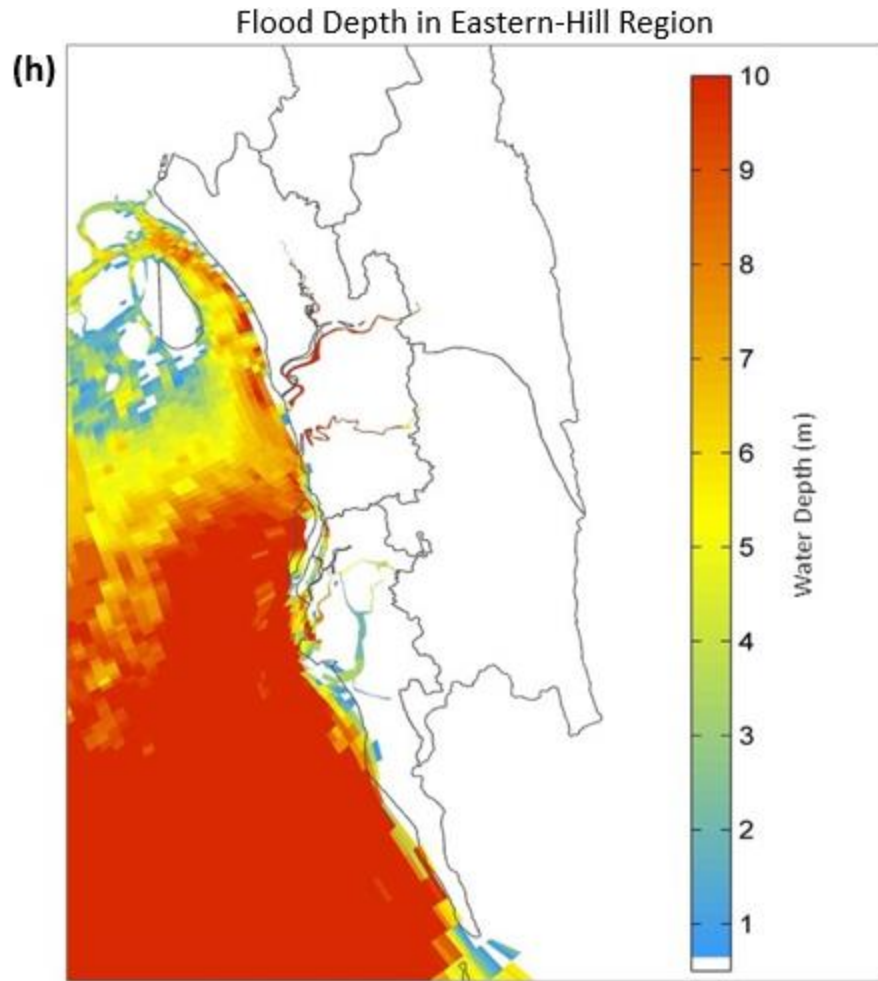


Flood Depth in South-Central Region



Flood Depth in South-East Region





Figures 4.22 : Flood depth maps for the (a) entire country (b) north-west region (c) north-central region (d) north-east region (e) south-west region (f) south-central region (g) south-east region and (h) eastern-hill region.

4.5 Simulation of Land Inundation during Storm Surge Flood in the Coast

BDM is applied to simulate inundation of land during cyclone SIDR. Comparison of land inundation depth between model simulation and inundation extent is shown in [Figure 4.23](#). Both the model result and the satellite image show that there is no land inundation inside polders. Inundation is observed only in unprotected regions.

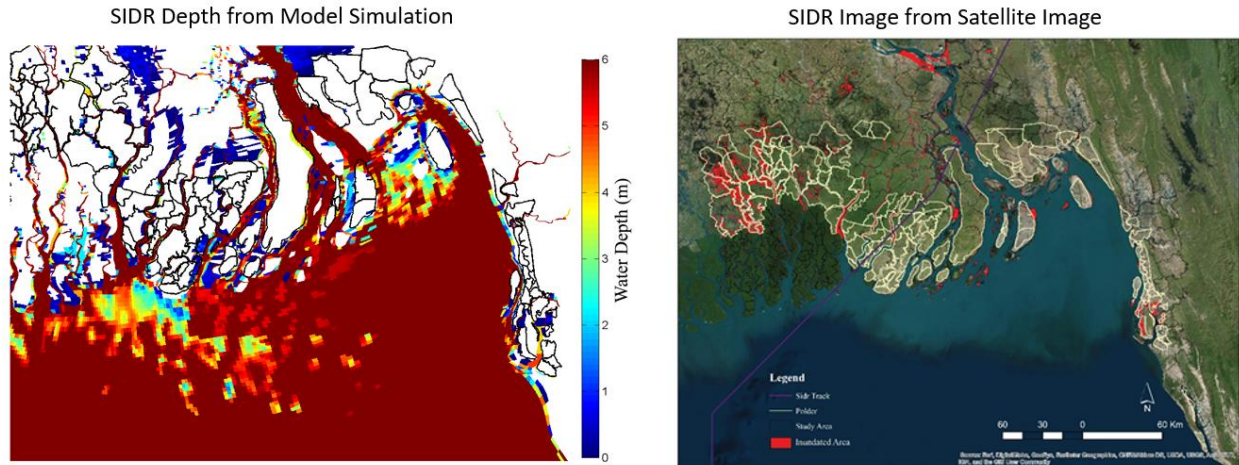


Figure 4.23: Inundation in the coast simulated from BDM (left image) and extracted from satellite image (right image).

4.6 Simulation of Sedimentation

Simulation of sedimentation is made by applying the morphology module of BDM. The results show the sediment movement path along the coast and sedimentation in the floodplains of the entire riverine and estuarine systems.

4.6.1 Sediment movement path along the coast

To determine sediment movement path along the coast, sediment is released from the main inflow systems and its movement is traced all along its travel path (Figure 4.24). The sediment movement path shows that the sediments from the Ganges-Brahmaputra-Meghna systems discharges into the Bay of Bengal through the Lower Meghna mouth, turn clockwise, part of the sediments deposit in the ocean and the rest of the sediments re-enter into the western estuarine systems. During cyclonic events, this equilibrium breaks down and bulk amount of sediments re-enters into the system through the estuary mouths.

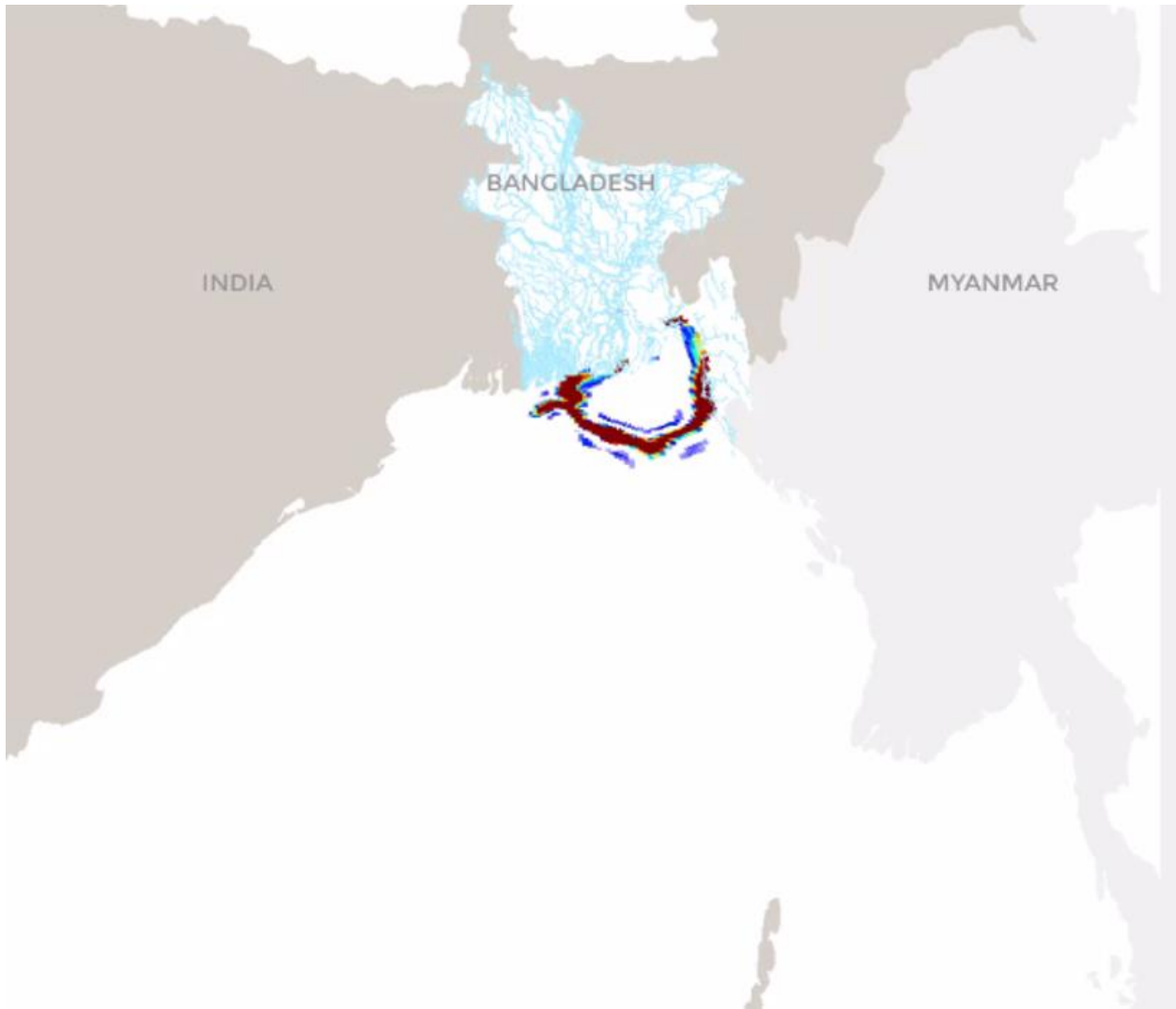
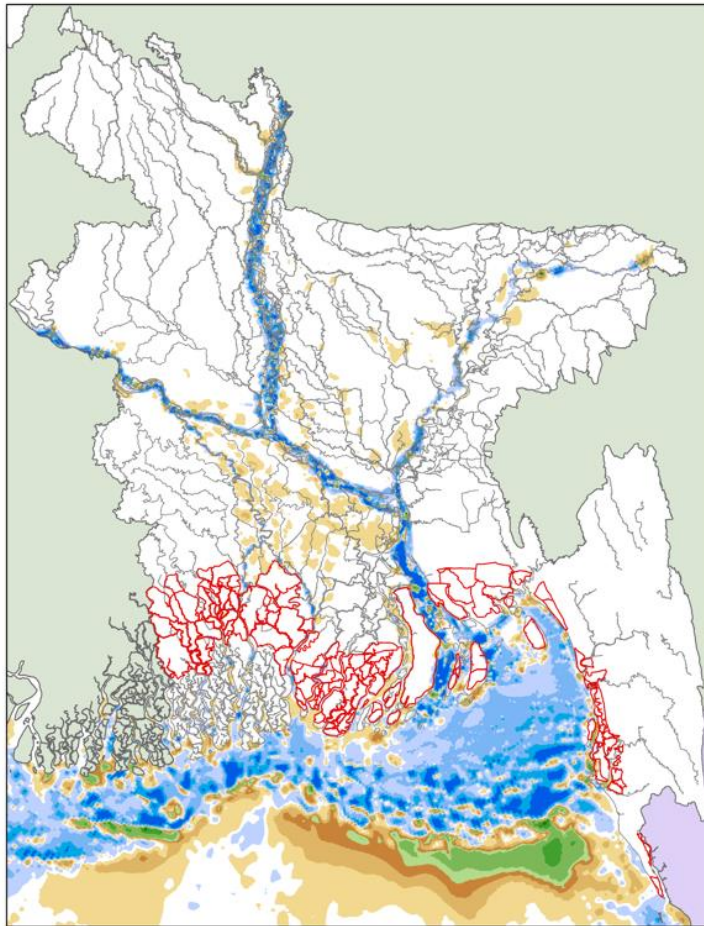


Figure 4.24: Sediment movement path along the coast. The red color shows high sediment concentration, green and blue colors show relatively low sediment concentration.

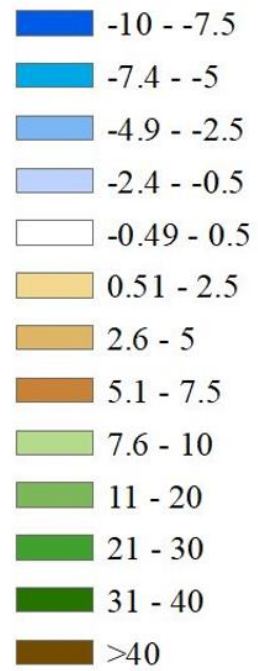
4.6.2 Sedimentation in the floodplains

Morphology module of BDM is applied to compute cumulative yearly erosion and sedimentation in all the rivers, estuaries, and their floodplains. Results are shown in Figure 4.25 (a- j). Sedimentation, as expected, is the maximum in the unprotected regions of the coast. No sedimentation is observed inside polders. Among the rivers and estuaries, maximum sedimentation is observed in the Sundarban system. In Meghna estuary region, a distinct sedimentation is observed in the region between Sandwip and Urir char which will eventually join these two land forms. Sedimentation is also observed in the Pyra port region in the mouth of Tetulia river, in the Kutubdia channel and in the Moheshkhali channel.

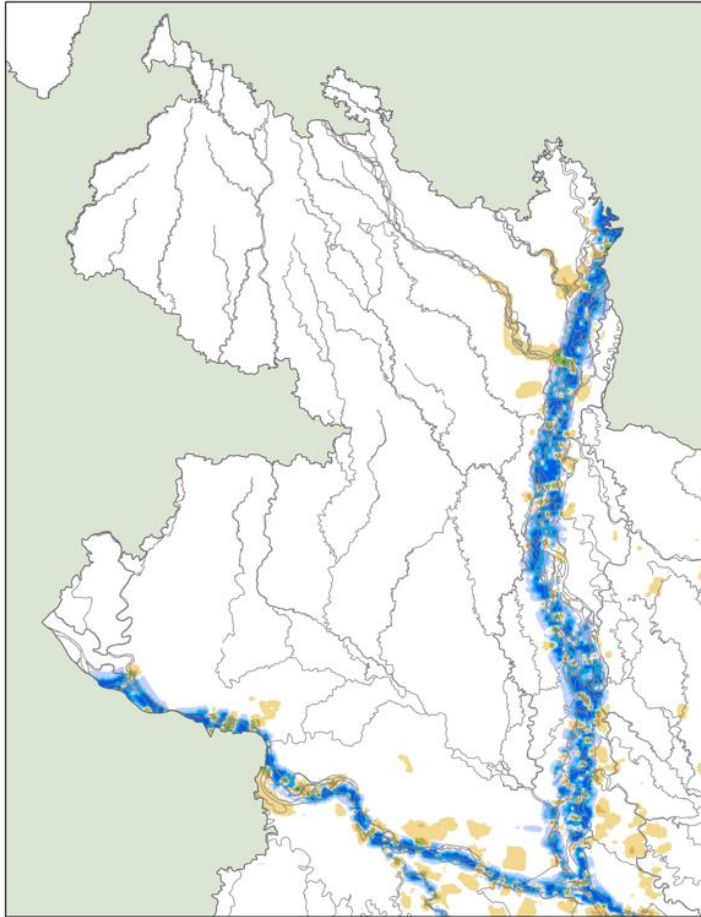
(a)



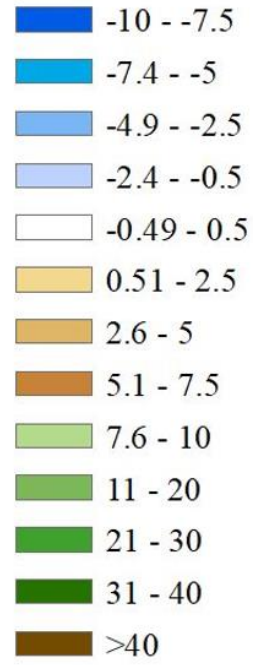
Yearly erosion-sedimentation (cm)
in entire Bangladesh



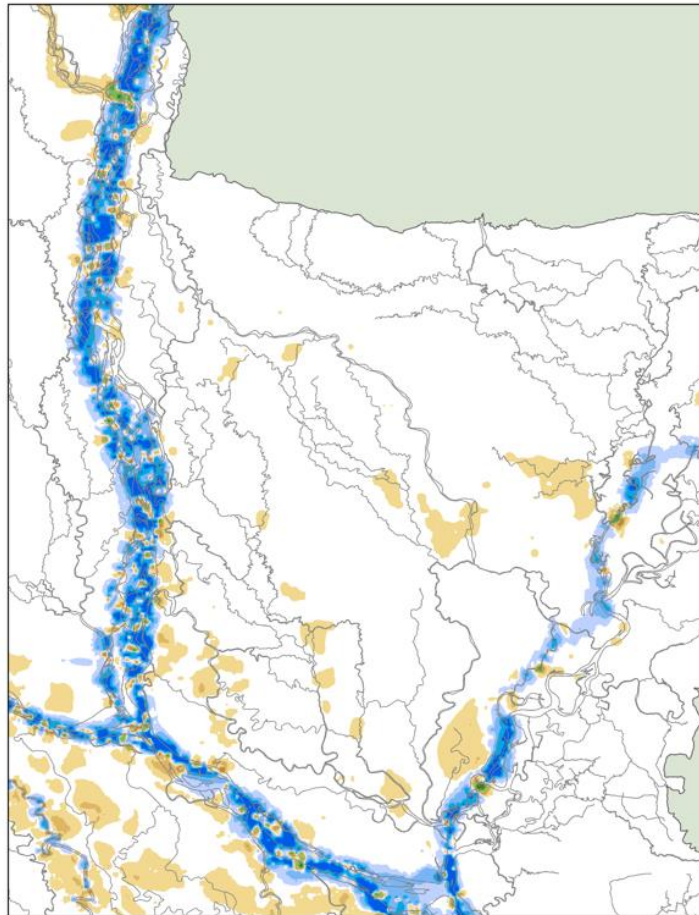
(b)



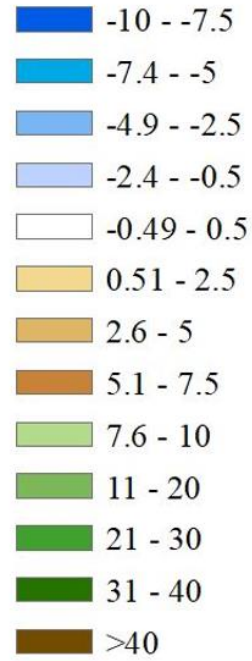
Yearly erosion-sedimentation (cm)
in North-West Region



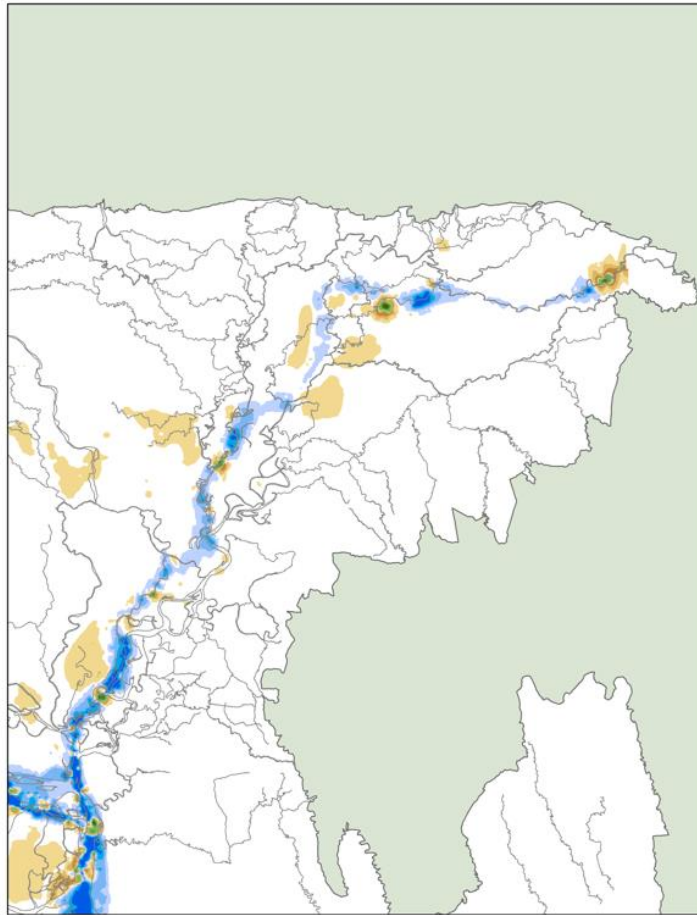
(c)



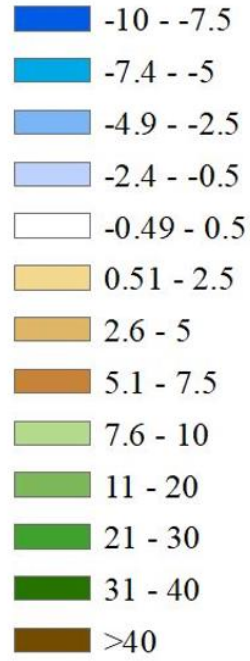
Yearly erosion-sedimentation (cm)
in North-Central Region



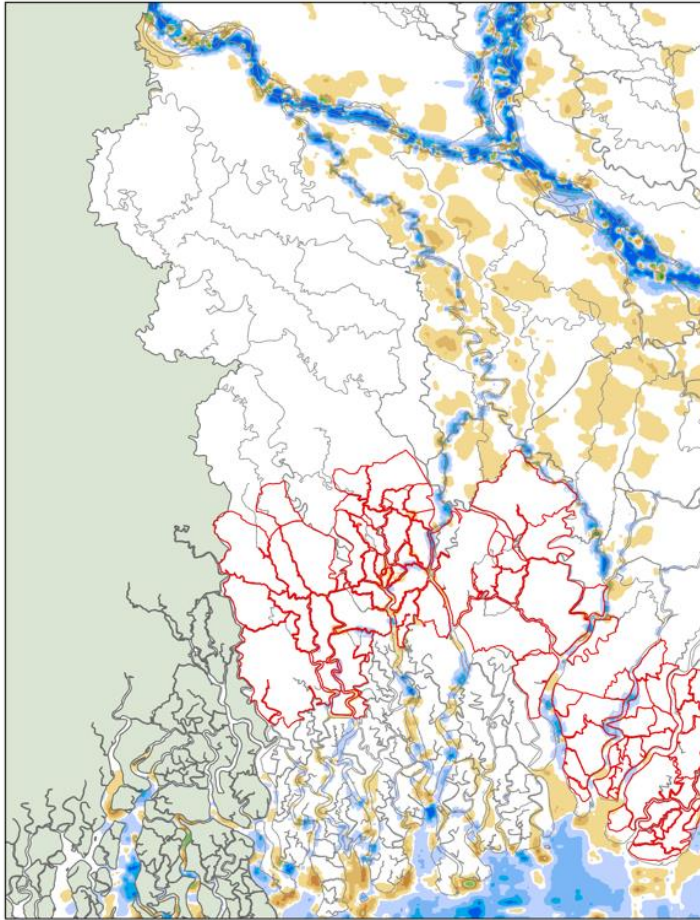
(d)



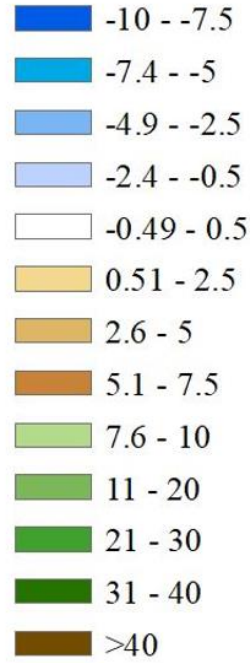
Yearly erosion-sedimentation (cm)
in North-East Region



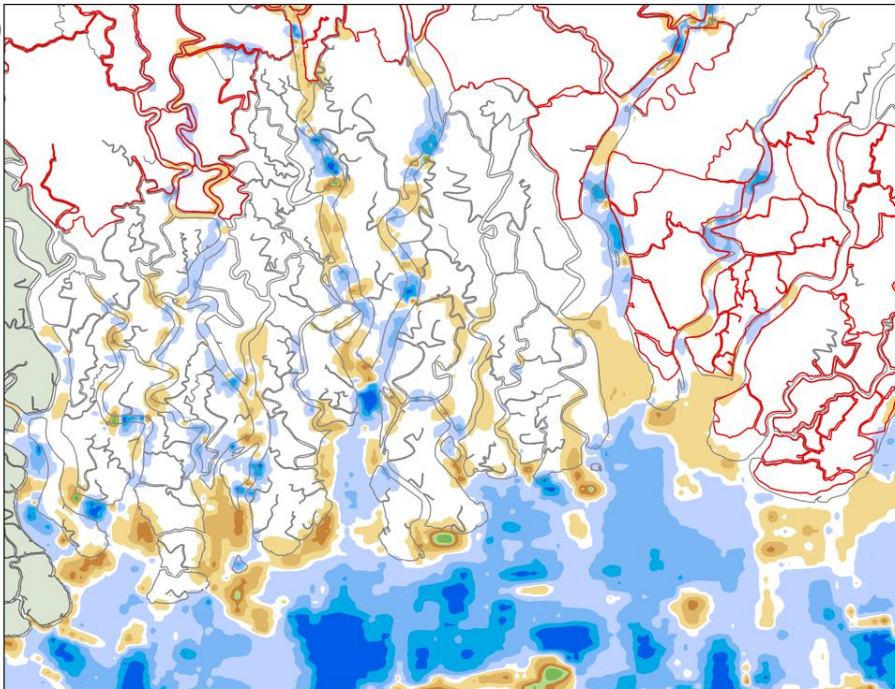
(e)



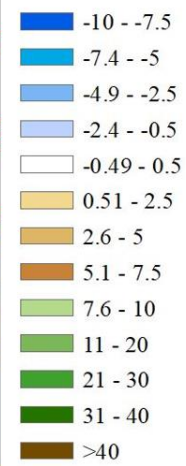
Yearly erosion-sedimentation (cm)
in South-West Region



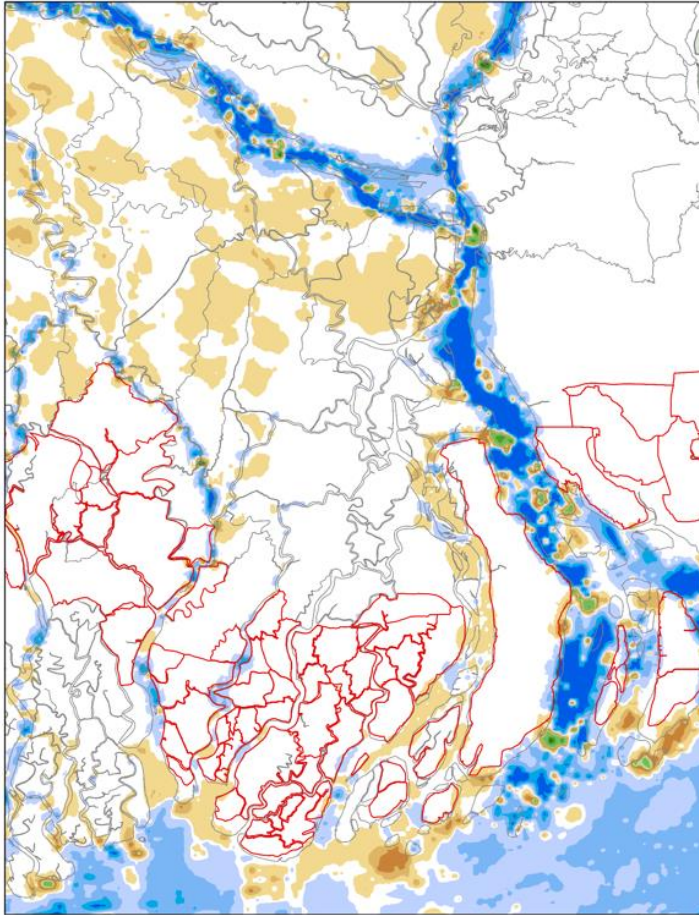
(f)



Yearly erosion-sedimentation (cm)
in Sundarban Region

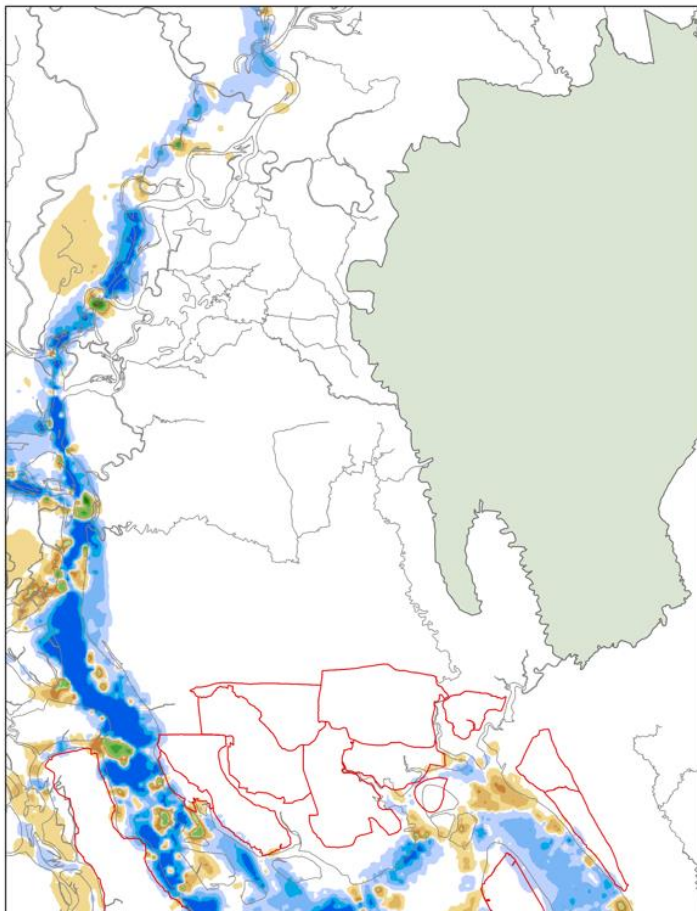


(g)

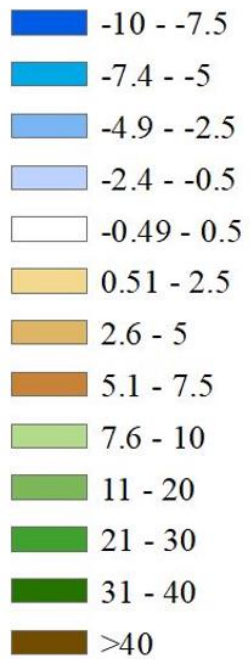


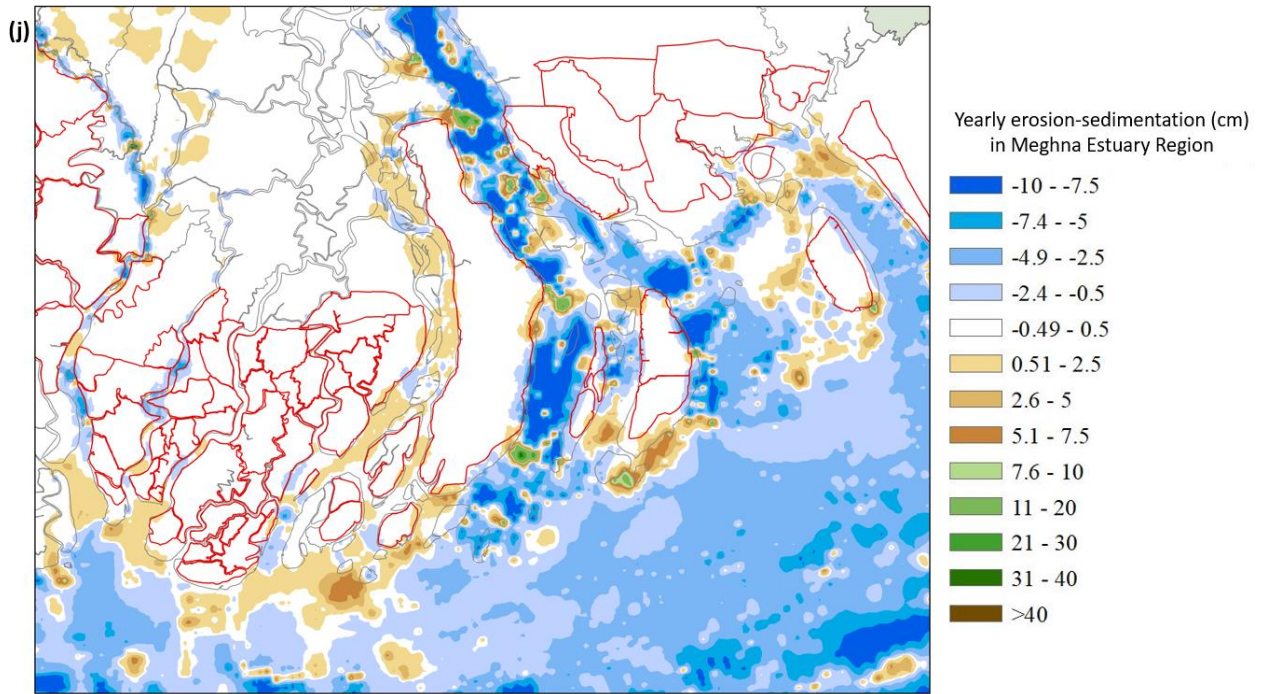
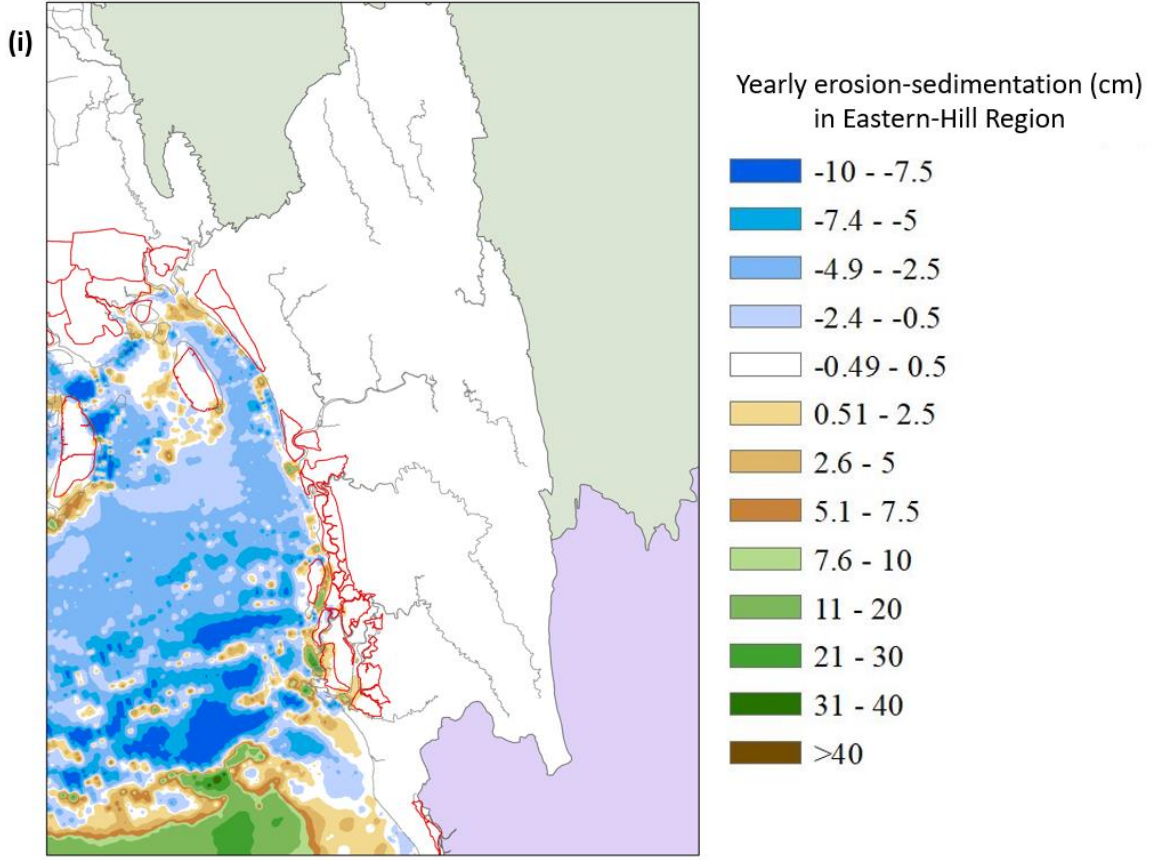
Yearly erosion-sedimentation (cm)
in South-Central Region

(h)



Yearly erosion-sedimentation (cm)
in South-East Region





Figures 4.25 : Yearly erosion-sedimentation maps for the (a) entire country (b) north-west region (c) north-central region (d) north-east region (e) south-west region (f) Sundarban region (g) south-central region (h) south-east region (i) eastern-hill region and (j) Meghna estuary region.

CHAPTER FIVE

Conclusions

A new modelling framework named Bangladesh Delta Model (BDM) is developed in this study. BDM is based on widely applied Delft3D modelling suite. BDM modeling framework integrates the entire processes of ocean, coast, Sundarban, polders, canal network, estuaries, inland rivers of different scales, embankments, wetlands, beels and haors. The model domain is extended southward to the Bay of Bengal down to Sri Lanka & Thailand coast and northward to the inflow points of all 54 transboundary rivers.

At this stage of the study, from the application of BDM, following conclusions are drawn related to sediment management in the coast:

- Relatively higher velocity along the mouth of the estuaries of the western coast during the flood tide causes ocean sediments to enter inside the western estuarine systems. Sources of these ocean sediments are Lower Meghna estuary which propagates along the continental shelf during the ebb tide and later re-enter into the system during the flood tide.
- Just at the beginning of the ebb tide in the ocean, there is a flow disaggregation line and a zone of stagnation occurs. This zone has significant impact on the sedimentation all along the estuary mouths.
- The Swatch-of-no-ground acts like a fast flowing channel and divides the entire oceanic circulation into two distinct patterns – eastern circulation and western circulation. Eastern circulation is dominated by the Lower Meghna flow and the western circulation is dominated by the western estuarine systems and flows from the West Bengal coast. Due to this fast-moving flow separation line, it appears that the sediments from the Lower Meghna system may not be able to deposit in the Swatch-of-no-ground.
- The sediments from the Lower Meghna estuary is mainly distributed along the continental shelf.
- Freshwater plume from Lower Meghna propagates a long distance up to the coast of Thailand.
- There is no vertical infiltration of freshwater inside the canyon even during the monsoon. The sediments are mainly carried in suspension by freshwater from the estuarine system. This sediment laden freshwater cannot enter inside the canyon, rather it is distributed within the first 50m zone from MSL.
- Stratification exists along the east coast throughout the year.

- For a similar sediment regime, cyclonic event creates increased sediment flux. This drive increased volume of sediments to re-enter into the estuarine systems through increased flood flow velocity created by cyclone.
- Flooding is observed in the north-eastern haor systems in the Sylhet region and the central part of the country by Brahmaputra-Jamuna system.
- In the coastal region, fluvial flooding is observed in the central part of unprotected region. During cyclone, there is no land inundation inside polders. Inundation is observed only in unprotected regions.
- Sedimentation, as expected, is the maximum in the unprotected regions of the coast. No sedimentation is observed inside polders.
- Among the rivers and estuaries, maximum sedimentation is observed in the Sundarban system.
- In Meghna estuary region, a distinct sedimentation is observed in the region between Sandwip and Urir char which will eventually join these two land forms. Sedimentation is also observed in the Pyra port region in the mouth of Tetulia river, in the Kutubdia channel and in the Moheshkhali channel.

References

- Al Masud, M. M., & Islam, A. K. A. M. S. (2018), The Challenges of Sediment Management in Tidal Basin: Application of Indigenous Knowledge for Tidal River Management in the Southwest Coastal Bangladesh.
- Amir, S.I.I., et al., (2013). River Sediment Management—A Case Study in Southwestern Bangladesh, *International Journal of Geological and Environmental Engineering*, Vol.7 (3), pp 175-184, 2013.
- As Salek, J. A. (1998), Coastal Trapping and Funneling Effects on Storm Surges in the Meghna Estuary in Relation to Cyclones Hitting Noakhali–Cox’s Bazar Coast of Bangladesh, *American Meteorological Society*, Volume 28, February 1998.
- BWDB (2013), Coastal Embankment Improvement Project, Phase-I (CEIP-I) Final Report-Volume-1, Bangladesh Water Development Board, Dhaka, Bangladesh, June 2013.
- Coleman, J. M. (1969). Brahmaputra River: channel processes and sedimentation. *Sedimentary geology*, 3(2-3), 129-239
- Bharati, L., and Priyantha J. (2011). Hydrological Impacts of Inflow and Land-Use Changes in the Gorai River Catchment, Bangladesh, *Water International*, 36(3), 357–369. [doi:10.1080/02508060.2011.586200.]
- Dasgupta, S., et al. (2014). River Salinity and Climate Change: Evidence from Coastal Bangladesh, Policy Research Working Paper No. 6817, The World Bank.
- EDP (2007), Estuary Development Programme, Technical Note EDP-01, DHV-Haskoning, May 2007.
- Goodbred, S.L. and Kuehl, S.A., (2000), The significant of large sediment supply, active tectonism, and estuary on margin sequence development: Late Quaternary stratigraphy and evolution of the Ganges-Brahmaputra delta, *Sediment. Geol*, 133, 227-248.
- Haque, A., Sumaiya, Rahman, M. (2016), Flow distribution and sediment transport mechanism in estuarine systems of Ganges-Brahmaputra-Meghna systems, *International Journal of Environmental Science and Development*, Vol.7, No.1, January 2016.
- Hussain, M. A., Tajima, Y., Hossain, M. A., & Rana, S. (2014). Asymmetry of tide and suspended sediment concentrations observed at the north-eastern part of the meghna estuary. *Coastal Engineering Proceedings*, 1(34), 77.

Hussain, N., Islam, M. H., & Firdaus, F. (2018). Impact of Tidal River Management (TRM) for Water Logging: A Geospatial Case Study on Coastal Zone of Bangladesh. *Journal of Geoscience and Environment Protection*, 6, 122-132.

Islam, S.N., and Gnauck, A. (2011). Water Shortage in the Gorai River Basin and Damage of Mangrove Wetland Ecosystems in Sundarbans, Bangladesh, 3rd International Conference on Water & Flood Management (ICWFM-2011), March 2011, Dhaka, Bangladesh

Milliman, J. D. (1991). Flux and fate of fluvial sediment and water in coastal seas. *RFC Mantoura*, 69-89.

Mirza, M. M. Q. (1998). Diversion of the Ganges water at Farakka and its effects on salinity in Bangladesh, *Environmental Management*, 22(5), 711–722. [<http://doi.org/10.1007/s002679900141>]

Rahman, M., Dustegir, M., Karim, R., Haque, A., Nichols, R.J., Darby, S.E., Nakagawa, H., Hossain, M., Dunn, F.E. and Akter, M. (2018), Recent sediment flux to the Ganges-Brahmaputra-Meghna delta system, *Science of the Total Environment* 643 (2018) 1054–1064, <https://doi.org/10.1016/j.scitotenv.2018.06.147>

Rahman, L., et al. (2014). Optimization of Alignment of Proposed Canal and Revetment in the old Madhumati River Using Physical Modelling : A Case Study, *International Journal of Hydraulic Engineering*, 3(2), 68–75. [<http://doi.org/10.5923/j.ijhe.2014030203>]

Sumaiya., et al. (2015). Modelling Salinity Extremes in Bangladesh Coast, 5th International Conf. on Water and Flood Management, ICWFM-2015, Dhaka, Bangladesh, pp. 259–266.

Tahsin Anika, Sadmina Razzaque, Anisul Haque, Imran Hossain Newton, Abul Fazal M. Saleh, Rowshan Mamtaz, Md Ibnul Hasan, Md. Aminul Islam Khan, Flavia Simona Cosoveanu, and Cecilia Borgia (2020), Impact of Internal Road Network on Water-Logging Inside Polders, A. Haque, A. I. A. Chowdhury (eds.), *Water, Flood Management and Water Security Under a Changing Climate*, Springer Nature Switzerland AG 2020, https://doi.org/10.1007/978-3-030-47786-8_2

Talchabhadel Rocky, Hajime Nakagawa, and Kenji Kawaike (2020), Selection of Appropriate Shifting of Tidal River Management, A. Haque, A. I. A. Chowdhury (eds.), *Water, Flood Management and Water Security Under a Changing Climate*, Springer Nature Switzerland AG 2020, https://doi.org/10.1007/978-3-030-47786-8_20

WARPO and BUET (2019), Research on the Morphological processes under Climate Changes, Sea Level Rise and Anthropogenic Intervention in the Coastal Zone, Final Report, IWFM, BUET, March 2019.

WARPO and BUET (2018), Research on the Morphological processes under Climate Changes, Sea Level Rise and Anthropogenic Intervention in the Coastal Zone, Progress Report-4, IWFM, BUET, January 2018.

WARPO and IWM, (2016), Sediment Transport in Rivers, Technical Report Volume 4, Comprehensive report on Assessment of State of Water Resources: Sediment Transport in Rivers (4.8s). WARPO, Ministry of Water Resources.